NASA Contractor Report 181806

TAILLESS AIRCRAFT PERFORMANCE IMPROVEMENTS
WITH RELAXED STATIC STABILITY

Irving L. Ashkenas and David H. Klyde

SYSTEMS TECHNOLOGY, INC.
Hawthorne, California

NASA

National Aeronautics and
Space Administration

Langley Research Center
Hampton, Virginia 23665

TABLE OF CONTENTS

LIST OF FIGURES

LIST OF FIGURES (CONCLUDED)

LIST OF TABLES

SYMBOLS AND DEFINITIONS

A, AR	Wing Aspect Ratio, b^2/S
a	Speed of Sound
A/C	Aircraft
AFCS	Automatic Flight Control System
APU	Auxiliary Power Unit
b	Wing Span
c	Specific fuel Consuption (see Table 3); also Wing Chord ($\bar{c}$ = Mean Aerodynamic Chord)
cg	Center of Gravity
C_D	Drag Coefficient D/qs
C_L	Lift Coefficient L/qs

C_ℓ — Rolling Moment Coefficient

C_M — Pitching Moment Coefficient $\Bigg\}$ $\dfrac{\text{moment}}{qSb}$

C_n — Yawing Moment Coefficient

C_y	Side Force Coefficient — Y/qS
D	Drag
F	Force
G	Generic Controller Transfer Function, Particularized by Subscript
g	Acceleration of Gravity, 32.2 ft/sec^2
h	Height, Altitude
HALE	High Altitude Long Endurance
HP	Horsepower
K	System Element Gain
kt	Knots

L	Lift
ln	Natural Log (to base e)
M	Mach Number
NLF	Natural Laminar Flow
n	Load Factor, L/W; also nautical as in n miles
q	Dynamic Pressure, $1/2 \; \rho U^2$, also Pitching Velocity
R	Range
r	Yaw Rate
RN	Reynold's Number
RPV	Remotely Piloted Vehicle
RSS	Relaxed Static Stability
S	Wing Area
s	Laplace Operator
SM	Static Margin $\equiv \partial C_M / \partial C_L$
T	Thrust, also First Order Time Constant
t	Time
TOGW	Takeoff Gross Weight
U	Forward Air Speed
UDF	Unducted Fan
V	Forward Velocity
W	Weight
X	Distance in Forward Direction
Y	Sideforce
y	Spanwise Distance from Center-line
Z	Vertical (down) Acceleration due to Lift

SYMBOLS AND DEFINITIONS (Concluded)

α	Angle of Attack
β	Angle of Sideslip, also $\sqrt{1-M_2}$
δ	Control Surface Deflection Angle
Δ	Designating an Increment e.g., ΔR, Δt
ζ	Oscillatory Damping Coefficient
η	Ratio y/b; also Propeller Efficiency
θ	Airplane Pitch Attitude
Λ	Wing Sweep Angle
λ	Wing Taper Ratio
ρ	Atmospheric Density
Σ	Summation/Total e.g., ΣR - Total Range
ϕ	Bank Angle
ω	Oscillatory Frequency

SUBSCRIPTS

a	Aileron, as in δ_a
CR	Designating Critical eg., M_{CR}
d	Dutch Roll e.g., ω_d
e	Elevator or Elevon
FFT	Free Flight (Wind) Tunnel (LaRC)
G, GR, gnd	Designating Ground e.g., X_G, X_{GR}, X_{gnd}
i	Initial, also Induced (Drag)
le	Leading Edge
M	Designating Pitching Moment eg., C_M; also Mach-/Related e.g., C_{D_M} = $\partial C_D / \partial M$

MAX	Designating Maximum e.g., $C_{L_{MAX}}$
MG	Main Landing Gear
n	Designating Yawing Moment, e.g., C_n
nom	Nominal
o	Designating "Design" (e.g., C_{L_o}) or Static (e.g., T_o)
p	Phugoid Oscillatory Mode; also Rolling-Associated e.g., $C_{\ell_p} \equiv \partial C_n/\partial \left(\dfrac{pb}{2u}\right)$; also Parasite as in C_{D_p}
P1, P2	Decomposed (2 First Order) "Phugoid" Modes
PT	Pressure (Wind) Tunnel (LeRC)
q	Pitching-Associated e.g., C_{M_q}
r	Yawing-Associated e.g, $C_{n_r} \equiv \partial C_n/\partial \left(\dfrac{rb}{2u}\right)$; also Rudder-Associated
R	Wing Root e.g., C_R
rotn, rot	Designating Rotation
s	Stall, e.g., V_s
sp	Short Period Oscillatory Mode
sp1, sp2	Decomposed (2 First Order) "Short Period" Modes
T	Wing Tip e.g., C_T; also Thrust e.g., ΔC_{n_T}, β_T
t	Designating (Outboard) Trim Flap e.g., δ_t
TO	Designating Takeoff
trim	Designating Trimmed Condition
w	Designating Plunging Velocity e.g., Z_w
x	Designating Crosswind
β	Designating Sideslip e.g., $C_{n_\beta} \equiv \partial C_n/\partial \beta$

SUBSCRIPTS (Concluded)

δ_a — Designating Aileron Deflection e.g., $C_{n_{\delta_a}} = \partial C_n / \partial \delta_a$

δ_r — Designating Rudder Deflection e.g., $C_{n_{\delta_r}} = \partial C_n / \partial \delta_r$

ϕ — Designating Roll Transfer Function Numerator, e.g., ω_ϕ

1, 2 — Initial, Final e.g., W_1, W_2

50 — Designating 50' (Obstacle) Height

INTRODUCTION AND SUMMARY

The concept of using active automatic control to allow stable flight at (ordinarily unstable) aft cg locations -- so-called relaxed static stability (RSS) -- has been shown to generally improve cruise efficiency thereby permitting either reduced weight or increased range-payload performance. The largest improvement for conventional aircraft appears to be for supersonic cruise; then the aft cg location acts to strongly reduce the required longitudinal tail size and the tail down-lift required to trim, and their associated drag. However, conventional subsonic transport aircraft also benefit from RSS as evidenced by the Refs. 1-3 series of studies which uniformly show about 4% improvement in fuel efficiency. Some of these benefits are due, not only to the impact of RSS which permits smaller tails and concomitant reduced weight and drag, but also to the underlying Active Control Technology which allows the use of automatic air-load-alleviating trailing edge surfaces to effect reductions in design loads and in wing structural weight.

Spanwise distributed fuel and payload is a better way to achieve wing load alleviation and weight reduction. In their purest embodiment such "span loader" aircraft become flying wings which then combine the benefits of both reduced structural weight and reduced profile drag. That is, the combined effects of a "good" (not the highest achievable) max L/D and of a high fuel/payload weight fraction, produce a superior range/payload performance.

The beneficial effects of relaxed static stability on such aircraft are potentially very significant -- all stemming from the fact that required trailing-edge trim surface deflections, normally negative for stable cg's are now positive for unstable cg locations. In other words, longitudinal trim, instead of involving reverse wing camber, now results in positive camber. The immediate effect is an increased trimmed maximum lift and attendant improved landing performance. This "classical" result was the primary reason for the original patent obtained by Northrop Aircraft in the early 1940's which foresaw these particular performance benefits of relaxed static stability for flying wing aircraft.

1

Notice that the favorable shift from down- to up-lift, similar in kind to that for conventional tailed aircraft, is now much more powerful in degree and exerts a dominant effect on (increased) trimmed maximum C_L. This effect permits a reduction in <u>wing</u> area, versus a reduction in <u>tail</u> area for the conventional aircraft. Obviously the former exerts the greater influence on the resulting weight saving.

The potential drag reduction due to positive (versus reverse) camber at trimmed cruise C_L is expected to be of roughly the same magnitude as that due to the smaller, uploaded tail on the conventional airplane. In addition, though, the cambered wing critical Mach number at cruising lift coefficients will also be improved with proper design. Finally, because trimming is now beneficial rather than detrimental from a drag standpoint, it appears that the conventional spanwise-distributed, discrete trailing edge surfaces (e.g., inboard-, mid-, and outboard-span) may be used to effect better lift distributions for both slightly reduced drag and wing bending moments. That is, positive inboard and mid-span camber can be countered with a little reverse outboard camber to shift the center of lift distribution inboard and reduce the high tip loadings due to wing sweep. Such "opposed" static and maneuver trimming is possible regardless of cg location, but is more effective at aft cgs because the net camber is positive rather than negative. However, it must be emphasized that such re-distributed lift possibilities, at best secondary effects, are not nearly as powerful regarding wing-load and -weight reduction as is the primary inertial relief afforded by span distributed fuel and payload. Perfect inertial relief, e.g., for a fully loaded condition, will shift the maximum wing bending moment to lighter weights or possibly to landing-impact conditions. This permits either a lighter wing structure or higher maneuver load factors for a given structure.

The maximum trimmed lift improvement potential of the RSS flying wing extends also to <u>any</u> <u>tailless</u> aircraft. Thus a tailless fighter airplane with RSS cg locations, can be designed with a smaller lighter wing, while retaining equivalent field takeoff and landing performance. Wing drag reductions due to positive camber will further enhance altitude performance. However, span-loading contributions to wing weight saving will be

negligible because of limited wing volume and the greater capacity of the center-body which is then the natural receptacle for most of the carried load.

If low observability is a desired characteristic of such a tailless fighter, it will have minimum appendages, so that most of the available control "surfaces" will be limited to devices attached to, or part of the wing. The smaller wings resulting from the RSS design process then exacerbate such control limitations; and the low resulting available control power emphasizes the importance of the wing-alone stability derivatives, some of which are not well quantified. In these respects the blended-body, tailless fighter and the flying wing can have similar control design problems. More conventional aircraft will have sufficient control power to swamp the wing derivatives with feedback-created artificial derivatives, so that the inherent derivatives are not so important.

On all the above counts, the flying wing configuration emerges as a limiting best/worst case for the study of potential benefits and penalties of RSS. The present study was undertaken to quantify this potential in terms of range-payload improvements; and to identify other possible operational and handling benefits or problems, including needed technology advances to convert the "promise" to reality, recognizing that such promise can be partially extended to tailless aircraft in general. The potential control power deficiencies are also explored especially with reference to the effects of poorly-quantifiable wing cross-control and cross-rotary derivatives (e.g. $C_{n_{\delta a}}$, C_{n_p}).

In the body of the report itself we progressively treat:

Configuration Selection — the process of deciding between two basic subsonic geometries: one a "modern" high aspect ratio, short-chord wing proposed as a high altitude long endurance (HALE) RPV; the other a wider, lower aspect ratio, high volume wing suitable for internal stowage of all fuel and payload required for a manned long range reconnaissance mission. The latter, the "old" Northrop YB-49 geometry, is selected for a variety of reasons (see Table 1) including the ready availability of much more complete baseline design data, and of studies updating the structure, power plant and other equipment.

Drag Relationships for the above-selected configuration are summarized in Table 2 and record the expected effects of

3

(stable) up- and (unstable) down-deflected controls on both $C_D(C_L)$ and $M_{CR}(C_L)$.

Specific Fuel Consumption for the power plant type selected-- an unducted fan (UDF) turbine combination, only two of which are required -- characterized and clarified in Tables 3 and 4, and the associated text.

RSS Effects on Max C_L and Weight develops and discusses the trimmed maximum C_L effects of RSS and the resulting allowable reductions in wing area and weight as summarized in Tables 5 and 6 respectively. The stable version has a "normal" 5% static margin; the unstable a negative 8% static margin as limited by stall-recovery pitch control power. The ratio of maximum C_L, unstable (RSS): stable is about 1.41 allowing a corresponding reduction in wing area from 4,000 (stable) to 2,800 (unstable) square feet. The weight considerations and calculations show about a 7,000 lb reduction (10.6%) in weight empty for the smaller wing; and apply specifically to the primary manned reconnaissance versions, both of which reflect takeoff weights of 194,000 lbs. A later expansion of the study to cover similarly stable and unstable light weight (30,000 lb) RPV versions is detailed in the section labeled Light Weight RPV Versions.

Range/Endurance Computations for the manned versions start with the variation of incompressible L/D and M_{CR} L/D with M and with C_L. The unstable (smaller) version shows about a 3-1/2% improvement in M_{CR} L/D at a slightly increased C_L and slightly reduced M. The differences in cruise C_L and wing loading result in lower cruise altitudes by about 7,000 ft, for the unstable version which is, however, arbitrarily held to an initial alti- tude of 35,000 ft. The resulting maximum ranges, developed in Table 7 favor the unstable version by about 14%. The maximum endurance, computed at 20,000 feet (Table 8) because of the improved specific fuel consumption arising from the lower cruise Mach numbers, shows about a 9% advantage for the unstable case.

Light Weight RPV Versions, using the same basic wings but reduced weights (30,000 lb T.O.G.W.), were formulated to explore possible differences due to the drastically decreased wing loadings and increased altitudes. The weight breakdowns shown in Table 9 reflect a weight empty saving of about 9% for the unstable version. As described in Table 10, the higher alti- tudes and resulting reduced Reynolds numbers permit a general drag reduction due to increased natural laminar flow (NLF); however the theoretical best cruise altitudes approach 83,000 ft (end of flight) and even "paper engine" performance at these high altitudes is considered doubtful. Accordingly, range and endurance are computed for a constant 60,000 ft cruise altitude. Furthermore, to increase the power absorbed by the propeller (UDF), one engine is shut down and the prop feathered for

weights <15,000 lbs; and the feathered prop drag is added to each configuration.

The resulting 60,000 ft endurance (Table 11) is greater for the unstable version by about 7%; and the range (Table 12) by a significant 23%. The components of the latter disproportionate increase are identified and shown to be due in part to a mismatch in the selected 60,000 ft cruise altitude for the larger stable version. When altitude is allowed to increase with decreasing weight so that both versions always cruise at best ML/cD, the range advantage of RSS (bottom of Table 12) is reduced to "only" 14-1/2% quite consistent with the manned aircraft result.

<u>Take-Off Performance</u> for the manned versions shows a marked dependence on assumed ground roll trim settings and resulting C_L and C_D. Initial comparisons (Figs. 6, 7) show that the best unstable 50 ft clearance distance is about <u>45% greater</u> than the best stable. However, taking advantage of the automatic trimming inherent in the flight control system, which is necessary to stabilize and fly the unstable version, permits a reduction in ground-roll C_L, C_D such that the resulting 50 ft clearance distance (Fig. 8) is now about <u>14-1/2% less</u> than the best stable distance. Take off performance for the unstable <u>RPV</u> version (shown in Fig. 9) is much improved because of the reduced wing loading (2,010 ft versus 6,500 ft for the manned version).

<u>Stability and Control Characteristics</u> are computed based on the estimated derivative coefficients given in Appendix A which were combined with inertial and geometric parameters to compute the dimensional derivatives and control input transfer functions given in Appendix B. The feedback and gains used to additionally stabilize both versions longitudinally are shown on page 36.

The computed longitudinal response to Step θ command inputs (Figs. 10, 11) show a considerably <u>reduced</u> delay (a factor of about 2) in the h response for the unstable case. This difference is traceable to the direct-lift contributions of the automatically downward trimmed elevon. Such delays, especially characteristic of tailless aircraft due to the strong down-lift associated with nose up elevator moments, sometimes constitute a handling problem; the reduced delay due to RSS is generally quite significant and beneficial.

The remaining stability and control situations studied are all for lateral control involving, in order:

- Cruise $\omega\phi/\omega d$ (Table 13) — lower (worse) values for the unstable configuration

5

- δ_r for engine out at T.O. (Table 14) — more
  marginal for the unstable case

- Crosswind trim (Table 15)

  Rudder limits worse for unstable case
  Rudder + diff thrust limits better unstable

  (Table 16) aileron, bank limits worse for
  unstable case.

- Yaw suppression in rapid rolls (Table 17)

  Available rudder power imposes a limit on usable
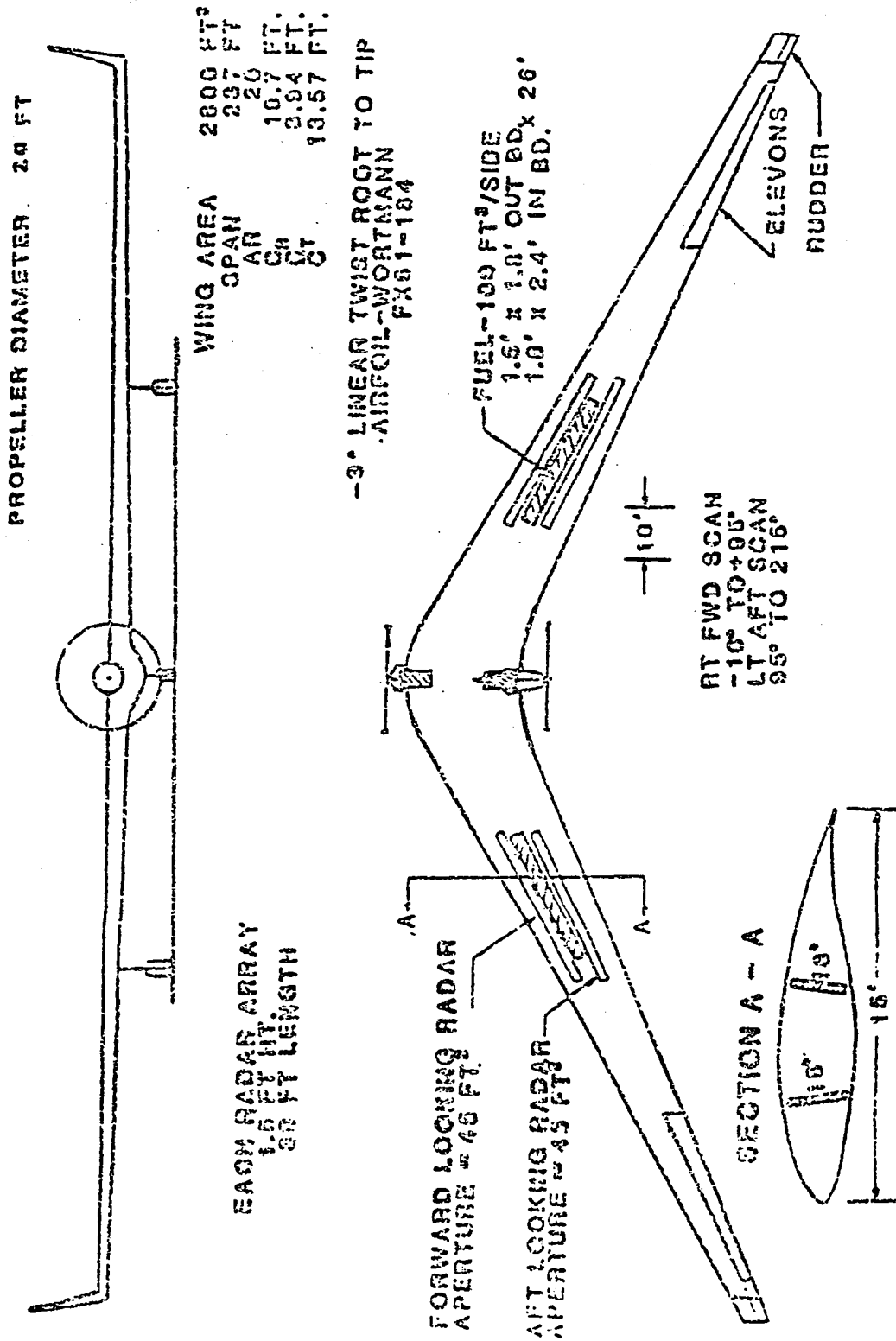 aileron for roll control for both versions.

Results, Conclusions, Observations and Recommendations are given in the final paragraphs of the main text, which follows now starting with, as noted above, the section concerning the choice of wing configuration.

CONFIGURATION SELECTION

To emphasize the area of greatly expected performance improvement, the design mission chosen for the study was high altitude long range/ endurance reconnaissance. This selection, in part, also reflected the existence of fairly recent design interest in, and information on, remotely piloted versions of these aircraft (Fig. 1). The availability of such baseline information was considered a prerequisite because of the very limited scope of our own study. In fact, we sought to expand the applicable database to the extent possible by also considering updated versions of the manned YB-49 (Fig. 2) as represented by the advanced technology version defined in unpublished NASA-sponsored studies by Kentron International (authored by R.V. Turriziani): NASA/ASO file 3-9200/4LTR-260, Sept. 14, 1984.

The considerations involved in choosing between these two configuration extremes are listed in Table 1. Here it may be seen that the YB-49 inertial and aerodynamic data and information are much more complete, as also evidenced by the listed Refs. 4-12. Furthermore, the YB-49 is not space limited so that reduced wing areas (reflecting increased max C_L) can still accommodate design gross weight fuel and payload consistent with a

Figure 1. Remotely Piloted High Altitude Long Endurance (HALE) Configuration (Ref. 14)

7

STATIC GROUND LINE 2°30'
TO ROOT CHORD

53.08'

4°

HORIZ. REF. PLANE
(ROOT CHORD)

14.98'

23.5'

WING AREA   4000 FT²
AR   7.4
CR   448 IN.
CT   112 IN.
$\bar{c}$ 314.5 IN.

18.91'
17.26'
31'
32.88'

TRIM FLAP, δ_t
& RUDDERS

ELEVON, δ_e

LANDING FLAP, δ_f

43.7'

WING SLOT

DORSAL FINS

BASIC AIRFOIL = NACA 65,3-018

172'
86'
36.63'

$\mathcal{C}$ OUTB'D. VERTICAL FIN
$\mathcal{C}$ INB'D. VERTICAL FIN

HORIZ. REF. PLANE

23.63'

0°53 DIHEDRAL AT LEADING EDGE

41.2'
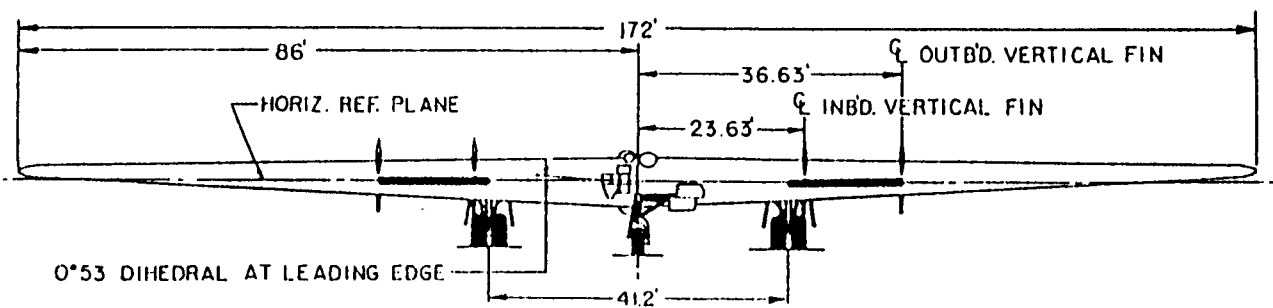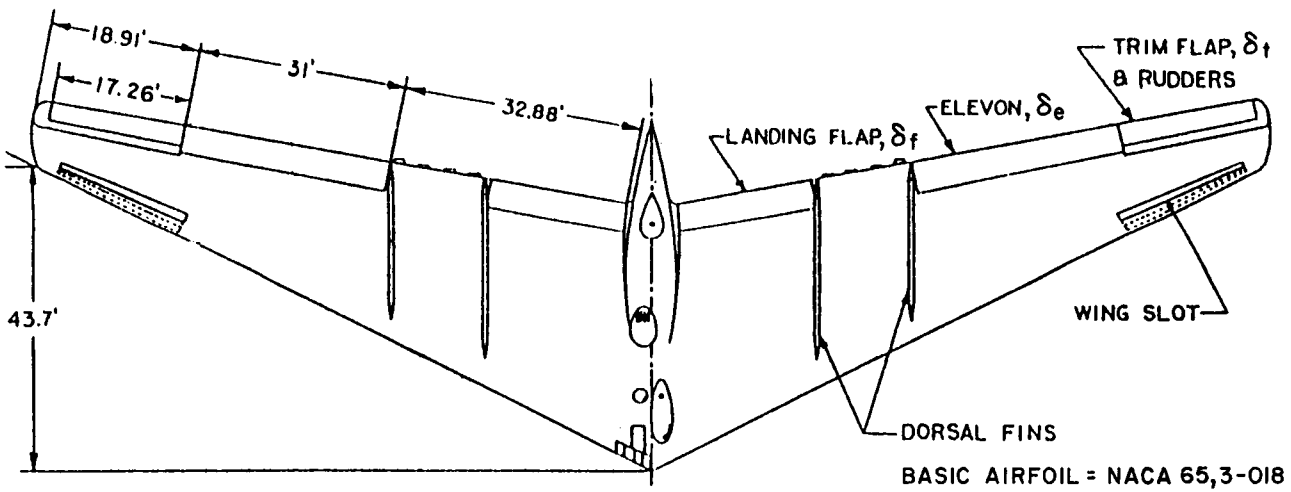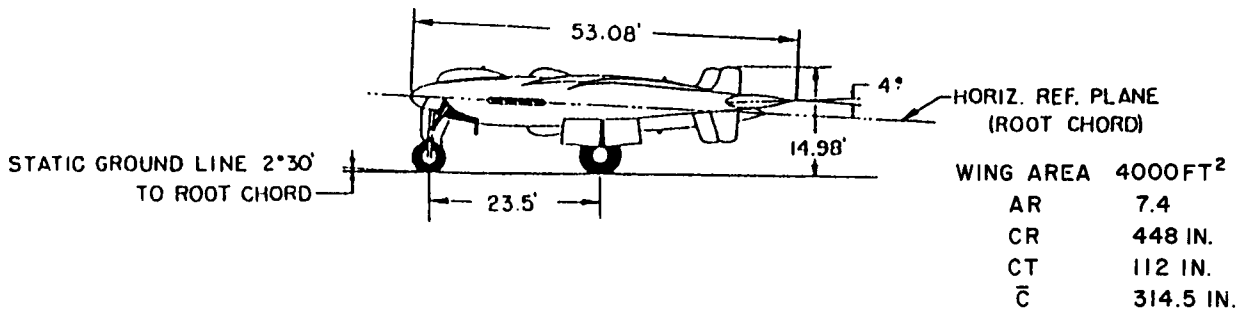
Figure 2.   YB-49 Three-View

TABLE 1. CONFIGURATION SELECTION CONSIDERATIONS

	MANNED YB-49	RPV HALE
Weight Data Quality	SOLID	[1]Questionable
Engine Alternatives	2	1
Control Effectiveness Data	Complete	Rudimentary
Stability Derivative Data	Wind tunnel and ltd Flight	Estimates
Inertial Data	Actuals	Estimates
Airfoil Type	Symmetric	[2]Camber-Reflex
Space Limited	No	Maybe
Wing Loading	48.5	6.1
Approx. T.O. Distance	7500'	[3](1000')

(1)   Conventional empirical wing weight formulas don't account for distributed span-loads.

(2)   Reference 19 discarded reflex because of expected upper surface B.L. separation at .70c̄.

(3)   Probably not critical: $C_{L_{MAX}}$ unimportant.

manned aircraft, whereas the Fig. 1 geometry probably cannot. The heavier manned versions are basically more efficient because the load will be distributed practically full-span; not so for the much lighter RPV's. Finally the RPV's will not be as critical as regards take-off or landing so that maximum C_L may be relatively unimportant. For these reasons we chose the YB-49 configuration as the basis for the study replacing the eight jets and four fins with two turbine-driven eight-bladed counter rotating 12.5' diameter unducted fan (UDF) propellers.

The hydraulic system hinge moments are proportional to scale[3] and may be taken as governing actuator sizes and weights; however, the hydraulic line weights will vary with length or directly with scale. Averaging these effects gives a factor again roughly equal to the ratio of wing areas (=scale[2]). Finally the surface control weights are dominated by surface area which is, again, proportional to the wing area ratio. Thus the general rule applied to the reduction of these items in the column 4 tabulations was to multiply the column 3 values by 0.7.

DRAG RELATIONSHIPS (TABLE 2)

The first line, basic drag, reflects the incompressible YB-49 drag data given in Ref. 5, as does the second line for $\Delta C_D(\delta)$. Substituting the stable (static margin SM=.05) variation of δ with C_L (Table 2 trim equation) results in the total incompressible $C_D(C_L)$ shown which yields a maximum L/D=26.4.

For the unstable cg (SM=-0.08), the ΔC_D variation shown reflects the improvement in section drag variation with C_L due to positive flap deflection (camber effect on "design" C_L) as inferred from the data in Ref. 15. Substituting the unstable variation of δ with C_L results in the incompressible $C_D(C_L)$ with a maximum L/D=27.6.

The next section of Table 2 relates to the estimation of the critical mach number M_{CR} to be used in the $C_D/C_{D_{inc}}$ multiplier (Ref. 5) given in the bottom Table 2 equation. The basic relationship shown is that in Ref. 5, extended for $C_L > C_{Lo}$ by the third term reflecting the theoretical $M_{CR}(C_L)$ variations in Ref. 14 for the basic YB-49 airfoil. The $\Delta M_{CR}(\delta)$

10

TABLE 2. TRIM ANGLE EFFECTS ON C_D, M_{CR}

$\underline{\text{BASIC}}$ ($\delta = 0°$) $\quad C_D = .0070 + .051C_L^2$

$\underline{\text{FOR STABLE CG}}$ $\quad \Delta C_D = .000058\delta°^2$

$\quad\quad$ SM = .05 $\quad \delta° = 1.83 - 7.04C_L$

$\quad\quad\quad\quad C_D = .00719 + .0539C_L^2 - .001494C_L$

$\quad\quad\quad\quad\quad\quad\quad\quad\quad\quad\quad\quad\quad$ MAX L/D = 26.4

$\underline{\text{FOR UNSTABLE CG}}$ $\quad \Delta C_D = .008 (C_L - .02\delta°)^2$

$\quad\quad$ SM = -.08 $\quad \delta° = 1.83 + 11.27C_L$

$\quad\quad\quad\quad C_D = .0070 + .0481C_L^2 - .000454C_L$

$\quad\quad\quad\quad\quad\quad\quad\quad\quad\quad\quad\quad\quad$ MAX L/D = 27.6

$\underline{\text{BASIC}}$ $\quad M_{CR} = .670 - .063C_L - \underbrace{.063(C_L - C_{L_o})}_{\text{for } C_L > C_{L_o}} + \Delta M_{CR}(\delta)$

$\underline{\text{FOR STABLE CG}}$ $\quad C_{L_o} = .35 \quad\quad \Delta M_{CR}(\delta) = 0$

$\quad\quad M_{CR} = .670 - .063C_L - \underbrace{.063(C_L - .35)}_{\text{for } C_L > .35}$

$\underline{\text{FOR UNSTABLE CG}}$ $\quad C_{L_o} = .35 + .02\delta° \quad\quad \Delta M_{CR} = -.00085\delta°$

$\quad\quad M_{CR} = .6684 - .0726C_L - \underbrace{.0488(C_L - 0.50)}_{\text{for } C_L > .50}$

$\underline{\text{GENERAL}}$

$$\frac{C_D}{C_{D_{inc}}} = 1.00 + .08\left(\frac{M}{M_{CR}}\right)^{10} + .01\left(\frac{M}{M_{CR}}\right)^{20} + .001\left(\frac{M}{M_{CR}}\right)^{50}$$

term is to account for small reductions in M_{CR} due to increments in design C_L (positive camber). For the stable cg this is zero as shown; and C_{Lo} is constant $=0.35$ in keeping with the original basic two-term equation which is considered applicable to the stable YB-49 (Ref. 5). For the unstable case the "design" C_L varies with control trim deflection as does ΔM_{CR}, both based on the Ref. 14 data.

SPECIFIC FUEL CONSUMPTION

The power plant characteristics as regards specific fuel consumption (c) were not directly available because the engine data document referred to in the above-cited unpublished Kentron study was declared proprietary and denied to this project. However, those data included maximum range and endurance results for given weights and associated average M, C_L, L/D, c values for a variety of configurations; and the Table 3 considerations show that the values of specific fuel consumption, also shown, can be considered equivalent to <u>thrust</u> specifics $\left[\dfrac{\text{lb/hr}}{\text{lb thrust}}\right]$ rather than shaft horsepower specifics as for conventional turbo props. This is consistent with the fact that the unpublished Kentron data do <u>not</u> include propeller efficiency, η, as a tabulated parameter; and with the relatively high disk loadings of the small diameter propellers. This renders their thrust variation with speed more akin to that of a Turbofan as shown for example in the Ref. 18 data, later used to support the selected propeller diameter. Table 3 progressively shows:

- the range equation pertinent to thrust specific characteristics

- the reserve used (in the Kentron study) to compute the final weight, W_2

- the derivation of a factor (1.36) to convert range to endurance conditions

- the use of this factor to compute the weight allowance corresponding to 30 min at SL max endurance $=462$ lb

- 5% of the initial fuel (6036 lb) the total reserve (6498 lb) and W_2, the final weight$=79914$ lb

- the range at M$=.64$, corresponding L/Dc, $W_1=194,143$ and W_2 as above $=19029$ nautical mi

- the Kentron study range $=18441$

TABLE 3. SPECIFIC FUEL CONSUMPTION BASIS (THRUST OR HP?)

Check Kentron study Tabulated Range, Weight, L/D etc. vs. Computed Range based on:

$$c \; = \; \frac{W/hr}{T} \quad \text{and corresponding Range} \; = \; a \, \frac{M}{c} \, \frac{L}{D} \, \ell n \, \frac{W_1}{W_2}$$

where

$$a = 573.8 \text{ kts } (h > 35k \text{ ft}), \; W_1 = 194,143,$$

$W_2 \sim$ reserves = 5% of initial fuel + 30 min at SL max endurance

Kentron (Table VII) Endurance/Range Comparisons for 40% Natural Laminar Flow (NLF) show

$$\frac{L/Dc \text{ endurance}}{L/Dc \text{ range}} \; = \; \frac{25.3}{.289} \times \frac{.373}{24.0} \; = \; 1.36$$

Use this factor for the more appropriate Table VI C (Kentron) example 25; then

$$L/Dc \text{ endurance} \; = \; 1.36 \times \frac{21.6}{.370} \; = \; 79.4$$

$$\Delta W(30 \text{ min}) \; = \; W(\frac{D}{L} c)\Delta t \; = \; \frac{73416}{79.4} \times 0.5 \; = \; 462 \text{ lb}$$

$$5\% \text{ initial fuel} \; = \; .05 \times 120727 \; = \; 6036$$

$$\text{total fuel reserve} \; = \; 6498$$

$$W_2 \; = \; 194,143 - 120727 + 6498 \; = \; 73416 + 6498 \; = \; 79914$$

Using Range formula (above) based on thrust specific

$$R \; = \; 573.8 \times .64 \times \frac{21.6}{.370} \, \ell n \, \frac{194143}{79914} \; = \; 19029 \text{ n miles}$$

$$\text{Kentron Range} \; = \; 18441 \text{ n miles}$$

3% error

Similar Comparisons for other Example Cases

$\therefore$ c based on thrust OK

- the conclusion that specific fuel consumption, c, based on thrust is a proper characterization for the selected engine-propeller combination.

The Ref. 19 thrust and fuel flow data, for a similar propulsive unit are converted to thrust-specific fuel consumption data in Table 4. These data are plotted beneath the Table and show a linear variation of thrust-specific fuel consumption (normalized by the value at M=.65, h=35 kft) with M which is consistent with the Kentron data which show that ratios of c for M=.3 to those for M=.64 lie between 0.760 and 0.775; the value given by the Table 4 equation fit to the data is 0.75.

RSS EFFECTS ON MAXC$_L$ AND WEIGHT

The first set of performance comparisons were made for a manned version; a later set considered a much-reduced-weight RPV version. For both versions there was a reduction in wing area for the unstable case because of the increased max C$_L$ as computed in Table 5. The general trim and lift equations in Table 5 are from Ref. 5; the C$_{L_{max}}$ relationship is consistent with the Ref. 12 data for an identical wing planform. The stable case has a 5% and the unstable case has a negative 8% static margin; i.e., X$_{cg}$/$\bar{c}$ − .303 = -.05 and +.08 respectively. The unstable static margin is limited to 8% because of nose down pitching moment requirements at stall corresponding to $\ddot{\theta}$ = .08 rad/sec^2, (Refs. 19,21) which requires +11.1° of elevon (δ_e) deflection. This, added to the trim deflection, practically saturates the elevon (which only has about 25° of linear effectiveness). The ratios of stable to unstable max C$_L$ are 0.7 for both 50° and 0° of landing flap so that the unstable wing can be reduced to 70% of the baseline 4000 ft^2 without landing or takeoff performance penalty.

The weight buildup data for the manned versions are shown in Table 6. The first three columns are assembled from the figures given in the Kentron study, with the first representing the baseline YB-49. The maximum ramp weight, constant for all columns in Table 6, is consistent with YB-49 and Kentron information. The major differences are between the first and second columns, both for aluminum construction; and are due to "advanced

14

TABLE 4. SPECIFIC FUEL CONSUMPTION (M, h)

Reference 19 fuel flow and thrust data converted to c with following results

h Kft \ M	0	.2	.4	.6	.75	.85
0	.352	.429	.539			
10		.419	514	.617		
20			.502	.595	.656	
30				.579	.635	.667
35				.580	.635	.667

Based on a "nominal" value ~ M = .65 at 35 Kft

$$c/c_{nom} = .54 + .74M$$

fits data within a max conservative error of 5% for all altitudes above 20,000 ft -- see plot below.
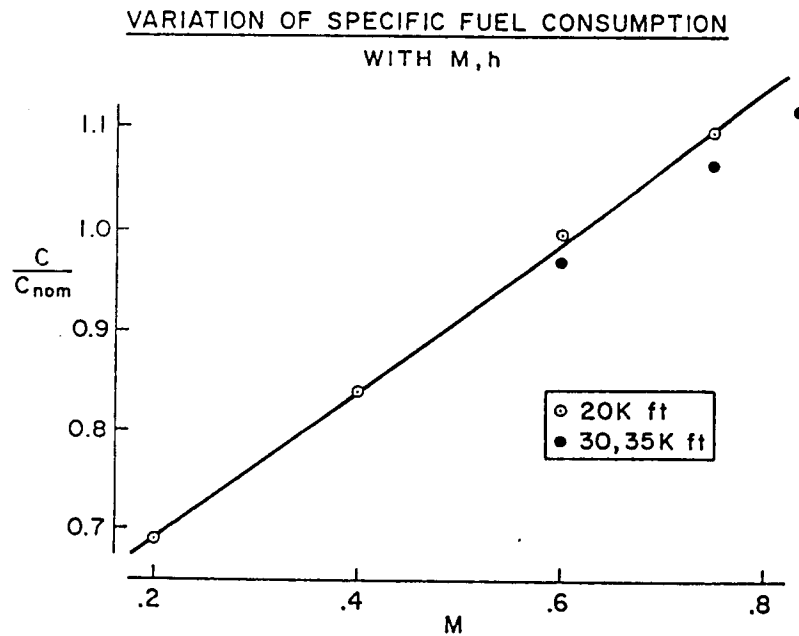

VARIATION OF SPECIFIC FUEL CONSUMPTION WITH M,h

TABLE 5. TRIMMED MAX C_L

GENERAL: $C_{L_{MAX}} = 1.34 + .0086\delta_f + .0129\delta_e + .0064\delta_t$

$C_{M_{TRIM}} = 0.13 + \left(\frac{X_{cg}}{\bar{c}} - .303\right)C_L - .0010\delta_f - .0046\delta_e - .0025\delta_t$

FOR $\delta_f = 50°$

	δ_t^o	δ_e^o	$C_{L_{MAX}}$
STABLE	-33.5	-6	1.48
UNSTABLE	+34.5	+10°	2.12

FOR $\delta_f = 0°$

STABLE	-34	+8	1.23
UNSTABLE	+39	+12	1.74

technology" and corresponding projected improvements in avionic equipment, use of carbon brakes and radial tires (reflected in "structure" savings-- other than wing), a reduced crew and associated service, and the more modern propulsion represented by 2 GE36D engines plus 8 bladed counter- rotating 12.5' diameter swept propellers (de-rated thrust at 100 kt = 2 × 17000 lb). The column 2 weights shown for the APU, avionics, furnishing and equipment, air conditioning and anti-icing are consistent with those given in Ref. 19 for these items.

The third column represents further improvements, due to composite materials and construction, in the wing, nacelle, and control surface weights; and due to a reduction in payload from 16000 to 7500 pounds. The final column is for the unstable version which has a reduced wing area (.70 × 4000 = 2800 ft²) reflecting, of course, the increased maximum C_L's shown in Table 2. The affected weights are those for the smaller wing, surface controls and hydraulic systems, as derived from the following considerations.

The various applicable wing weight formulas of Refs. 22,23 yield values of .679, .765 and .84 for the ratio of the 2800 to 4000 ft² wing weights. However, the formulas do not reflect span loading effects, being

TABLE 6. ESTIMATED WEIGHTS

	YB-49	STABLE ADV TECH(Aℓ)	STABLE COMPOSITE	UNSTABLE COMPOSITE
Structure	41746	36901	30277	24994
Wing	23285	23285	17613	12330
Propulsion	23383	11731	---	---
Systems & Equipment	23891	14345	13465	11857
Surface Controls	4313	3613	2733	1913
APU	907	907	---	---
Instruments	832	532	---	---
Hydraulic	3082	2586	---	1798
Electrical	2058	1658	---	---
Avionic	6623	2512	---	---
Furnish-Equipment	4640	2000	---	---
Air Conditioning	1049	349	---	---
Anti-Ice	387	188	---	---
Weight Empty	89020	62977	55473	48582
Crew	1675	900	---	---
Crew Service	2450	1000	---	---
Crew Container	1050	0	---	---
Operating Weight	94195	64877	57373	50482
Payload	16000	16000	7500	7500
Weight Empty	110195	80877	64873	57982
Total Fuel	83948	113266	129270	136161
Ramp Weight	194143	---	---	---

rather fits to statistical, historic data. Because the fuel load is about 5.2% higher for the smaller unstable version (column 4) and the span is only 83% as long, the distributed span loading will be denser and the resultant load relief higher. Accordingly, we would expect somewhat lower weight ratios by some 5% to 10% than those listed; and applying such correction places the above median value near 0.70, the ratio of wing areas.

RANGE/ENDURANCE COMPUTATIONS

Figure 3 is an initial cut at determining maximum range. It shows incompressible L/D and M_{CR} L/D vs both M and C_L for the stable (solid) and unstable (dashed) variants. The most significant maximum values are those for $(M_{cr}L/D)_{max}$ which are listed below

M_{CR} L/D	C_L	
17.088	.34	stable
17.079	.36	
17.683	.36	unstable
17.685	.38	

These values of C_L are used to determine and to plot the variation of cruise altitude with weight shown in Fig. 4. In this case δ is the atmospheric pressure ratio $p(h)/p_0$. This plot graphically illustrates that the smaller wing, unstable version has a cruise altitude deficit of about 6000-7000 ft. In fact, the max range calculation shortly to follow assumes that the minimum cruise altitude is 35,000 feet as indicated by the dotted vertical line.

Figure 5 is an example plot of the compressible M L/D vs M/M_{CR} for the stable, C_L-0.34 case. This plot is typical and illustrates that the maximum range-relevant (compressible) ML/D-15.663 occurs for M/M_{CR} between 1.00 and 1.005.

Table 7 is the max range computation using the foregoing results, a 3% weight allowance for initial climb to 35K ft in 200 miles of range, weight empty for end of cruise, and a nominal specific fuel consumption,
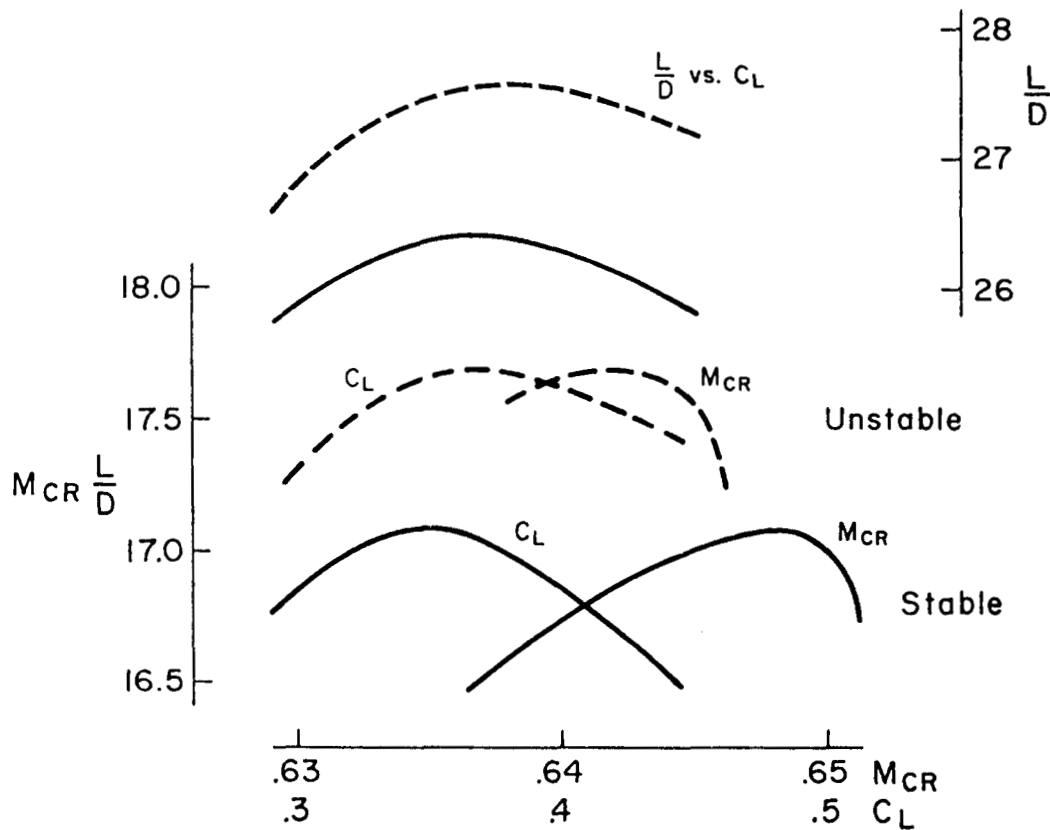
18

Figure 3. Incompressible L/D and $M_{CR}L/D$

c=.368, (from Kentron). Accordingly the stable range, corresponding to the cruise altitudes of Fig. 4 is 30,125 mi as shown.

For the unstable case, the initial segment at a constant 35K ft is above the best cruise altitude (Fig. 4) and is flown at constant M=0.65 for the conditions tabulated and weights ranging from 188,319 at end of climb to 150,000 lbs where 35K ft is the optimum cruise altitude. From 150,000 lbs to weight empty =64900 lbs the remaining range is at increasing cruise altitude as shown in Fig. 4. The total range, shown in Table 7, 34,392 mi is a 14% increase over the stable case.

Table 8 is the max Endurance Calculation. The altitude chosen, 20,000 ft, is not in keeping with the originally described "high altitude" mission, but it yields greater endurance because of the better specifics due to the lower cruise Mach numbers at lower altitudes. Later calculations for the lightly loaded RPV versions will be at high altitude.
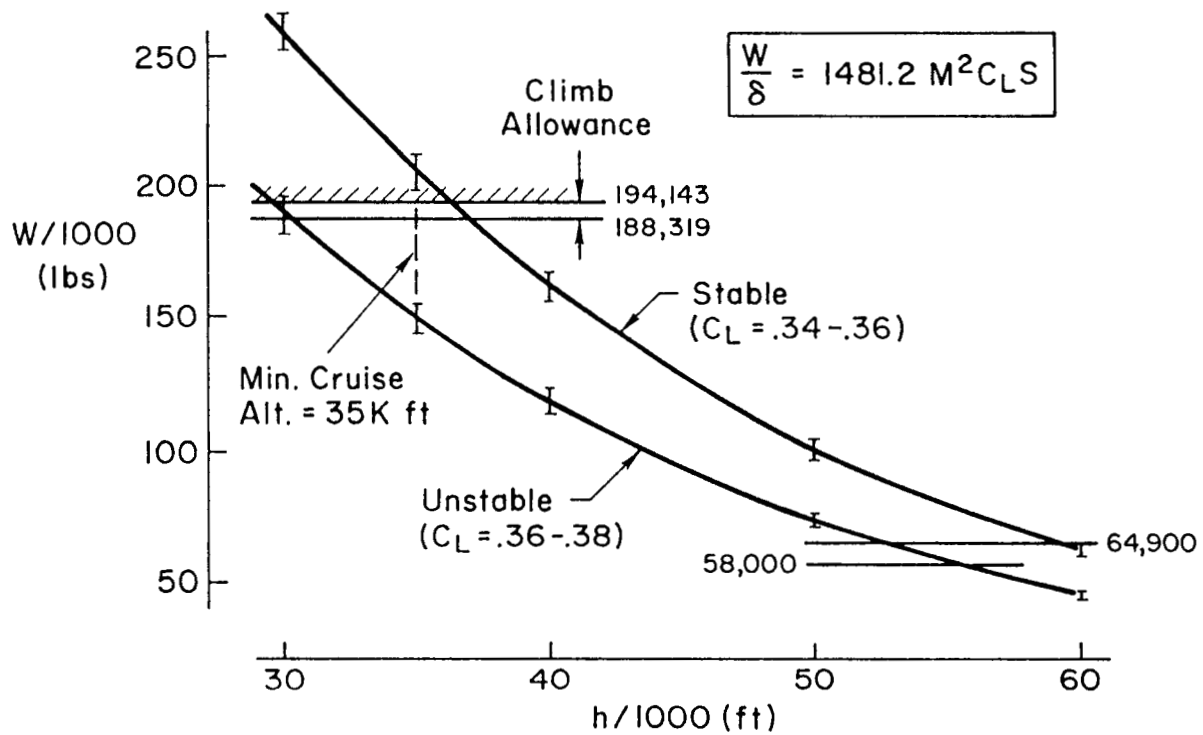
$$\boxed{\dfrac{W}{\delta} = 1481.2 \, M^2 C_L S}$$
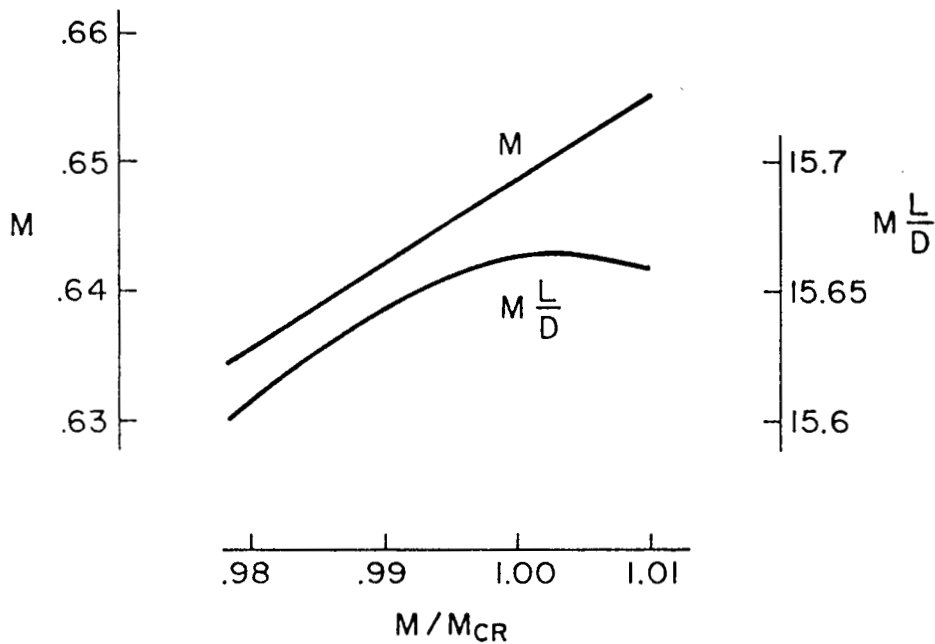
Figure 4. W vs h for Maximum M_{CR} L/D

Figure 5. Typical M, Compressible L/D vs M/M_{CR}
Stable, $C_L=0.34$

20

TABLE 7. MAX RANGE

Assume $.03 W_{TO}$ — fuel to climb to 35,000' in 200 mi (Ref. 19)

W_1 = start cruise weight = .97 (194143) = 188319 lbs

W_2 = weight empty (no allowance) = 64900 stable, 58000 unstable

c_{nom} = .368 for similar M and altitude

For Range at cruise altitude:

$$R = a \frac{M}{c} \frac{L}{D} \ln \frac{W_1}{W_2} + 200$$

Stable $= \frac{660}{.368} \; 15.663 \; \ln \frac{188319}{64900} = \underline{30,125 \text{ mi}}$

Unstable - initial segment at 35K ft is above alt for best range; fly at:

$$M = \text{const} = 0.65$$

W/1000	c_L	$c_{D_{inc}}$	M/M_{CR}	M L/D	ΔR
188.32	.457	.0168	1.0245	15.766	
180	.436	.0159	1.0209	15.971	1286.0
170	.412	.0150	1.0180	16.055	1642.4
160	.388	.0141	1.0153	16.129	1749.7
150	.364	.0132	1.0125	16.221	1872.3

The remaining cruise alt range + climb allowance is:

$$\frac{660}{.368} \; 16.221 \; \ln \frac{150,000}{58,000} + 200 = 27842$$

$$\text{Total} = \underline{34392 \text{ mi}}$$

21

TABLE 8. MAX ENDURANCE AT 20,000 FT

$$C_L = 0.37 \qquad \frac{C_D}{C_{D_{inc}}} = 1.00 \qquad \frac{L}{D} = 26.39/27.59$$

$$M^2 = \frac{W}{1,007,305} \text{ (stable)} = \frac{W}{705114} \text{ (unstable)}$$

$$\Delta t = \left(\frac{1}{c}\frac{L}{D}\right)_{avg} \ln \frac{W_i}{W_{i+1}}; \qquad c = \frac{c}{c_{nom}} \times .368$$

W/1000	M		c/c_{nom}		Δt	
	STABLE	UNSTABLE	STABLE	UNSTABLE	STABLE	UNSTABLE
194.143	.439		.869			
		.522	(.8675	.932)$_{av}$		
190	.434		.866		1.78	1.74
		.498	(.8525	.9135)$_{av}$		
160	.399		.839		14.45	14.10
		.453	(.824	.8797)$_{av}$		
130	.359		809		18.07	17.70
		.404	(.7925	.843)$_{av}$		
100	.315		.776		23.74	23.33
		.349	(.757	.800)$_{av}$		
70	.264		.738		33.79	33.43
			(.734)$_{av}$			
64.9	.253		.730		7.39	
		.301		(.766)$_{av}$		18.41
58						
Total Endurance (hours)					99.22	108.71

Getting on with Table 8, max L/D's as listed occur at about $C_L=0.37$ (Fig. 3) for both stable and unstable cases. The tabulated computations, using the relationships above the table, are for the weight progression shown and proceed from the cruise Mach number to the value of $c/c_{nom}(M)$, as given by the Table 6 equation, to the time increment, Δt. The c/c_{nom} values in parenthesis are averages for weights halfway between those tabulated; and these were used to compute Δt. For the stable case these were obtained by averaging c/c_{nom} for the starting and ending weights (and M) in a given weight range, and they are shown interpolated between such values. For the unstable case we simply computed M and c/c_{nom} for the average weight a priori; hence only the parenthetical c/c_{nom}'s are shown.

Notice that the higher M's for the unstable smaller wing area increase c/c_{nom} so that the endurance for given weight increments is smaller than that for the stable case. However the smaller final (unstable) weight takes over at the end and produces a net increase in endurance of about 9.5%.

LIGHT WEIGHT RPV VERSIONS

To expand the scope of the study we also examined light weight HALE RPV type configurations for the same wing areas: 4000 and 2800 ft^2 respectively for stable and unstable conditions at a takeoff gross weight of 30,000 lb each. As the acronym implies, HALE RPVS are remotely operated unmanned reconnaissance vehicles which carry fixed surveillance payloads to high altitude, remain on station hopefully for days, return to base and land intact, requiring only refueling for the next mission. Weight Breakdowns for the stable, 4000 ft^2 wing are shown in the first column of Table 9. These weights are based on ratios of various items to gross weight for the heavy manned version as "verified" by comparison with similar Ref. 14 ratios. For example, the Table 3, column 3, structure plus surface controls is about 17% of the T.O. (ramp) weight. A similar ratio is "achieved" in Ref. 14, although landing gear is apparently not included, and the wing aspect ratio is 20 (Fig. 1) vs a modest 7.4 for the YB-49 planform. Neglecting these opposing differences for the time being, the structural weight in the first column is shown as 0.17×30,000 = 5100 lbs. The propulsion fraction in Table 3 is .0604 and this translates to

TABLE 9. WEIGHT ESTIMATES FOR RPV VERSIONS

TOGW = 30,000 LBS

Based on Ref. 14 and heavy version weight ratios, and corrections to reflect the weight breakdown, given in an unpublished Northrop HALE study (Dec. 1987).

	EST'D FROM WT RATIO	DIRECT FROM REF. 15
Structure	5100	4846
Fuel Tank	--	520
Propulsion	1812	2709
Avionics	581	200
Landing Gear	incld'd	450
Actuators	--	360
Payload	1578	1500
Deicing	368	--
Weight Empty	9439	10585

add 1500 lbs our estimate = 10939 (4000 FT^2)

Reduce wing, control surface and
hydraulic system weights (3870) by 25%   9968 (2800 FT^2)

*S = 3761, b = 230', AR = 14.1, $\Lambda_{1.e.}$ = 30°, all-moving 14' winglets

the 1812 lbs shown in Table 9; for comparison the propulsion weight in Ref. 14 is 1690 lb although this does not include an 8 blade counter rotating propeller. The deicing, avionics and payload are taken directly from Ref. 14 to yield a total (first column) of 9439 lbs.

The second column in Table 9 shows the weights estimated in the above cited HALE study for the configuration described in the Table 9 footnote. Considering the differences, especially in power plant, fuel tank, and landing gear weights, it was decided to add 1500 lbs to the column 1 estimate as indicated. Accordingly the stable (4000 ft^2) version zero fuel weight is 10,939 lbs. For the unstable (2800 ft^2) case the wing, control surface and hydraulic system weights are scaled down by 25% to yield a zero fuel weight of 9968 lbs.

Maximum Range/Endurance considerations listed in Table 10 need a little expansion as follows:

1. self-evident

2. at optimum cruise altitudes between 57K and 83K ft, root chord RN's vary from 12 to 4x10^6 which theoretically allows 60% NLF

3. 60% NLF would theoretically reduce drag more than the 20 counts assumed, which is therefore slightly conservative

4. although we are talking paper engines, flight at 83K for the scaled down engines seems an unconservative "hope"

5. therefore both range and endurance were computed at 60,000 ft, and one engine cruise (other engine feathered), to increase the power absorbed by the propeller, for weights less than 15,000 lb; the feathered prop drag coefficients (Ref. 18, referred to wing area) are shown for stable/unstable versions.

Endurance Computations shown in Table 11 start with the max L/D column which shows the decrease due to feathered prop drag at 15000 lbs. The corresponding C_Ls for best L/D are .310 and .322 (30,000-15,000 lbs) and .322 and .338 (below 15,000 lbs). The succeeding columns show the corresponding loiter Mach number, the relative specific fuel consumptions per the Table 6 equation, and finally the endurance time increments. The

TABLE 10. RPV-TYPE MAX RANGE/ENDURANCE CONSIDERATIONS

1. Lower wing loading leads to higher cruise altitudes.
2. Resulting Reynolds Numbers (RNs) are appropriate for Natural Laminar Flow (NLF).
3. Accordingly reduce C_{D_o} by .0020 each configuration.
4. Optimum cruise altitudes→ 83k ft at end of flight -- probably too high for good propulsion power/thrust.
5. Assume 60k ft for endurance and range; further, fly one engine (prop feathered) from mid to final weight to raise power. Increases drag by .00039/.00056 for W < 15000 lb.

TABLE 11. RPV TYPE ENDURANCE AT 60K FT

W/1000	(L/D) STABLE	(L/D) UNSTABLE	M STABLE	M UNSTABLE	c/c_{nom} STABLE	c/c_{nom} UNSTABLE	Δt STABLE	Δt UNSTABLE
30	31.29	32.72	.48	.56	.900	.960		
25			.44	.51	.870	.923	17.52	17.23
20			.39	.46	.833	.885	22.42	21.95
15			.34	.40	.795	.840	30.05	29.67
15	30.13	31.00	.33	.39	.788	.833		
10.939			.27		.743		33.79	
9.968				.32		.780		42.69
TOTALS							104.23	111.54

$$\Delta t = \frac{L/D}{.368(c/c_{nom})_{av}} \, \ell n \, \frac{W_i}{W_{i+1}}$$

26

latter show, as for the heavy manned version (Table 8), that the unstable version only catches up at the end because of its larger fuel fraction (lower final weight). The endurance advantage of the unstable case is about 7.3%.

Range at 60,000 ft is compared in Table 12 which displays some of the components of the range calculations, again assuming one-engine operation for W<15000 lb. The big advantage accruing to the unstable, smaller-wing case — some 23% improvement — is partly due, of course, to the fuel fraction advantage i.e., $\frac{\ln(28.2/9.968)}{\ln(28.2/10.939)} -1 = 9.8\%$. The remaining 13% or so is due to differences in $\frac{M\ L/D}{C/C_{nom}}$ which, for a typical condition (in this case 15,000 lb with one feathered prop) is made up of the following increments for the ratio of unstable to stable values:

$\qquad$ +12% for increased M

$\qquad$ -4% for increased c/c_{nom}

$\qquad$ -.18% for increased $C_D/C_{D_{inc}}$ due to increased M/M_{CR}

$\qquad$ +6% for increased incompressible L/D

$\rule{4cm}{0.4pt}$

$\qquad$ +13.8% for increased $\dfrac{M\ L/D}{c/c_{nom}}$

Best Cruise Range. Some of these differences, e.g., in M, are due in part to a mismatch in altitude for the stable case. When the altitude is allowed to increase with decreasing weight so that both configurations always cruise at best ML/cD the range comparisons (at the bottom of the last column) show "only" a 14 1/2% advantage for the unstable case; almost identical to the Table 7 comparison for the manned versions. Remembering that about 10% of this is due to the improved fuel fraction (above) leaves only about 4%, which is directly traceable to the difference in incompressible L/D. That is, both best cruise cases occur at $M \doteq .617$, $C_L = 0.30$, and $M/M_{CR} \doteq .95$ so $C_D/C_{D_{inc}}$, c/c_{nom} and M are the same; and differences in $\frac{M\ L/D}{c/c_{nom}}$ are due only to $(L/D)_{inc}$. Note that the effect of c/c_{nom} variation with M, considered negligible for the manned version Range computation, reduces "best" M/M_{CR} from 1.0025 in Fig. 5 to 0.95 in the present case. Also there is, of course, a difference in cruise altitude

TABLE 12. RPV VERSION RANGE AT 60k ft

Assume 400 mi climb to 60,000' uses fuel = .06 W;
feather one prop for W < 15,000 lbs

best range conditions

W/1000	M		C_L		$\dfrac{M\ L/D}{c/c_{nom}}$		ΔR	
	STABLE	UNSTABLE	STABLE	UNSTABLE	STABLE	UNSTABLE	STABLE	UNSTABLE
28.2	.519	.566	.25	.30	16.917	18.860		
21.6	.463	.532	.24	.26	15.738	17.913	7811.7	8796.8
15	.403	.461	.22	.24	14.096	16.257	9760.5	11179.0
15	.394	.443	.23	.26	13.399	15.289		
12.2	.356		.23		12.542		4808.8	
11.000		.395		.24		13.910		8125.2
10.939	.340		.22		12.058		2408.0	
9.968		.375		.24		13.778		2447.3

$$\Delta R = \frac{660.34}{.368} \left(\frac{M\ L/D}{c/c_{nom}}\right) \ell n \frac{W_i}{W_{i+1}} \text{ miles}$$

Max Range = 400 + $\Sigma \Delta R$ =

25189	30948

For continued 2-engine operation at best cruise altitude

Range =

31736	36383

28

with about a 7000 ft advantage accruing to the stable, larger-wing, ver-
sion version which starts at 71K ft.(vs64) and ends at 91K ft(vs85). This
same altitude difference also applies to the manned versions as depicted
in altitude difference also applies to the manned versions as depicted
in Fig. 4. On the whole there is satisfying consistency between the
manned heavy, and the RPV, light versions except for the "constrained"
60,000 ft. altitude comparison.

TAKE-OFF PERFORMANCE

The reduced wing area for the unstable configuration(s) is predicated
on achieving the same take-off (T.O.) performance, for given T.O. weights
and thrusts, by virtue of maintaining constant wing area x max C_L. In
this regard, take-off rather than landing is deemed more critical because,
for the latter, the unstable case has a reduced landing weight for the
same wing area x max C_L. Accordingly we compared only take-off per-
formance to ascertain whether the reduced wing area, unstable version was,
in fact, equivalent in critical T.O. performance.

The thrust variation entering into the take-off calculation was com-
puted using the Ref. 18 propeller data and the Kentron study shaft horse-
power, de-rated somewhat, to allow a 12.5' diameter propeller for the
manned versions. The T.O. thrust variation with speed was estimated from
applicable data in Ref. 18 as $T = 41,447-44 \ V_{fps}$.

Drag and Lift coefficients were computed for control surface deflec-
tions corresponding to trim ($C_M=0$) at 1.2V stall, equivalent to
Max $C_L/1.44 = .85$(stable), 1.21(unstable), where the landing gear pitching
moment increment, modifying the Table 2 equation for C_M, is (Ref. 5)
$\Delta C_M = .011(4000/S)^{3/2}$. For the ground run, the C_L due to α was set to
zero and the trim increments in C_L computed according to the Table 5 equa-
tion for MAX_{C_L}. A landing gear drag increment, $\Delta C_D = .0190(4000/S)$ was
added to the basic, Ref. 5, $C_{D_{inc}} = .0070 + .051 \ C_L^2 + .000030 \ \delta_e^2 +$
$.000017 \ \delta_t^2$ which was used for both stable and unstable versions. For
the trim conditions (inset) in Figs. 6 and 7, the corresponding ground
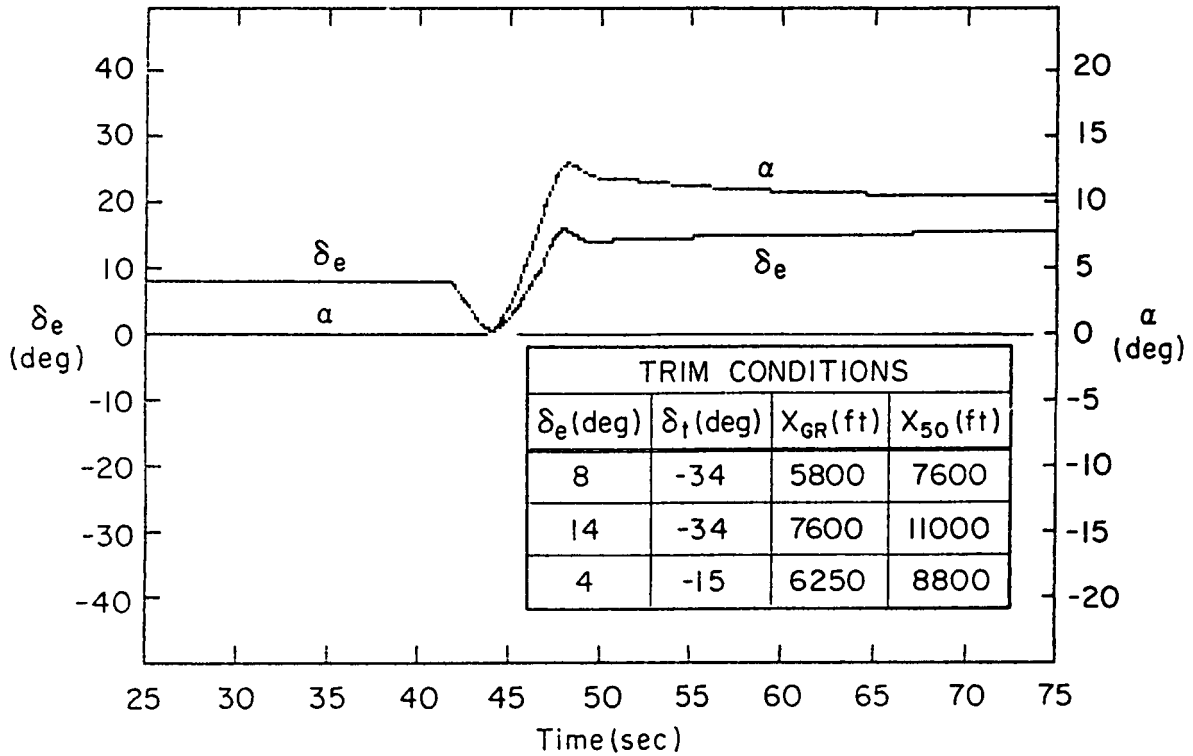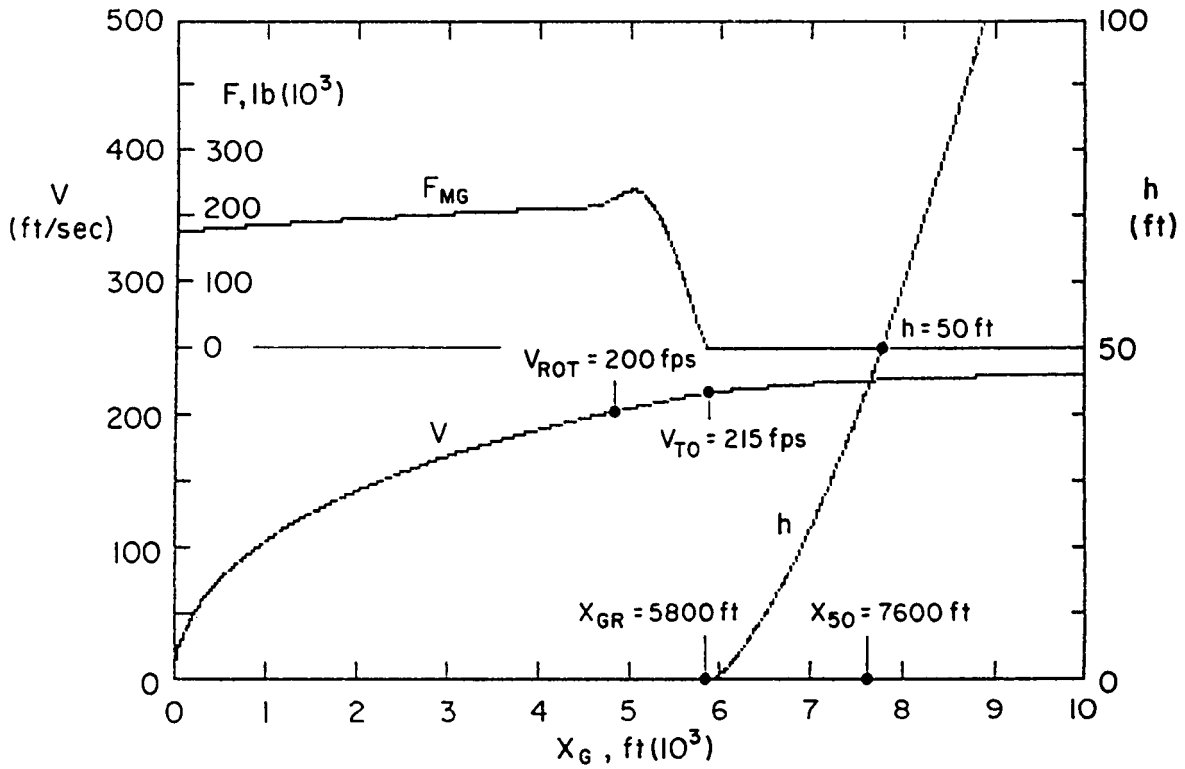roll lift and zero-lift drag coefficients are:

Figure 6. Takeoff Performance (Stable Configuration)
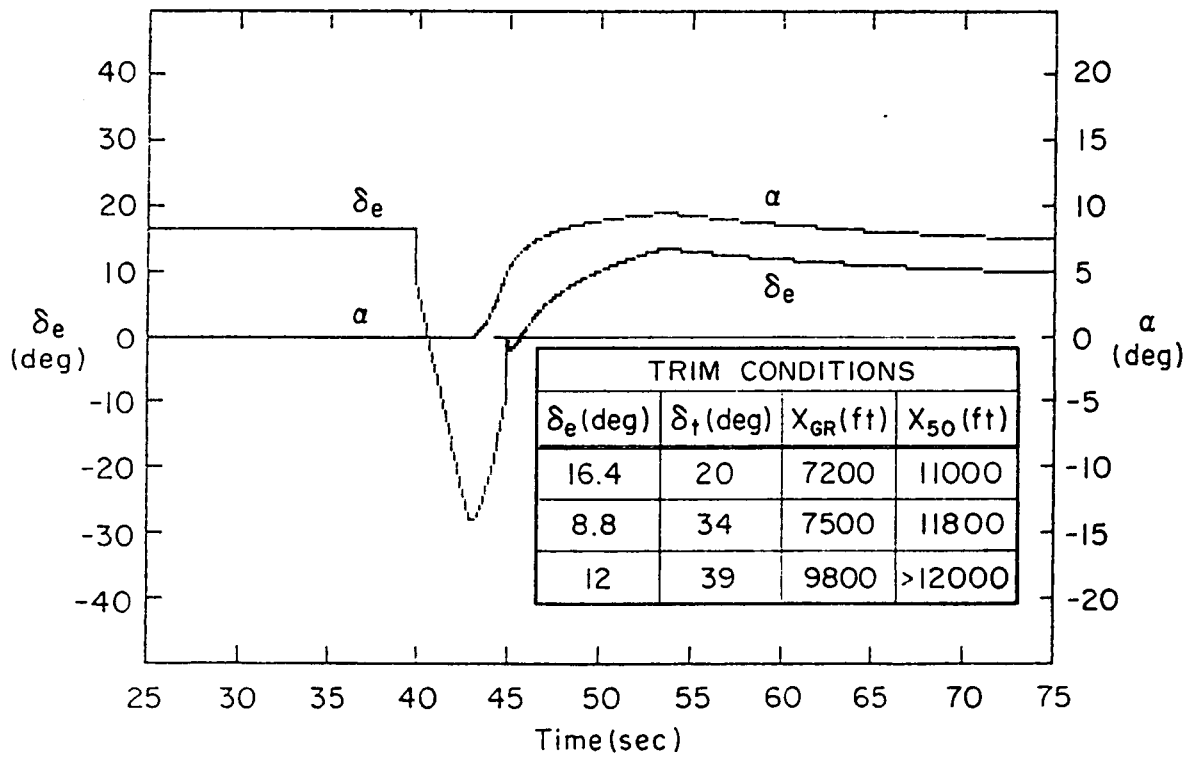$\delta_{e_{trim}} = 8^{\circ}$, $\delta_t = -34^{\circ}$

30
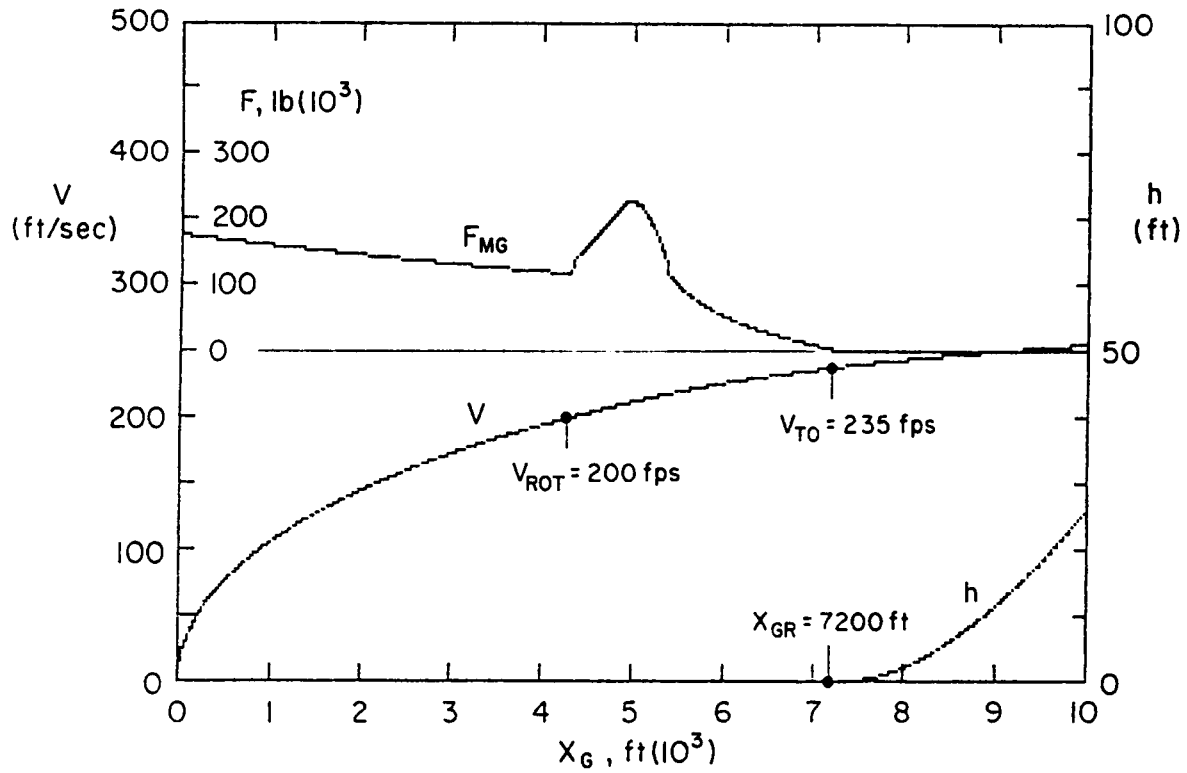
Figure 7. Takeoff Performance (Unstable Configuration)
$\delta_{e_{trim}} = 16.4°$, $\delta_t = 20°$

31

	δ_e	δ_t	$C_{L_{gnd}}$	C_{D_o}
Fig. 6 Stable	8	-34	-.1144	.0476
	14	-34	-.0370	.0516
	4	-15	-.0444	.0303
Fig. 7 Unstable	12	39	.4044	.0643
	8.8	34	.3311	.0561
	16.4	20	.3396	.0490

The first of the above-tabulated conditions in each set corresponds to trim at max C_L with the landing gear retracted which represents one extreme of the possible trim variants. The remaining two conditions in each set are for trim at $1.2V_s$ with gear extended as stated above. The rolling friction coefficient was fixed at 0.02.

Figure 6 displays take-off performance for rotation, initiated by a $10°$ pitch command ramp (5 sec) to the AFCS (discussed later), at V=200 fps corresponding to about $1.1V_s$. The upper plot displays main gear reaction force, speed buildup, and altitude vs the ground distance traveled. The lower plot shows the variation of α and δ_e with time. For the example trim condition plotted, the T.O. distance to clear fifty feet is 7600 ft. The importance of selected trim condition is shown in the tabulated ground roll and fifty foot clearance distances. From the corresponding ground roll C_L's and C_{Do}'s tabulated above it can be appreciated that the X distances tabulated are not quite in the order of the drag coefficients, although the distances to rotation speed (not given in Fig. 6) are: 4700', 4850', and 4200' for the order given in Fig. 6. The differences in X distances following rotation are apparently due to differences in lift buildup as influenced by the $\delta_e(t)$ time history. For the first tabulated trim condition the lift first exceeds weight at about 47.5 sec corresponding to the Fig. 6 peak δ_e at about the same time. However, for the last tabulated trim set (which has lower C_{Do} and X_{rot} distance), the lift $\geq$ weight condition occurs later at about 50.0 sec and the δ_e trace does not overshoot but rather flares into, the final trim value.

For Fig. 7 which is a similar set for the unstable vehicle, the δ_e variation with time is smooth and exponential-like (as illustrated) for

32

all cases so that the performance shown is more governed by the basic drag coefficients than by variations in lift-off elevator timing. Thus the tabulated X distances increase with increasing values of the above-listed C_{Do}s.

Figure 8 shows what happens if we take advantage of the self-trimming capacity of the unstable, AFCS-stabilized version and reduce all trim settings during the take-off roll to zero. The corresponding zero lift drag is calculated to increase after rotation by not only the induced drag proportional to $C_L^2(\alpha,\delta)$ but also by the parasite drag increase due to δ_e^2 (which is not a significant contribution) as indicated. The result is a spectacular improvement in performance, reducing the best of the Fig. 7, 50 foot clearance distances, 11,000 ft, to 6500 ft. A corresponding zero trim calculation for the stable case (not presented) actually showed a performance deterioration apparently due to the long δ_e "tail," fairing into the final trim value at about 56 seconds; the corresponding X distances are about 100 to 200 ft. longer than the worst in the Fig. 6 table. Note that for the "good" performance plotted both in Fig. 6 and in Fig. 8, the rapid lift buildup due to the positive δ_e rotation and overshoot provides fast liftoff in about 5 sec., which, incidentally is the time for the 10° pitch command to ramp up.

Figure 9 illustrates the zero trim take-off for the lighter (30,000 lb) unstable RPV case. Despite the disproportionately lower T/W (T - 4950-5.25V), the 50 ft. clearance height is achieved in about 2100 ft. due, of course, to the much reduced wing loading.

A significant feature of both Figs. 8 and 9 is the rapid and large positive elevator deflection which contributes directly to the rapid lift buildup and short take-off performance. The point is, take-off performance may not be crucial for the RPV versions (depending on available field lengths); but the similarities between Figs. 9 and 8 argue that regardless of a large range in weights and wing loadings, it is possible to achieve similar or better take-off performance with a smaller wing, deliberately unstable (relaxed static stability) configuration.
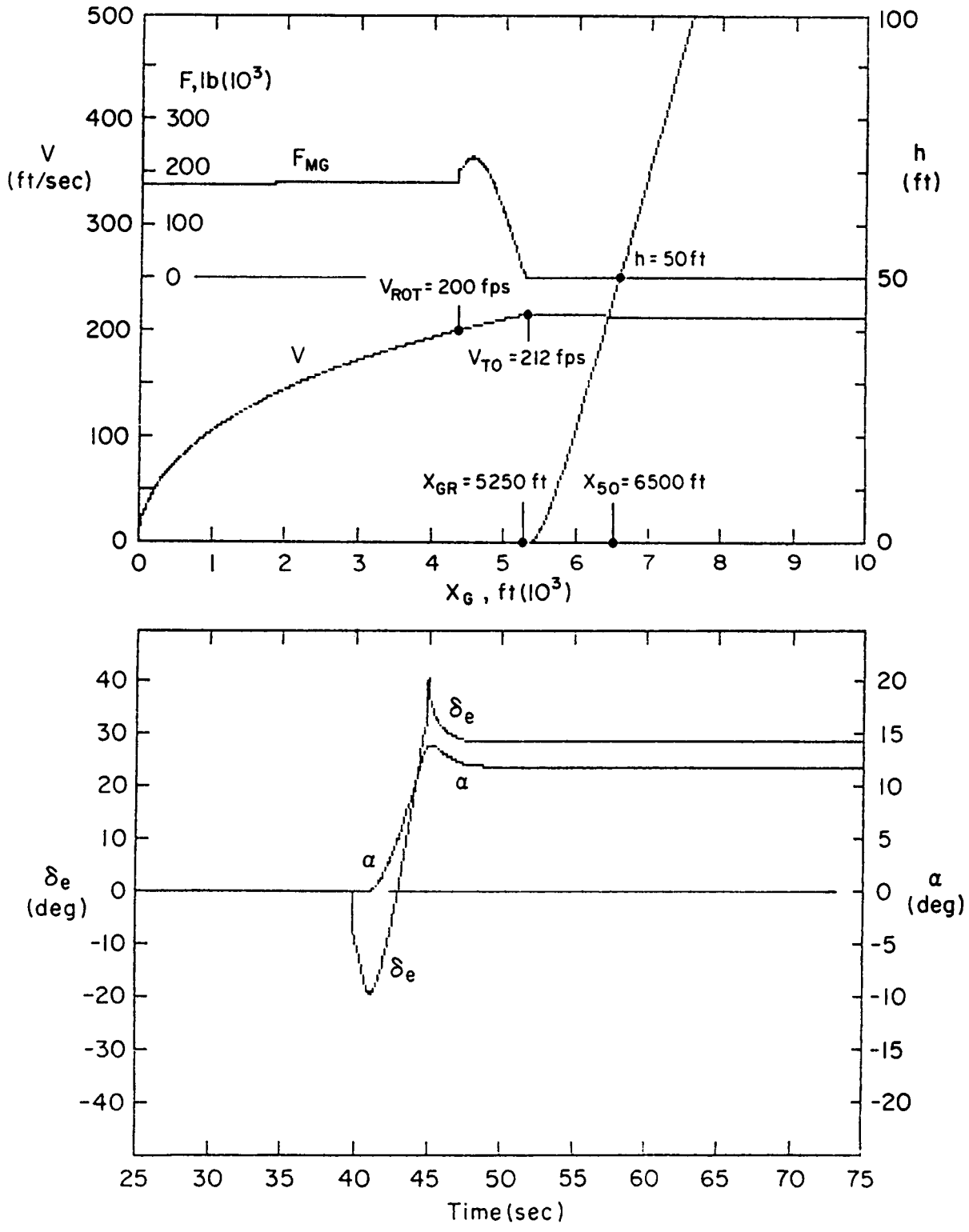
Figure 8. Takeoff Performance (Unstable Configuration)
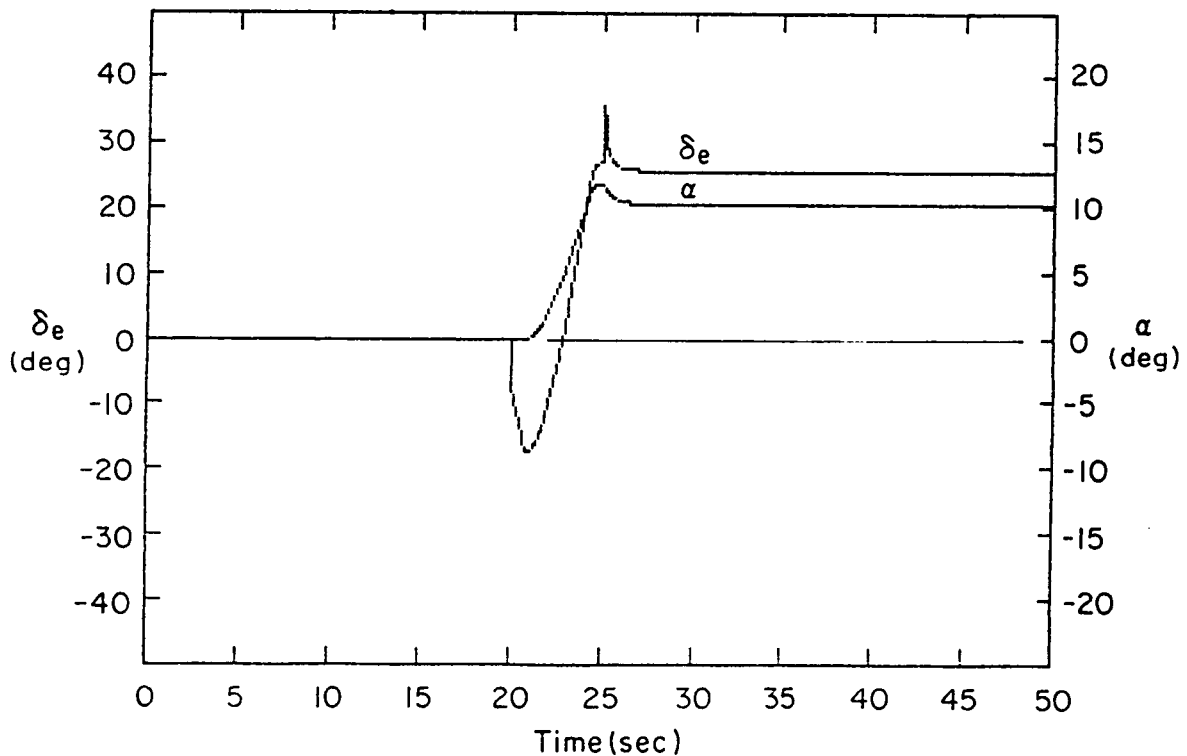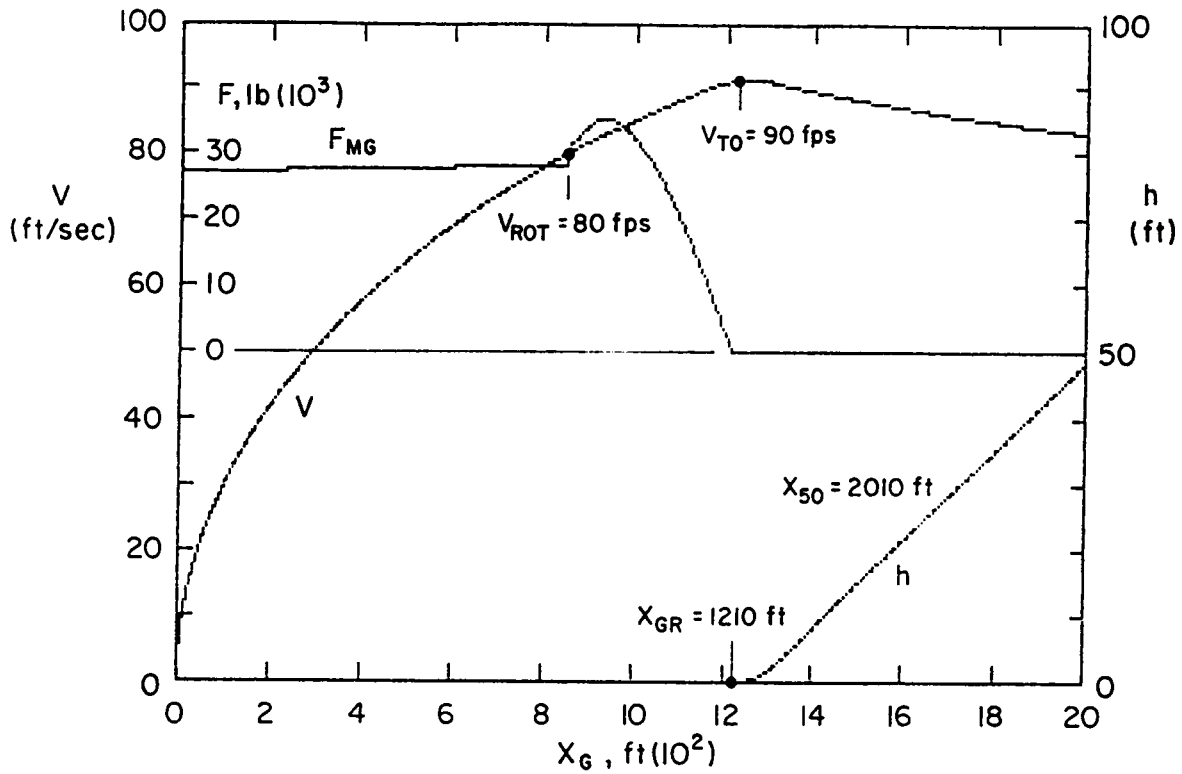$\delta_{e_{trim}} = 0$, $\delta_t = 0$, with δ_e^2 drag component

34

Figure 9. Takeoff Performance (RPV Unstable Configuration)

$\delta_{e_{trim}} = 0$, $\delta_t = 0$, with δ_e^2 drag component, $T_o = 4950$ lbs

$T = 4950 - 5.25\ V$

STABILITY AND CONTROL CHARACTERISTICS

The stability and control derivatives in coefficient form were estimated/computed and are given in Appendix A. These data were utilized together with inertial and geometric parameters to compute dimensional derivatives and control input transfer functions as given in Appendix B. The longitudinal transfer functions for landing were combined with a second order actuator model ($\zeta = .707$, $\omega = 12$ rad/sec) and used to determine suitable longitudinal AFCS feedbacks and gains as follows:

$$\text{Stable} \qquad \delta_e = 2\theta + q = q(\frac{s + 2}{s})$$

$$\text{Unstable} \qquad \delta_e = 3.5 \ (\frac{s + 1.73}{s})q$$

These are, in fact the control laws used in the above-discussed take-off computations. Their effect for landing on the longitudinal characteristic frequencies, dampings, etc., are as follows:

		ω_{sp} $\begin{bmatrix} 1/T_{sp_1} \end{bmatrix}$	ζ_{sp} $\begin{bmatrix} 1/T_{sp_2} \end{bmatrix}$	ω_p $\begin{bmatrix} 1/T_{p_1} \end{bmatrix}$	ζ_p $\begin{bmatrix} 1/T_{p_2} \end{bmatrix}$
Stable					
	FCS off	1.11	.533	.197	.127
	FCS on	1.92	.446	.248	.99
Unstable					
	FCS off	(-.745	1.501)	.237	.231
	FCS on	2.52	.786	(.103	.935)

Figures 10 and 11 show the time history responses to step θ commands for the augmented stable and unstable versions respectively. The altitude responses at the cg and pilot's station for the unstable configuration are faster for either location by at least a factor of 2. That is, the flat spot or effective time delay is about 1/2 to 3/4 sec for the unstable, and about 1-1/2 seconds for the stable case. The latter is close to that shown in Ref. 27 for a "current jet transport, so neither response is bad," however, for larger, higher inertia tailless aircraft (e.g. SST) the
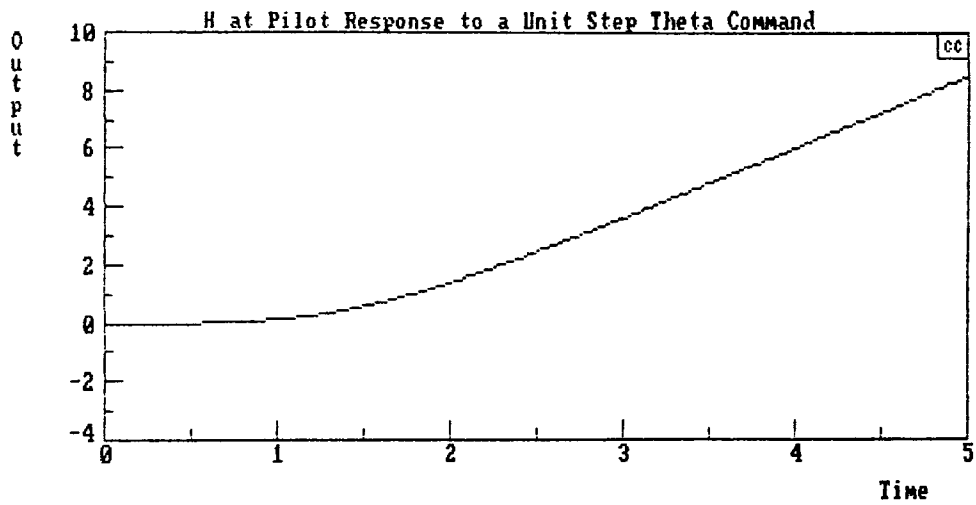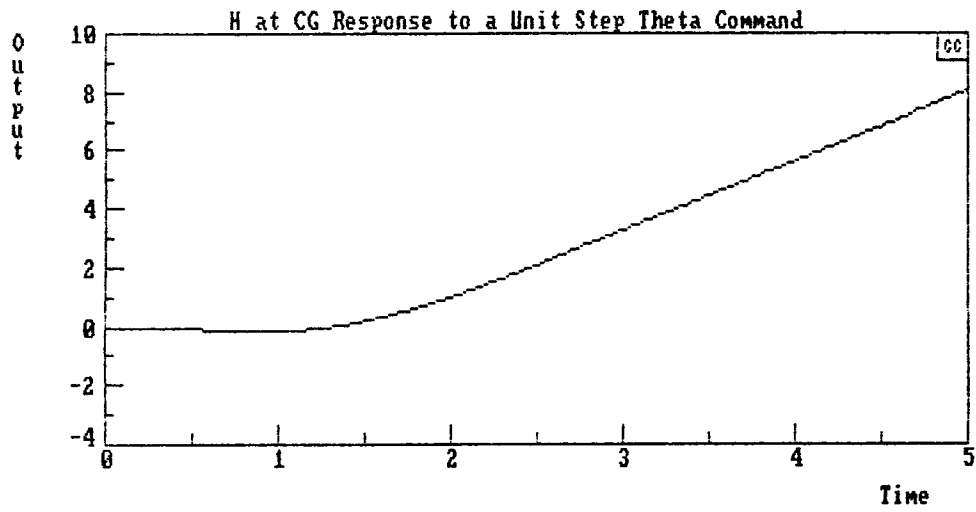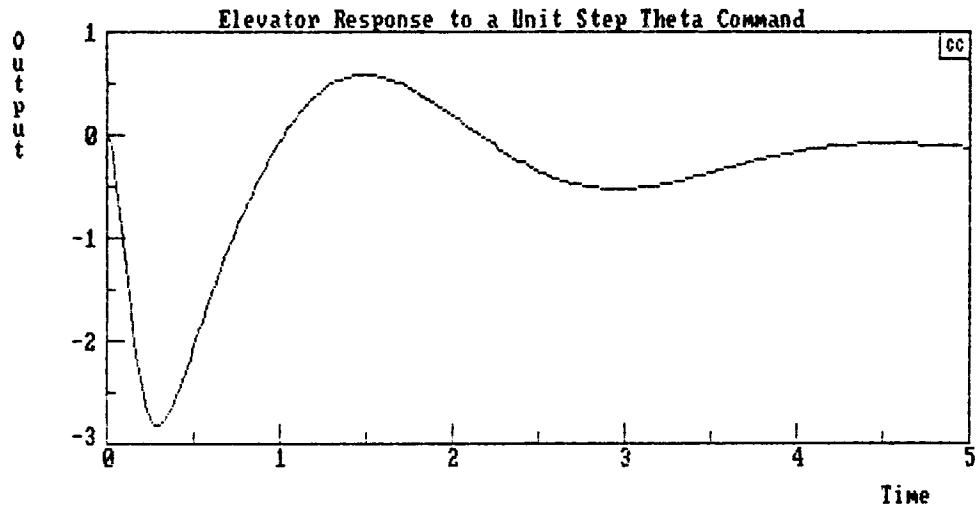
36

Figure 10. Responses to Step Theta Command
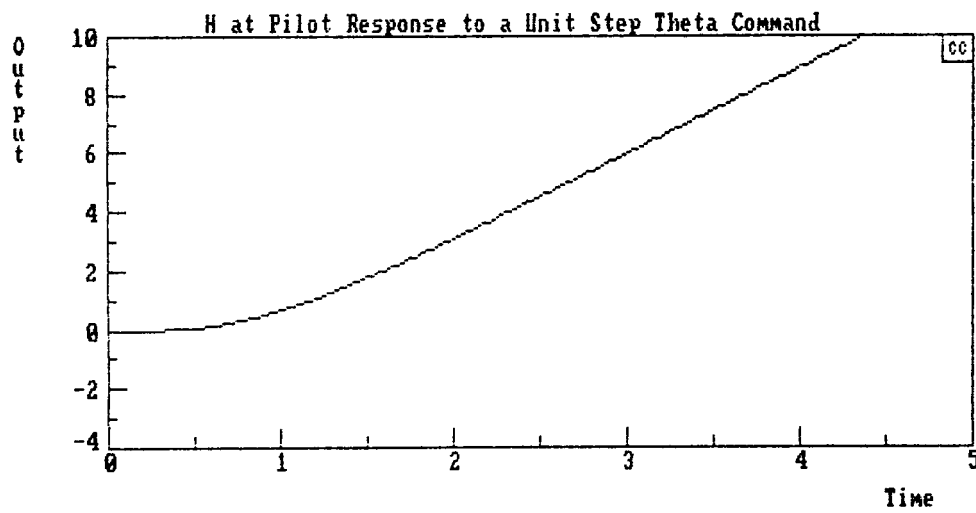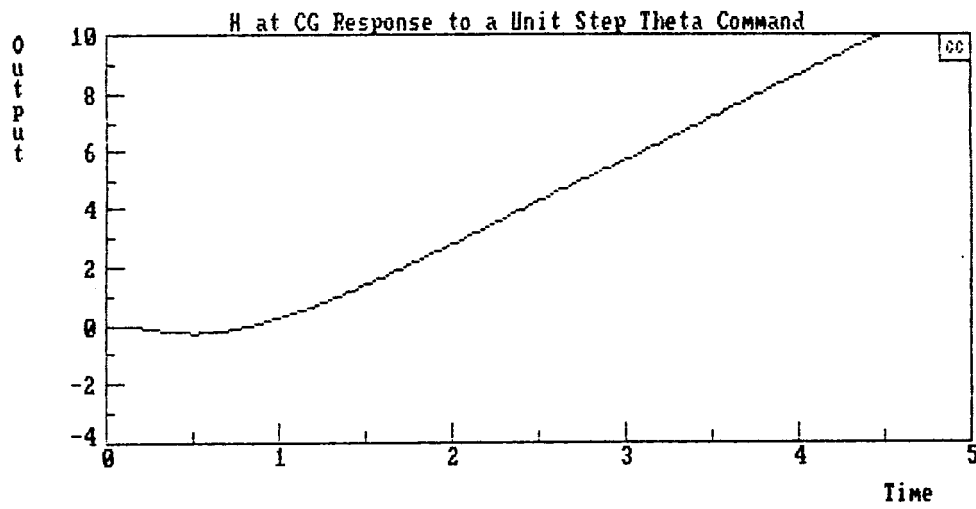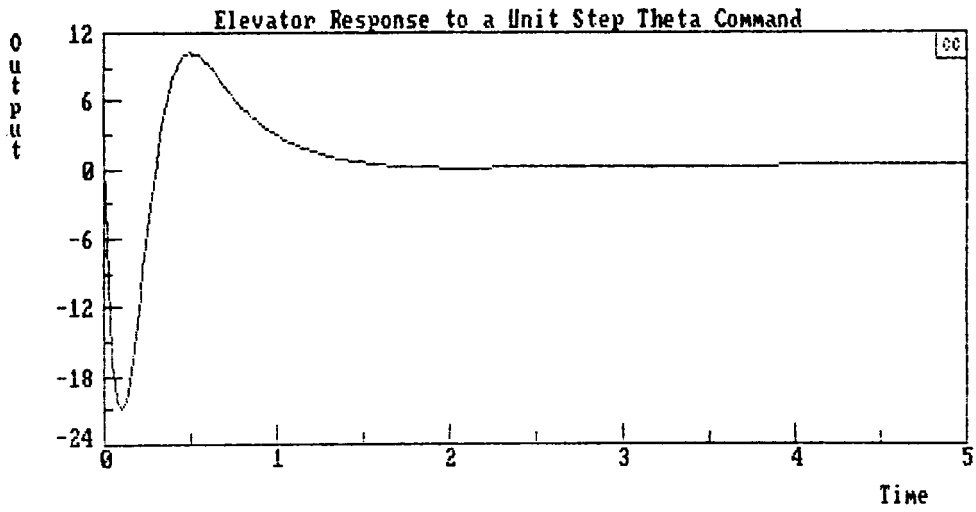Stable Configuration

Figure 11. Unstable Configuration

two fold reduction afforded by the RSS version could be crucial to good handling. The elevator traces show that the difference is due to the strongly positive elevator pulse, and attendant direct-lift contribution, for the unstable case.

Table 13 displays the values of the aileron yaw parameter, ω_ϕ/ω_d as collected from the computed ϕ/δ_a transfer functions in Appendix B: The differences between the stable and unstable versions, are due primarily to the values of $Cn_{\delta a}$ as affected by the negative/positive trim surface settings estimated from the data in Ref. 17 and documented in Appendix A. The already marginal values for the stable case are pushed into the definitely poor region (Ref. 21) for the unstable version. Good flying qualities in this regard would demand an aileron-to-rudder crossfeed to counter the aileron yaw; but rudder power is already marginal for the YB-49-type (double split flap) drag rudder assumed as shown below.

Table 14 computes the thrust offset yawing moment for loss of an engine just beyond lift-off speed. Despite the "tight" engine lever arm assumed (10' for a 12.5' propeller) and the omission of windmilling or even feathered propeller drag, the required percentage of available rudder power approaches 90% for the unstable case as opposed to slightly more than 50% for the stable configuration. This difference is directly ascribable to the (scale)^3 effect of the smaller wing and control surfaces for the constant thrust, propeller diameter etc., needed to obtain comparable cruise and take-off performance.

TABLE 13. CRUISE $\omega\phi/\omega_d$

C_L = .36 ± .01			$\omega\phi/\omega_d$	
			STABLE	UNSTABLE
W = 194,000	h = 40,000		.836	.723
		20,000	.786	.719
= 65,000/58,000		20,000	.764	.698

TABLE 14. RUDDER FOR ENGINE OUT T.O.

$$W = 194{,}000 \qquad C_L = .7\, C_{L_{max}}$$

$$V = 237 \text{ fps}$$

$$T = 17{,}000 \text{ lbs}$$

$$\Delta C_n = \frac{T}{W}\, C_L\, \frac{y}{b}$$

	STABLE	UNSTABLE
$C_{L_{max}}$	1.04	1.48
ΔC_n	.00368	.00626
δ_r	.526	.894

$$\delta_r \text{ available} = 1.00$$

Table 15 further illustrates the rudder control-power problem with estimates/computations of the trimmable (β-o) crosswind at $1.2V_s$ for the landing weights shown. Note that these computations cover both the manned and RPV versions, with figures for the latter given in parenthesis. The values shown for β are the maximum trimmable with: full rudder, subscript r (the same for both manned and RPV); full asymmetric thrust $\Delta T = 17{,}000/$ (2300) lbs, subscript T; and for both full rudder and asymmetric thrust, $\Sigma\beta$. The corresponding trimmable crosswinds are shown for the combined rudder and thrust, and for the rudder only. For the latter, the trimmable maximum crosswind in a wingdown sideslipping approach, is 10 ± 1.2 kt for the manned, and $4.2 \pm .5$ kt for the RPV, version; with the positive and negative increments accruing to the stable and unstable versions respectively. Using maximum asymmetric thrust and full rudder raises the allowable crosswinds to 38.2 ± 3.9 kts for the manned, and 13.6 ± 9 kts for the RPV, version, with the positive and negative increments now accruing to the unstable and stable versions respectively. That is, the unstable versions are more controllable with combined thrust and rudder and less controllable with rudder alone. This is consistent with the fact that constant thrust moments are more effective on the smaller shorter-span wing; and rudder is less effective because of the higher C_L-related values of $C_{n\beta}$, $C_{\ell\beta}$. The big difference between the RPV and manned versions is

40

TABLE 15. YAW TRIM IN CROSSWINDS FOR FLAPPED WING AT 1.2 V_s

BASIC DATA -- FROM REF. 4*

$$\beta = \frac{-\Delta C_{n_T} - C_{n_{\delta_r}} \delta_r{}^{\neq}}{C_{n_\beta} - C_{\ell_\beta} \dfrac{C_{n_{\delta_a}}}{C_{\ell_{\delta_a}}}}$$

$$\Delta C_{n_T} = \frac{\Delta T}{W} C_L \frac{y}{b}$$

landing weight includes $\underline{1000}$ lb reserve
$\phantom{\text{landing weight includes }}(600)$

	STABLE	UNSTABLE
C_L	1.04	1.48
C_{ℓ_β}	-.060	-.100
C_{n_β}	.045	.065
$C_{\ell_{\delta_a}}$	.048	
$C_{n_{\delta_a}}$	-.033	-.0058
$C_{n_{\delta_r}}$	.007	
$C_{n_\beta} - C_{\ell_\beta} \dfrac{C_{n_{\delta_a}}}{C_{\ell_{\delta_a}}}$	.0413	.0529
W	65900 (11500)	59000 (10500)
ΔC_{n_T}	.0156 (.0121)	.0296 (.0225)
(full rudder = 1 rad) β_r	.170	.132
β_T	.377 (.293)	.560 (.425)
$\Sigma\beta$	.547 (.463)	.692 (.557)
1.2 V_s kt =	66(28)	
max V_x kt	34.3 (12.8)	42.1 (14.5)
rudder only V_x kt	11.2 (4.8)	8.7 (3.7)

*trim δ_e and propeller effects not included

$\neq$assumes $C_{\ell_{\delta_r}} = 0$

due to the lower wing loading and reduced landing speed (28 vs 66 kts) of the former.

Operational viability would seem to require the use of some asymmetric thrust for reasonable conventional crosswind landing capability; rudder alone is marginal to inadequate.

Table 16 is a check on the aileron power and bank angle requirements for the same (Table 15) landing conditions. The final result is that for maximum values of δ_a limited to $\pm 15^\circ$ (remember that the mid-span elevon serves as both elevator and aileron and elevator is first priority), the maximum trim values of β are .42 and .25 rad which translate to allowable crosswinds of 26.9(11.4) and 16.3(6.9) knots for the stable and unstable cases respectively. These values are lower than those shown in Table 15 for max V_x although exceeding those shown for rudder only V_x. We conclude therefore that the sideslip conditions corresponding to full asymmetric thrust, as assumed in Table 15, are untenable from the standpoint of available aileron roll control, which will limit maximum crosswind conditions, using partial asymmetric thrust, to the values shown above. Finally, the values of ϕmax shown in Table 16, appear to be sufficiently low (because of inherent low side forces) so that possible wing tip ground contact during landing operations will not be a problem.

The calculations in Table 17 are intended to roughly delineate the magnitude of the yaw control problem during rapid rolls. As shown in the first equation (for yaw balance) the rudder must be able to counter at least the aerodynamic yawing moments due to rolling motions and aileron inputs. Inertial and kinematic coupling effects are neglected in this simple approximation because products of inertia are small for flying wing aircraft, and rolling is about the velocity vector. To the extent that the aero balance can be "perfect" there will be little β excitation during rapid turn entry and exit. Once the desired bank angle is achieved, the yawing moment due to yaw rate, $r = g/U_o \phi$, takes over, but this is seldom as crucial a problem as the rapid roll. Accordingly, we substitute the single-degree of freedom approximation for the roll parameter, $pb/2U_o$, to obtain the simple (third equation) relationship between the δ_a input and the δ_r required at the peak p response in the turn entry/exit maneuver.

42

TABLE 16. AILERON, BANK LIMITS IN STEADY CROSSWINDS FOR FLAPPED WING AT 1.2 V_s

		STABLE	UNSTABLE
	c_L	1.04	1.48
BASIC DATA REF -- FROM REF. 4	$c_{y_\beta}^*$	-.184	-.235
	c_{y_β}	-.265 (-.236)	0.351 (-.310)
$\dfrac{\delta_a}{\beta} = \dfrac{-c_{\ell_\beta}}{c_{\ell_{\delta_a}}}$	c_{ℓ_β}	-.060	-.100
	$c_{\ell_{\delta_a}}$	.048	
	$-\delta_a/\beta$	1.25	2.08
$\dfrac{\phi}{\beta} = -\dfrac{c_{y_\beta}}{c_L}$	ϕ/β	.255 (.227)	.237 (.209)
for $\delta_{a_{max}} = 30^\circ$(.524 rad),	β_{max}	.42	.25
	max V_x kt	26.9 (11.4)	16.3 (6.9)
	ϕ_{max}	6.1 (5.5)	3.4 (3.0)

*propeller effects included in the next row, amount to $-\Delta C_{y_\beta} = .0518$ and .0746 for RPV, and 1.56 × these for heavy, versions.

TABLE 17.   YAW SUPPRESSION IN RAPID ROLLS

$$C_{n_p} \frac{pb}{2U_o} + C_{n_{\delta_a}} \delta_a + C_{n_{\delta_r}} \delta_r = 0$$

$$\frac{pb}{2U_o} \doteq \frac{C_{\ell_{\delta_a}} \delta_a}{-C_{\ell_p}}$$

$$C_{\ell_{\delta_a}} \delta_a \left(- \frac{C_{n_{\delta_a}}}{C_{\ell_{\delta_a}}} + \frac{C_{n_p}}{C_{\ell_p}}\right) = C_{n_{\delta_r}} \delta_r$$

$$.048\delta_a \underbrace{(+ 0.2 + .332)} = .007\delta_r$$

some "typical" large values

$$\frac{\delta_r}{\delta_a} = 3.65$$

allowable $\delta_a \quad = \frac{60^o}{3.65}$

$$= 16.4^o$$

The numerical values shown for the ratios Cnδa/Cℓδa and Cnp/Cℓp are, as indicated, typical large values for fairly high C_L's (.7 $C_L$max — .86 stable, 1.22 unstable) as shown in Appendix A. Both of these parameters are very difficult to estimate with any accuracy so the values chosen are deliberately shaded to the high side to avoid over-optimism. The final result shows that the permissable maximum value of δ_a which can be balanced by full rudder is 16.4° which is only a little more than half of the (30°) available. That is, the maximum aileron input (and resulting roll rate) must be limited to 55% of that available. Possible differences between the unstable and stable cases are within the accuracy of this rough calculation which is therefore considered applicable to both.

RESULTS, CONCLUSIONS AND OBSERVATIONS

The foregoing results are collected and summarized below in two categories; significant quantitative Conclusions regarding performance and control/handling improvement or degradation and Observations which explain and generalize the results and conclusions

Conclusions

1.   An unstable flying wing configuration, flying at best cruise altitude, shows a 14% improvement in range over a stable configuration for either a manned (heavy) or RPV (light) version; maximum endurance at given constant altitudes are increased by 9% to 7% for the unstable case.

2.   Trim surface deflections during ground roll have a large effect on takeoff performance. Best unstable takeoff was achieved with zero trim and, following rotation, the automatic increasing C_L due to stabilizing, positive δ_e motions (akin to direct lift control). The 50' obstacle distance improvement, over the stable version is about 15%.

3.   The unstable version shows improved height response to elevator control because of similar positive δ_e motions which reduce the apparent delay to about 1/2 that of the stable case.

4.   The unstable configuration has higher adverse yaw than the stable because of the downward trimmed elevon surface. The resulting values of $\omega_\phi/\omega_d \doteq 0.7$ accentuate the aileron-induced Dutch roll excitation, and will probably be critical from the standpoint of Level 1 Flying Qualities.

5.   Rudder control for loss of an engine at Take-off, holding $\beta = 0$, is marginal, (89% of capacity) for the unstable and quite comfortable (53%) for the stable version (partly a consequence of the relatively small thrust offset $\approx 10'$). However, a delay in applying corrective, rudder could lead to dynamic overshoots which would require larger deflections thereby eroding both margins and making the unstable version definitely critical.

6.   Rudder only control in crosswind conditions appears totally inadequate for either configuration. The rudder saturates at very low β, with the unstable 22% lower than the stable case. Adding asymmetric thrust, as might be possible for landing operations, offers good potential improvement, with the unstable now some 25% better, but leaves aileron power as the limiting factor, with the unstable now some 40% worse than the stable case. The maximum trimmable β's for

the unstable condition go from .132 radians for rudder only to .692 for rudder plus asymmetric thrust to .25 for the aileron limit (see Tables 15 and 16). The latter translates to allowable crosswinds of only 16.2 and 6.9 knots respectively for the manned heavy and RPV light cases; and does require full rudder plus some asymmetric thrust for yaw balance.

7. Rudder control in rapid rolls, which may not be required operationally, is inadequate to allow use of more than 55% of aileron power.

Observations

1. The differences in RSS range improvement for the flying wing, 14% vs 4% for conventional configurations, can be traced primarily to increases in max C_L for the former. This permits a direct reduction in wing area and associated weight vs a reduction in tail area for the conventional case. Both cases offer C_D improvements, the conventional due to the smaller tail, the flying wing due to positive camber.

2. Best cruise altitudes for the stable version are about 7000' higher than for the higher wing loading unstable version.

3. The weight-favorable span-distributed payload characteristic of the heavy manned version would be difficult to achieve for the RPV version. In this regard, the absolute weights estimated for the latter may be optimistic, but the relative weight differences due to RSS are probably representative.

4. The allowable degree of RSS instability is limited by an assumed requirement of .08 rad/sec^2 nose down control for stall recovery. Removal or reduction of this requirement would allow smaller wings and greater improvement of RSS performance; however control limitations and problems could be exacerbated (see below).

5. Because of the direct-lift effect of downward trim (noted above in Conclusion 2), takeoff performance for the unstable version, set up to be equal on the basis of stalling speed, was actually better (15%) than for the lower wing loading stable version. Taking advantage of this effect would permit further wing area reduction and concomitant additional weight and performance improvement. If landing rather than take off were critical, the RSS reduced weight empty (Table 3) could be invoked for similar further reductions (11%) in wing area.

6. Because the study was conducted for only a nominal cg location for each version, the issue of nose wheel lift-off for maximum forward cg did not arise. However, the unstable is better than the stable version in this regard because there is more nose-up pitch control power available due to down or zero, rather than up, elevator carried for take-off trim.

7. The shortened delay in altitude response for the RSS version is not particularly significant since the longer delay for the stable case is still considered satisfactory. However for larger, higher inertia aircraft where such delays do become critical, the reduction factor of almost 2 for the unstable case would offer significant handling improvement.

8. The "poor" values of $\omega\phi/\omega d$ discussed for the unstable case can, of course be improved by crossfeeding aileron to rudder to modify the "effective" value of $C_{n_{\delta_a}}$. However, as noted earlier, rudder power is in short supply and such usage could exaggerate the general rudder control problem. Moreover, finite values of the difficult to estimate rudder cross-control parameter, $C_{\ell_{\delta_r}}$, assumed zero for this study, reduce the effectiveness of the crossfed rudder.

9. Control power deficiencies of the unstable, over the stable, version are due to the higher takeoff and landing C_Ls; and to the positive (downward) deflected trailing edge surfaces. Both these effects contribute to higher estimated static and rotary stability, and cross-control, derivatives.

10. However, the prediction of wing geometry and trailing edge control surface deflection effects on wing-only yawing and rolling derivatives is not in good shape. CFD codes to do this are apparently non-existent; and analytic-empirical methods are quite incomplete and not well supported by experimental data. This may also be true for the incremental zero-lift and lifting drag contributions of trailing edge surface deflections.

11. The above conclusions and observations regarding marginal rudder power are for a double split flap drag rudder occupying approximately the outer 20% span of a 7.4 aspect ratio wing (see Fig. 2). Longer rudder span, and other types of rudders, e.g., all movable wing tips, could conceivably increase rudder power somewhat but probably by less than a factor of 2. Increasing aspect ratio but keeping rudder percent span constant is not effective because rudder area x lever arm is proportional to Sb which means that the rudder effectiveness in coefficient

form, $C_{n_{\delta r}}$, remains essentially unchanged by changes in aspect ratio. Accordingly, any improvement in rudder control due to increased aspect ratio would have to come from <u>reductions</u> in the most critical, but not too well understood, yawing derivatives C_{n_p} and $C_{n_{\delta a}}$. On the other hand, the ΔC_n due to differential thrust would definitely be reduced — bad for crosswind control but good for engine loss at T.O.

12. A more refined unstable flying wing would encompass distributed camber and twist to provide self-trimming (zero trailing edge deflections) at cruise, and ideal lift distribution to minimize induced drag. The technology to do this is currently available.

13. The foregoing conclusions and observations apply in kind, if not totally in degree, to all tailless aircraft as noted in the Introduction and Summary. The control-related problems are then most appropriate where the tailless type in question is configured as a low observable with minimum control appendages. The flying wing then becomes a limiting best/worst case for all such aircraft.

An overall conclusion of the study is that the promise of considerably improved range and endurance performance for an RSS, over a normally stable, flying wing configuration, <u>is</u> realizable; that take-off performance is comparable to better, depending on control surface trim settings; and that the delay in altitude response on landing approach is cut in half. On the debit side, rudder power, generally crucial for any flying wing, or low observable tailless aircraft, is more marginal for the unstable RSS version; aileron control-power, also marginal for crosswind control is more so for the RSS version.

RECOMMENDATIONS FOR FURTHER STUDY

1. The requirement of .08 rad/sec^2 nose down control for stall recovery, which limits the degree of allowable instability, should be explored for its applicability to low pitch inertia all-wing and tailless aircraft.

2. The DLC-like automatic stabilizing, downward δ_e motions which improve unstable take-off performance and landing path response, should be further studied to determine their general handling and operational applicability and suitability.

48

3.   Because of low $C_{y\beta}$, flight at $\beta \neq 0$ is a possible option for the one-engine cruise postulated for the latter portions of the long range cruise. The performance and handling aspects of such operation, perhaps akin to the oblique wing, need exploration if the concept is deemed viable after preliminary studies.

4.   In the same vein, and reflecting the common rudder deficiency problem, the practical possibilities of non side-slipping (i.e., yawed) approach and the details of the accompanying final landing maneuver and control power required should be explored in an operational and handling context. (Of course a non-maneuvering landing using a castoring crosswind landing gear is a <u>design</u> possibility.)

5.   The generally deficient rudder control problem, itself, deserves further consideration and study to establish limits of achievable control power for possible new (as yet undiscovered) or old types of effectors.

6.   Of course the Item 5 rudder power problem is intimately tied to the uncertainties in the wing rotary and control derivatives, e.g., C_{n_p}, $C_{n_{\delta a}}$, C_{n_r}, $C_{\ell_{\delta r}}$. Methods of estimation and computation for these derivatives, especially as influenced by trailing edge surface deflections, should be initiated and diligently pursued (see Item 10 "observation").

Note that the last 4 recommendations are important whether or not the flying wing or tailless fighter aircraft is to be flown in an RSS or normally stable mode.

REFERENCES

1. Hanks, Glen, Henry Shomber, et al., _Selected Advanced Aerodynamics and Active Control Technology Concept Development_, Boeing Commercial Airplane Co. D6-49363, Sept. 1981.

2. Hays, A. P., W. E. Beck, W. H. Morita, et al., _Integrated Technology Wing Design Study_, NASA CR-3586, August 1982.

3. Sizlo, T. R., R. A. Berg and D. L. Gilles, _Development of a Low-Risk Augmentation System for an Energy-Efficient Transport Having Relaxed Static Stability_, Douglas Aircraft NASA CR-159166, Dec. 1979.

4. Koerner, W. G., _Dynamic Lateral Stability YB-49 Model_, Northrop Aircraft Inc., Report A-119, Mar. 1949.

5. Friend, C. G. and I. L. Ashkenas, _Aerodynamic Characteristics of XB-35 and YB-49 All-Wing Airplane Configurations_, Northrop Aircraft, Inc., Report A-88, Oct. 1947.

6. Amann, John R., and R. L. Cardenas, _Phase II Tests of the YB-49 Airplane_ USAF No. 42-102368, Flight Test Division AMC Memo Report CRFT-2156, Sept. 1948.

7. Stevens, Victor I. Jr., and G. M. McCormack, _Power Off Tests of the Northrop N9M-2 Tailless Airplane in the 40-by-80-Foot Wind Tunnel_, NACA MR A4L14, Dec. 1944.

8. Campbell, John P., and C. L. Seacord Jr., _Determination of the Stability and Control Characteristics of a Tailless All-Wing Airplane Model with Sweepback in the Langley Free-Flight Tunnel_, NACA Wartime Report (WR-L-50), Feb. 1945.

9. Anon, _Description Dimensions and Leading Particulars (of YB-49)_, Excerpts from Document _Bureau of Aeronautics_, AN 01-15EAB-2, 1949.

10. Hauser, George H. Jr., and R. E. Schlech, _Stability and Control Flight Tests of the YB-49 Airplane_, USAF No. 42-10236, HQAMC Memo Report MCRFT-2280, June 1950.

11. Maloney, Edward T., "Northrop Flying Wings," _World War II Publications_, Library of Congress Card 74-25469, ISBN No. 0-915464-0-4, 1980.

12. Letko, William and David Feigenbaum, _Wind Tunnel Investigation of Split Trailing-Edge Lift and Trim Flaps on a Tapered Wing with 23° Sweepback_, NACA TN 1252, July 1947.

REFERENCES (CONCLUDED)

13. Donlan, Charles J., _An Interim Report on the Stability and Control of Tailless Airplanes_, NACA Report 796, Aug. 1944.

14. Henderson, Campbell, Edward McQuillen, _High Altitude Long Endurance RPV Design Technology Study_, NADC-85060-60, Mar. 1985.

15. Abbott, Ira H., A. E. Von Doenhoff, L. S. Stivers Jr., _Summary of Airfoil Data_, NACA Report 824, 1945.

16. Toll, Thomas T., and M. J. Queijo, _Approximate Relations and Charts for Low Speed Stability Derivatives of Swept Wings_, NACA TN-1581, May 1948.

17. Rogallo, F. M., _Collection of Balanced-Aileron Test Data_, NACA Wartime Report (ACR) 4A11, Jan. 1944.

18. Black, D. M., R. W. Menthe, and H. L. Wainauski, _Aerodynamic Design and Performance Testing of an Advanced Eight Bladed Propeller at Mach Numbers from 0.2 to 0.85_, NASA CR-3047, Sept. 1978.

19. Jernell, Lloyd S. and C. B. Quartero, _Design of a Large Span-Distributed Load Flying Wing Cargo Airplane_, NASA TM X-74031, Apr. 1977.

20. Ribner, Herberts, _Formula for Propellers in Yaw and Charts of the Side-Force Derivative_, NACA Report 819, 1945.

21. Hoh, Roger H., David G. Mitchell, I. L. Ashkenas, et al., _Proposed MIL Standard and Handbook, Flying Qualities of Air Vehicles_, AFWAL TR 82-3081, Vol-I, Vol-II, Nov. 1982.

22. Stinton, Darrol, _The Design of the Airplane_, Van Nostrand Reinhold Co., N.Y., N.Y., 1983.

23. Nicolai, Leland M., _Fundamentals of Aircraft Design_, METS, Inc. San Jose, CA, 1975.

24. Hoerner, S. F., _Fluid-Dynamic Lift_, Hoerner Fluid Dynamics, Great Britain, 1975.

25. Roskam, Jan, _Methods For Estimating Stability and Control Derivatives of Conventional Subsonic Airplanes_, Roskam Aviation and Engineering Corporation, Kansas, 1971.

26. Seckel, Edward, _Stability and Control of Airplanes and Helicopters_, Academic Press, New York-London, 1964.

27. Kehrer, W. T., "Longitudinal Stability and Control of Large Supersonic Aircraft at Low Speeds," ICAS Paper No. 64-586, Aug. 1964.

APPENDIX A
STABILITY & CONTROL DERIVATIVES

LONGITUDINAL DERIVATIVES

1. $C_{L\alpha}$

For an XB-35 type aircraft, the wing effect dominates $C_{L\alpha}$

$C_{L\alpha} \approx C_{L\alpha_W}$

$C_{\ell\alpha} = \dfrac{[1.3 - (-.8)]}{[12° - (-8°)]} = 0.105/\text{deg} = 6.016/\text{rad} \leftarrow$ NACA $65_3\text{-}018$

(a) [Ref 24]

$C_{L\alpha_W} = \left[10 + \dfrac{20}{AR} + \dfrac{9}{AR^2}\right]^{-1} \times \dfrac{C_{\ell\alpha}}{0.100}$

$\qquad = \left[10 + \dfrac{20}{7.4} + \dfrac{9}{(7.4)^2}\right]^{-1} \times \dfrac{0.105/\text{deg}}{0.100} = 0.0816/\text{deg}$

$C_{L\alpha} = 4.68/\text{rad}$

(b) [Ref 15]

$C_{L\alpha_W} = f\left[\dfrac{a_e}{1 + (573a_e/\pi AR)}\right], \quad f(AR, TR) = f(7.4, 0.25) = 1.00$

$C_{L\alpha_W} = 1.00\left[\dfrac{0.105/\text{deg}}{1 + (57.3)(0.105)/\pi/7.4}\right] = 0.0834/\text{deg}$

$C_{L\alpha} = 4.78/\text{rad}$

(c) [Ref 25]

$\kappa = \dfrac{C_{\ell\alpha}}{2\pi} = \dfrac{6.016/\text{rad}}{2\pi/\text{rad}} = 0.957$

$\beta \approx 1$, No Mach Number Effects

$C_{L\alpha_W} = \dfrac{2\pi AR}{2 + \sqrt{\dfrac{AR^2\beta^2}{\kappa}\left(1 + \dfrac{\tan\Lambda_{c/2}}{\beta^2}\right) + 4}}$

(c) continued

$$C_{L\alpha_W} = \frac{2\pi(7.4)}{2 + \sqrt{\frac{7.4^2}{0.957^2}\left(1 + \frac{\tan(23.17°)}{1}\right) + 4}}$$

$$C_{L\alpha} = 4.06/\text{rad}$$

This result may be most valid, since it takes into account the sweep of the wing.

2. $C_{m\alpha}$

(a) <u>The stable configuration</u>

$$C_{m\alpha} = C_{L\alpha} SM$$

$$C_{m\alpha} = (4.06/\text{rad})(-.05)$$

$$C_{m\alpha} = -.203/\text{rad}$$

Using the average of the two higher $C_{L\alpha}$ values

$$C_{m\alpha} = (4.73/\text{rad})(-.05)$$

$$C_{m\alpha} = -.237/\text{rad}$$

(b) <u>The unstable configuration</u>

$$C_{m\alpha} = (4.06/\text{rad})(0.08)$$

$$C_{m\alpha} = 0.325/\text{rad}$$

or...

$$C_{m\alpha} = (4.73/\text{rad})(0.08)$$

$$C_{m\alpha} = 0.378/\text{rad}$$

3. C_{m_q} [Ref 25]

$$C_{m_q} = C_{m_{q_W}} + C_{m_{q_H}} \quad \nearrow^{\emptyset, \text{ No Tail}} \qquad ; A = AR = \text{Aspect Ratio}$$

$\beta \approx 1$

$$C_{m_{q_W}}\bigg|_M = C_{m_{q_W}}\bigg|_{M=0} \left[\frac{\dfrac{A^3 \tan^2 \Lambda_{c/4}}{A\beta + 6\cos\Lambda_{c/4}} + \dfrac{3}{\beta}}{\dfrac{A^3 \tan^2 \Lambda_{c/4}}{A + 6\cos\Lambda_{c/4}} + 3} \right]^{\nearrow 1}$$

$$C_{m_{q_W}}\bigg|_{M=0} = -K C_{\ell_{\alpha_W}} \cos\Lambda_{c/4} \left[\frac{A\left[2\left(\frac{x_w}{\bar{c}}\right)^2 + \frac{1}{2}\left(\frac{x_w}{\bar{c}}\right)\right]}{A + 2\cos\Lambda_{c/4}} + \frac{1}{24} \frac{A^3 \tan^2 \Lambda_{c/4}}{A + 6\cos\Lambda_{c/4}} + \frac{1}{8} \right]$$

[Ref 25] Fig 5.1, $K = 0.73$

$$C_{m_{q_W}} = -(.73)(6.016/\text{rad})\cos 23.12° \left[\frac{7.4\left[2(.05)^2 + \frac{1}{2}(.05)\right]}{7.4 + 2\cos(23.12°)} + \frac{1}{24} \frac{7.4^3 \tan^2(23.12°)}{7.4 + 6\cos(23.12°)} + \frac{1}{8} \right]$$

$$C_{m_{q_W}} = -1.56/\text{rad}$$

This formula is the same as that found in NACA TN No. 1581,

Approximate Relations and Charts For Low-Speed Stability

Derivatives of Swept Wings

Check of $C_{L\alpha}$ & $C_{m\alpha}$ from existing data:

Reference: NACA Report, Campbell & Seacord, NACA ACR, LSA13 [8]

Fig. 7, find $C_{L\alpha}$

No Flaps:

$$C_{L\alpha}\Big|_{PPT} = \frac{[0.9 - 0.04]}{[8° - (-4°)]} = 0.072/\text{deg} = 4.11/\text{rad}$$

$$C_{L\alpha}\Big|_{19\text{-ft PT}} = \frac{[1.18 - (-.7)]}{[16° - (-2°)]} = 0.077/\text{deg} = 4.39/\text{rad}$$

XB-35 Type Aircraft

Stability Derivative Data:

Reference : Power-Off Tests of the Northrop N9M-2 Tailless
[7]   Airplane in the 40-By-80 Foot Wind Tunnel
          Stevens & McCormack

Note : N9M-2 - model of the XB-35

$e = 0.8$

Landing Drag Effects: [Ref 5]

Landing gear : $\Delta C_m = 0.011$

$$\Delta C_{D_0} = 0.0190$$

$$\Delta (\delta C_D / \delta c_L) = -0.0110$$

Landing

Needed Information:

l_{x_a} , $l_{x_n} = 0$, l_{x_d}

V_{T_0} or Mach

C_D eqn. , $C_{D\alpha}$, $\frac{\partial T}{\partial M}$

1. a V_{T_0} (stable)

$C_{L_{max}} = 1.48 = \dfrac{W}{qS}$

$$V_{T_0} = \left[\frac{(194143 \text{ lbs})}{\frac{1}{2}(2.377 \times 10^{-3} \text{ slugs/ft}^3)(4000 \text{ ft}^2)(1.04)}\right]^{1/2} = 198 \text{ fps}$$

1. b V_{T_0} (unstable)

$$V_{T_0} = \left[\frac{(194143 \text{ lbs})}{\frac{1}{2}(2.377 \times 10^{-3} \text{ slugs/ft}^3)(2800 \text{ ft}^2)(1.48)}\right]^{1/2} = 198 \text{ fps}$$

2. C_D (from NACA TN No. 1352)

   a. Stable

   Fig. 6a $C_{D_p} = 0.18$, $C_D = 0.268$

   $$C_{D_i} = \frac{C_L^2}{\pi e A} = \frac{(1.04)^2}{\pi(0.6)(7.4)} = 0.078$$

   b. Unstable

   $C_{D_p} = 0.25$, $C_D = 0.407$

   $$C_{D_i} = \frac{C_L^2}{\pi e A} = \frac{(1.48)^2}{\pi(0.6)(7.4)} = 0.157$$

3. $C_{D\alpha} = \dfrac{2 C_L \, C_{L\alpha}}{\pi e A}$

a. Stable

$$C_{D\alpha} = \dfrac{2(1.04)(4.39/\text{rad})}{\pi \, (0.6)(7.4)} = 0.655$$

b. Unstable

$$C_{D\alpha} = \dfrac{2(1.48)(4.39)}{\pi \, (0.6)(7.4)} = 0.932$$

4. $\dfrac{\partial T}{\partial M}$

a. Stable

$$D = \tfrac{1}{2}(2.37 \times 10^{-3} \, \text{slg/ft}^3)(198 \, \text{fps})^2 (4000 \, \text{ft}^2)(0.258) = 48085 \, \text{lb} = T$$

$$\dfrac{\partial T}{\partial M} = \dfrac{(-48085)(198)}{1116.4} = -8528$$

b. Unstable

$$D = (46.59 \, \text{lbs/ft}^2)(2800 \, \text{ft}^2)(0.407) = 5309 \times 10 = T$$

$$\dfrac{\partial T}{\partial M} = \dfrac{(-5309 \times)(198)}{1116.4} = -9417$$

5. ℓ_{x_a}

a. Stable

$\ell_{x_a} \sim 20 \text{ft}$

b. Unstable

$\ell_{x_a} \sim 16.7 \text{ft}$

6. $\ell_{x_{\dot{d}}}$

a. Stable

$\ell_{x_d} \sim 25.5 \text{ft}$

b. Unstable

$\ell_{x_d} \sim 21.3 \text{ft}$

LATERAL-DIRECTIONAL DERIVATIVES

XB-35 Type Aircraft [YB-49 - Lateral Case, Koerner] [4]

	$C_L = .35$ Stable	$C_L = .37$ Unstable	$C_L = .525$ Stable	$C_L = .555$ Unstable	$C_L = 1.04$ Stable	$C_L = 1.48$ Unstable
C_{Y_p}	.0917	.0981	.148	.157	.313	.454
C_{n_p}	-.0262	-.0278	-.0398	-.0421	-.0797	-.114
C_{ℓ_r}	.0722	.0763	.108	.114	.214	.305
C_{Y_β}	-.138	-.152	-.162	-.205	-.191	-.265
C_{ℓ_β}	-.0328	-.0459	-.0466	-.0594	-.0350	-.130
C_{n_β}	.0155	.0171	.019	.0206	.0365	~
C_{Y_r}	-.00206	-.00413	-.0329	-.0378	-.130	~
C_{n_r}	-.0075	-.007	-.007	-.007	-.01	~
C_{ℓ_p}	-.343	-.343	-.343	-.343	-.343	-.343

XB-35 Type Aircraft

Stability Derivative Data: [Reference, Kconner]

$$C_{Y_p} = -.0205 + .3205 C_L$$

$$C_{n_p} = .0009 - .0775 C_L$$

$$C_{\ell_r} = .235 C_L \left[\frac{1}{\sqrt{1-M^2} + .0012q} \right] \quad @ \ 40 \ Kft, \ q = 113 \ lb/ft^2$$

$$C_{Y_{\beta \, prop}} = -1.32/prop = \frac{\partial y/\partial \psi}{q \pi D^2/4} \quad (NACA \ TR819)$$

Stable:

$$C_{Y_{\beta \, prop}} \Big|_{wrt \ S_w} = \frac{-1.32 \left[\pi (10 ft)^2/4 \right]}{4000 \ ft^2} = -.0259/prop \times 2 \ props$$

$$= -.0518$$

Unstable:

$$C_{Y_{\beta prop}} \Big|_{wrt \ S_w} = \frac{-1.32 \left[\pi (9.35 ft)^2/4 \right]}{2800 \ ft^2} = -.0324/prop \times 2 \ props$$

$$= -.0647$$

$$C_{Y_\beta} = C_{Y_{\beta \, WING + FINS}} + C_{Y_{\beta prop}}$$

$$C_{\ell_\beta} = \Delta C_{\ell_\beta} + C_{\ell_{\beta \, WING + FINS}}$$

$$\Delta C_{\ell_\beta} = -.01594 \left(\frac{W}{135000} \right) + (.000696 - .000182 \delta_L)\left(\frac{V_E}{100} \right)^2$$

@ 40 Kft, V_E = 313 kts

$$C_{Y_r} = -.0740 C_L^2 + C_{Y_{r \, wing + fin}}$$

$$C_{\ell_p} = -.391 \left[\frac{1}{\sqrt{1-M^2} + .0012q} \right] = -.0000S$$

$$C_{n_\beta} \big|_{prop} = \frac{-(-.0518)(5ft)}{172 \ ft} = .0015 \quad or \quad \frac{-(-.0647)(4.7ft)}{144 \ ft} = .0021$$

Landing

Lateral - Directional : Estimate C_{l_β} a C_{n_β}

Koerner, Figure 3   [4]

$C_{l_\beta} = -.0355$ (stable)

$C_{l_\beta} = -.0755$ (unstable)

Koerner, Figure 4   [4]

$C_{n_\beta} = .0235$ (stable)

$C_{n_\beta} = 0.04$ (unstable)

Estimate : C_{l_β} [Reference Seckel] [26]

$$C_{l_\beta} = \Delta_w C_{l_\beta} + \Delta_{wf} C_{l_\beta} \quad (\text{No Horizontal or Vertical Tail})$$

$M\cos\Lambda < 1$

$$\Delta_w C_{l_\beta} = -\tfrac{1}{6} \frac{1+2\lambda}{1+\lambda} \left[\Gamma C_{L\alpha} + \frac{\tan\Lambda}{1-M^2\cos^2\Lambda} C_L \right]$$

$$\Delta_{wf} C_{l_\beta} = 1.2\sqrt{A} \frac{z_w}{b} \left(\frac{h+w}{b} \right)$$

For a flap:

$$\Delta_{flap} C_{l_\beta} = -\tfrac{1}{6} \frac{b_f}{b} \frac{1+2\lambda_f}{1+\lambda_f} \frac{\tan\Lambda_f}{1-M^2\cos^2\Lambda_f} \Delta C_{Lf}$$

Parameters :

Parameter	Stable	Unstable
λ	.25	.25
Γ	.92°	.92°
$C_{L\alpha}$	4.39/rad	4.34/rad
Λ	23.12°	23.12°
M_{cruise}	.65	.65
M_{land}	.18	.18
A	7.4	7.4
b	172 ft	144 ft
z_w	0	0
h	6.6 ft	5.5 ft
w	6.6 ft	5.5 ft

C_{ℓ_β} [Seckel]   [26]

Cruise: (Clean)

$$\Delta_W C_{\ell_\beta} = -\frac{1}{6} \frac{1+2(.25)}{1.25} \left[(.016)(4.39) + \frac{\tan 23.12}{1 - (.65)^2 \cos^2 23.12} C_L \right]$$

$$= -(.014 + .133 C_L)$$

$$\Delta_{W_f} C_{\ell_\beta} = 1.2 \sqrt{7.4} \,(0) = 0$$

C_{ℓ_β} (stable, unstable) $= -(.014 + .133 C_L)$ @ cruise

C_L	C_{ℓ_β} Seckel	C_{ℓ_β} Koerner
.1	-.0273	-.015
.2	-.0406	-.019
.3	-.0539	-.025
.4	-.0672	-.0315
.5	-.0805	-.0405
.6	-.0938	-.049
.7	-.1071	-.054
.8	-.1204	-.0545
.9	-.1337	-.051
1.0	-.147	~

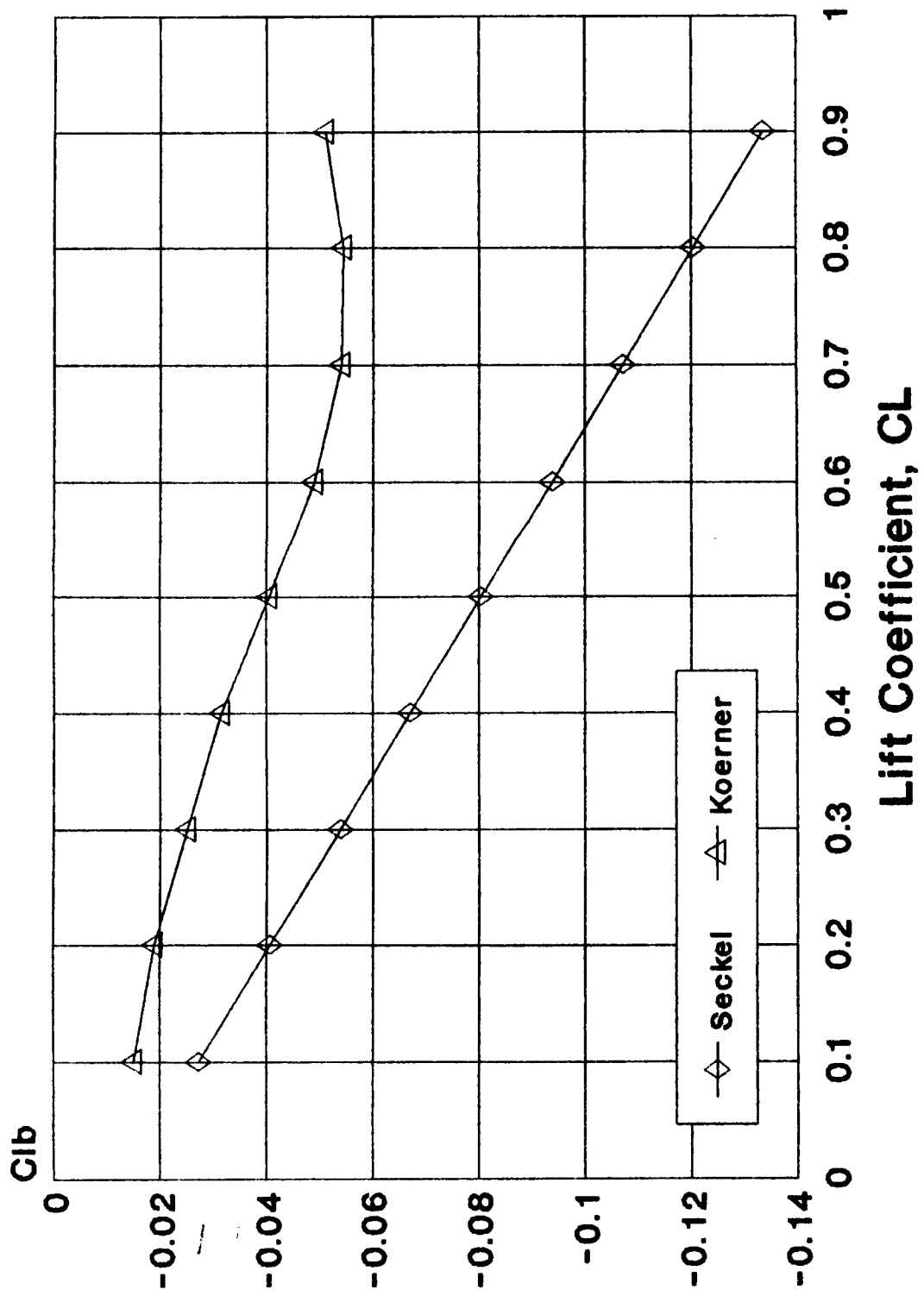See Figure A-1 For Comparison Plot

Figure A-1. Flying Wing Clb

XB-35 Type Aircraft : Stability Derivative Data

Reference: Aerodynamic Characteristics of XB-35 & YB-49
All-Wing Airplane Configurations - Friend [5]

Note: source C_m, C_L, C_D, X_{CG}, C_{D_0} (as a function of Reynolds No.)
& aircraft Geometry

Reference: Campbell & Seacord [8]

$$C_{L\alpha}\Big|_{FFT} = .072/deg = 4.11/rad$$

$$C_{L\alpha}\Big|_{19ft\ PT} = .077/deg = 4.39/rad$$

$C_{m\alpha}$ & $C_{D\alpha}$ are easily estimated w/ $C_{L\alpha}$ available

	$\alpha=12°, C_L=1.05$ FFT	$\alpha=0°, C_L=.3$ FFT	$\alpha=6°, C_L=.7$ FFT	$\alpha=4°, C_L=.3$ 19ft PT	$\alpha=8°, C_L=.6$ 19ft PT	$\alpha=15°, C_L=1.02$ 19ft PT
$C_{n\beta}$	.0006	.00025	.00029	.00015	.00025	.0006
$C_{l\beta}$	-.00075	-.00036	-.0007	-.0007	-.00125	-.00135

For Split-rudder : FFT

$$C_{n\delta_r} = 0.007/rad$$

CONTROL DERIVATIVES

<u>Aileron Control Derivatives</u> [Ref, Datcom & Roskam] [25]

$AR = 7.4$, $\lambda = 0.25$, $\Lambda_{c/4} = 23.12°$, $\pm 15°$

NACA 65,3018

$\eta_i = 0.1936$, $\eta_o = 0.3934$, $C_f/c = 0.144$, $M = 0.65$, $\beta = 0.76$, $R_E = 32 \times 10^6$

Find $C_{\ell_{\delta_A}}$

$(C_{\ell_\alpha})_M = C_{\ell_\alpha}/\beta = (6.016/rad)/.76 = 7.92/rad$

$K = \dfrac{(7.92/rad)}{2\pi/.76} = .957$

$\dfrac{\beta AR}{K} = \dfrac{(.76)(7.4)}{.957} = 5.87$

$\Lambda_\beta = \tan^{-1}(.427/.76) = 29°$

$(\beta C'_{\ell_\delta}/K)_{\eta_o} = 0.075$

$(\beta C'_{\ell_\delta}/K)_{\eta_i} = 0.18$

$C'_{\ell_\delta} = \dfrac{.957}{.76}\left[.18 - .075\right] = .132$

$(C_{\ell_\delta})_{Theory} = 3.2$

$\dfrac{C_{\ell_\delta}}{(C_{\ell_\delta})_{Theory}} = .92$

$K' = .98$

Aileron Control Derivatives (cont)

$$\Delta C_{\ell} = \delta \left[\frac{C_{\ell_\delta}}{(C_{\ell_\delta})_{Theory}} \right] (C_{\ell_\delta})_{Theory} \, K'$$

$$= \frac{15°}{57.3} (.92)(3.2)(.98) = .755$$

$$\alpha_\delta = \frac{-\Delta C_{\ell}}{(C_{\ell_\alpha})_M \delta} = \frac{-(.755)}{(7.92)(15°/57.3)} = -.364$$

$$C_{\ell_{\delta_A}} = C'_{\ell_\delta} |\alpha_\delta| = (.132)|-.364|$$

$$C_{\ell_{\delta_A}} = .048/rad$$

$C_{n_{\delta_A}}$

1. $\delta_e = 0°$

a) $C_L = .39$

δ	C_ℓ	C_n	C_n/C_ℓ
± 4°	.0125	-.001	-.08
± 8°	.0248	-.0016	-.064
± 12°	.0357	-.0024	-.067
± 16°	.0447	-.0031	-.069
± 20°	.0512	-.0037	-.072

$C_{n_{\delta_A}} = -.0034/\text{rad}$

b) $C_L = .73$

δ	C_ℓ	C_n	C_n/C_ℓ
± 4°	.012	-.0012	-.1
± 8°	.024	-.0024	-.1
± 12°	.034	-.004	-.12
± 16°	.044	-.005	-.11
± 20°	.052	-.006	-.12

$C_{n_{\delta_A}} = -.0053/\text{rad}$

c) $C_L = 1.05$

δ	C_ℓ	C_n	C_n/C_ℓ
± 4°	.012	-.0022	-.18
± 8°	.021	-.0043	-.20
± 12°	.03	-.0065	-.21
± 16°	.038	-.008	-.21
± 20°	.043	-.0097	-.23

$C_{n_{\delta_A}} = -.0099/\text{rad}$

2. $\delta_e = +4°$, $C_L = .39$

δ		C_ℓ	C_n	$-C_\ell/C_n$
16	+20° -12°	.0404	-.0041	-.10
12	+16° -8°	.0335	-.0031	-.092
8	+12° -4°	.0243	-.0024	-.099
4	+8° 0°	.0133	-.0012	-.090

$C_{n_{\delta_A}} = -.0046/rad$

3. $\delta_e = -4°$

a) $C_L = 0.39$

δ		C_ℓ	C_n	C_n/C_ℓ
16	+12° -20°	.0465	-.002	-.043
12	+8° -16°	.036	-.0016	-.044
8	+4° -12°	.024	-.0012	-.05
4	0° -8°	.0015	-.0004	-.27

$C_{n_{\delta_A}} = .0022/rad$

b) $C_L = .73$

δ		C_ℓ	C_n	C_n/C_ℓ
16	+12° -20°	.0462	-.004	-.087
12	+8° -16°	.0357	-.0027	-.076
8	+4° -12°	.0237	-.0021	-.089
4	0° -8°	.0118	-.0012	-.10

$C_{n_{\delta_A}} = -.0042/rad$

4. $\delta_e = +8°$

   a) $C_L = .39$

δ	C_ℓ	C_n	C_n/C_ℓ
$\pm 12 \begin{bmatrix} 20° \\ -4° \end{bmatrix}$	.029	-.0039	-.13

$C_{n_{\delta_A}} = -.0062/rad$

   b) $C_L = .73$

δ	C_ℓ	C_n	C_n/C_ℓ
$\pm 12 \begin{bmatrix} 20° \\ -4° \end{bmatrix}$	.0284	-.0051	-.18

$C_{n_{\delta_A}} = -.0086/rad$

5. $\delta_e = -8°$, $C_L = 1.05$

δ	C_ℓ	C_n	C_n/C_ℓ
$\pm 12 \begin{bmatrix} 4° \\ -20° \end{bmatrix}$	.0283	-.0049	-.17

$C_{n_{\delta_A}} = -.0082/rad$

$C_{n_{\delta_{ELEVON}}}$ Trim Effects

$$C_M = .013 + \left(\frac{x_{cg}}{\bar{c}} - .303\right)C_L - .0010\delta_F - .0046\delta_E - .0025\delta_t$$

For trim, $\delta_F = \delta_t = 0$, $C_M = 0$

Stable Configuration

$$O = .013 - (.05)(.35) - .0046\delta_E$$

$$\delta_E = \frac{.013 - (.05)(.35)}{.0046} = -.978° \approx -1°$$

Unstable Configuration

$$O = .013 + (.08)(.35) - .0046\delta_E$$

$$\delta_E = \frac{.013 + (.08)(.35)}{.0046} = 8.913° \approx 9°$$

From the C_n/C_ℓ plots, Figures A-2, A-3

$\delta_E = 8°$, $C_n/C_\ell = -.12$

$\delta_E = -1°$, $C_n/C_\ell = -.062$

$$C_{n_{\delta_A}}\bigg|_{\delta_E=8°} = (.048/rad)(-.12) = -.0058/rad$$

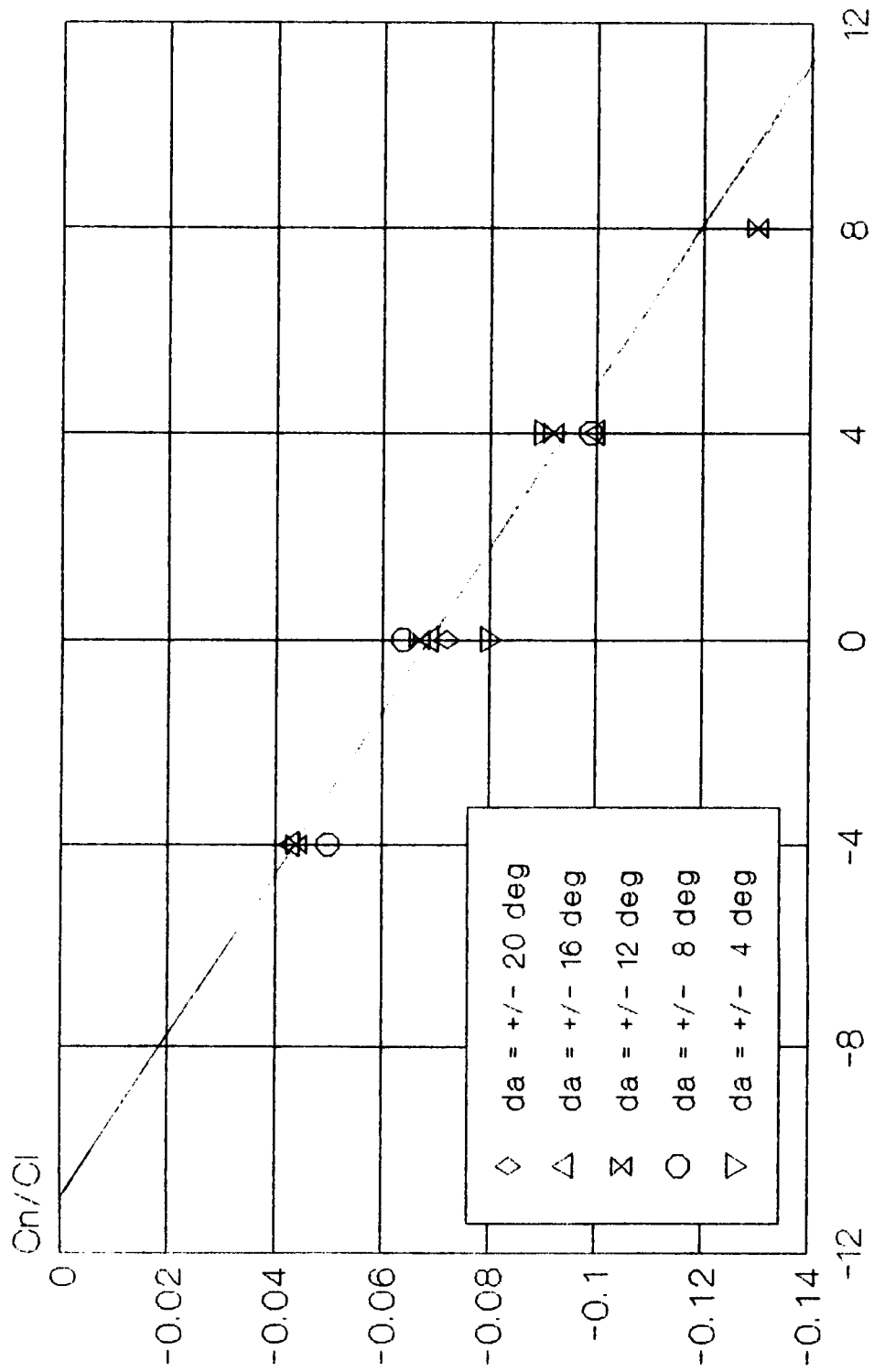$$C_{n_{\delta_A}}\bigg|_{\delta_E=-1°} = (.048/rad)(-.062) = -.0030/rad$$
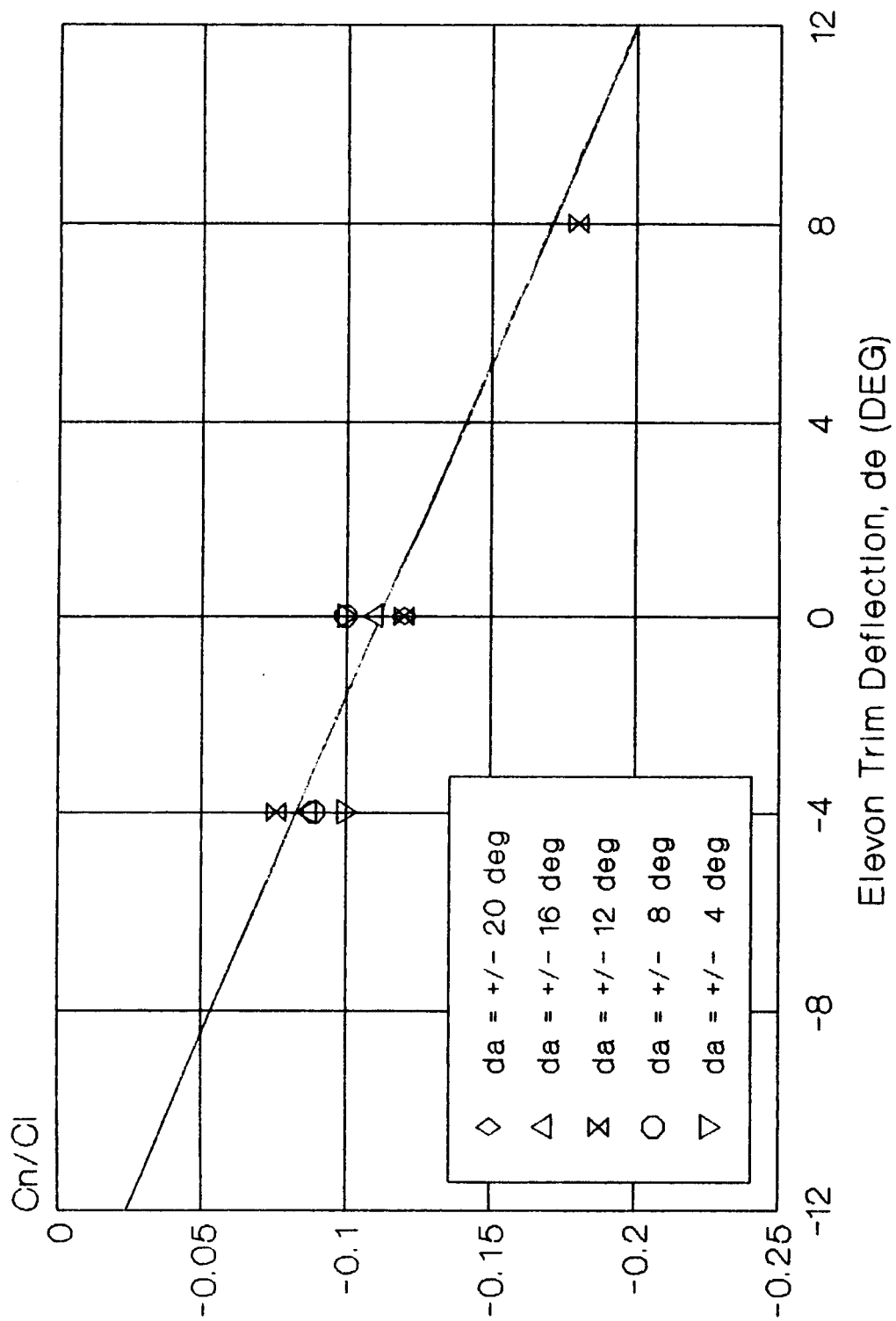
Figure A-2. CnCl vs. Elevon Trim Deflection
CL = 0.39

Figure A-3. Cn/Cl vs. Elevon Trim Deflection
CL = 0.73

Review of NACA ACR 4411 Collection of balanced-ail test data to see if useful re $C\ell_{\delta a}$ on flying wing project.

Consider only non-protruding overhangs to begin with, e.g., C series, D series, E-V to VIII:

   Look at: <u>1/2 span</u> wings 1st with C_n (rather than C_D) data.

   Eliminate: C VIII, XIV, XV, D I, III, IX, D IV, V level TR
               E III, IV, (⊐ ⊂⊃) VII, VIII

Search remaining for α n C_L variations

C36	plain sealed .155C aileron	±20°	-4.5<α <16.6	
37	1/3c internal bal aileron	±14°	-4.4 17.7	

C40, 41 poor print   Reasonable scale on C_n plots

42	internal .563 bal	±20°	-.36 <C_L<1.25
43	internal .563 bal	±20°	-.36 <C_L<1.25 ail extended to tip

C46a	plain unbal .150C	±30° - 40°	α = 1, 8, 15
46b	.30 internal bal	±20° - 30°	α = 1, 8, 15
47	.35 internal bal	±20° - 25°	α = 1, 8, 15 + <u>inbd flap</u>

C50   .29 internal bal .150C ±20° α = 0, 8, 12
                    1/2 scale C_n plots

C71	.30 internal bal .18C	±30°	-4.2 <α<17.7 full span
72	.56 internal bal .18C	±15°	-4.2 <α<17.7 ail

                    1/2 scale C_n plots

C75   .35 internal bal   ±15° α = .3, 5.7, 10.9
  76; 77 ditto flaps = 50°;   ditto bal plate removed (unsealed)
                    1/2 scale C_n plot

E16	plain .155c	+30	C_L=0.1, 1.06 full span tab
17	.005C gap	+30	C_L=0.1, 1.06 full span tab

                    1/2 scale C_n plot

E20	internal .688 bal .15C	±15°	C_n = .02,? full span tab
21	internal .688 bal .15C	±15°	C_L = .02 1/2 span tab
22	.563 bal .162C	±20	C_L = .02, .71, 1.25 1/2 span tab

$$C_n$$

	$C_L = -.25$	.06	.39	.73	1.05	1.24
δ	$\alpha = -4.5$	0	-4.5	8.8	13.3	16.6

Left Wing

+20	-.0005	- 0022	-.0037	- 0045	- 0060	- 0070
16	0	- 0012	-.0027	- 0035	- 0050	- 0055
12	0	- 0008	-.0020	- 0025	- 0040	- 0040
8	0	- 0006	-.0012	- 0012	- 0025	- 0025
4	0 - +.0002	-.0002	-.0008	- 0006	- 0012	- 0012
0	0	0	0	0	0	0
-4	-.0005	0	-.0002	+ 0006	0010	0014
-8	-.001	-.0002	+.0004	+ 0012	0018	0025
-12	-.0015	-.0005	+.0004	+.0015	0025	0036
-16	-.002	-.001	+.0004	+ 0015	0030	0040
-20°	-.003	-.0015	0	+.0015	+ 0037	+ 0045

$$C_P$$

(C_n/C_ℓ) vs δ_e

+20	+ 0225	.0225	0232	0225	020	--
16	+.021	.0205	0220	0205	0182	--
12	0168	.0167	0185	0167	0147	--
8	0120	0120	0133	0120	0105	--
4	.006	.006	.0067	.006	.0053	--
0	0	0	0	0	0	--
-4	-.0051	-.0053	-.0058	-.0059	-.0054	--
-8	- 0102	- 0105	- 0115	- 0118	- 0108	
-12	-.0146	-.0158	- 0172	- 0177	- 0152	--
-16	- 0185	-.0208	- 0227	- 0237	- 0194	--
-20	-.021	-.025	- 0280	- 0295	- 0230	--

Supposed trimmed: $\alpha = +4.5$ at $\delta = -4°$ $\delta\alpha = $ ' $\pm 16 = $ +12   -20

		+12	-20	
		.0185	-.0280	C_ℓ
		-.0020	0	C_n

$\delta = 44°$

		+20	-12	
		.0232	-.0172	C_ℓ
		-.0037	+.0004	C_n

Consider $+ \delta_a$ on ℓh wing; then

$- +$ for $-\delta_a$ on rh wing $\therefore$ change signs of C_ℓ, C_n for

$-\delta_a$ and add both sides: $\delta_a = -4$ $C\ell = .0455$ $C_n = -.0020$

                                                    $= +4$ $C\ell = .0404$ $C_n - .0041$

Repeat Above

			$\alpha = 4.5$	8.8	13.3
$\delta_\ell = -4°$	$\delta = +12$	C_ℓ	0185	0167	0147
		C_n	-.0020	-.0025	-.0040
	-20	C_ℓ	-.0280	- 0295	-.0230
		C_n	0	+.0015	+ 0037
	Σ	C_ℓ	0465	.0462	.0377
		C_n	-.0020	-.0040	-.0077
		C_n/C_ℓ	-.0430	-.0866	-.2042
+4°	$\delta = +20$	C_ℓ	.0232	0225	0200
		C_n	-.0037	-0045	-.0060
	-12	C_ℓ	-.0172	-.0177	-.0152
		C_n	+.0004	+.0015	+.0025
	Σ	C_ℓ	.0404	.0402	0352
		C_n	-.0041	-.0060	-.0085
		C_n/C_ℓ	-.1015	-.1493	-.2415

Trimming with down elevon increases adverse yaw!

Hinge-moment coefficient, C_h

Rolling-moment coefficient, C_l'

Yawing-moment coefficient, C_n

α (deg)	C_L
∇ -4.5	-0.25
$\bigcirc$ 0	.06
$\triangle$ 4.5	.39
$\square$ 8.8	.73
$\times$ 13.3	1.05
$\diamondsuit$ 16.6	1.24

Aileron deflection, δ_a, deg

(a) Plain sealed aileron.
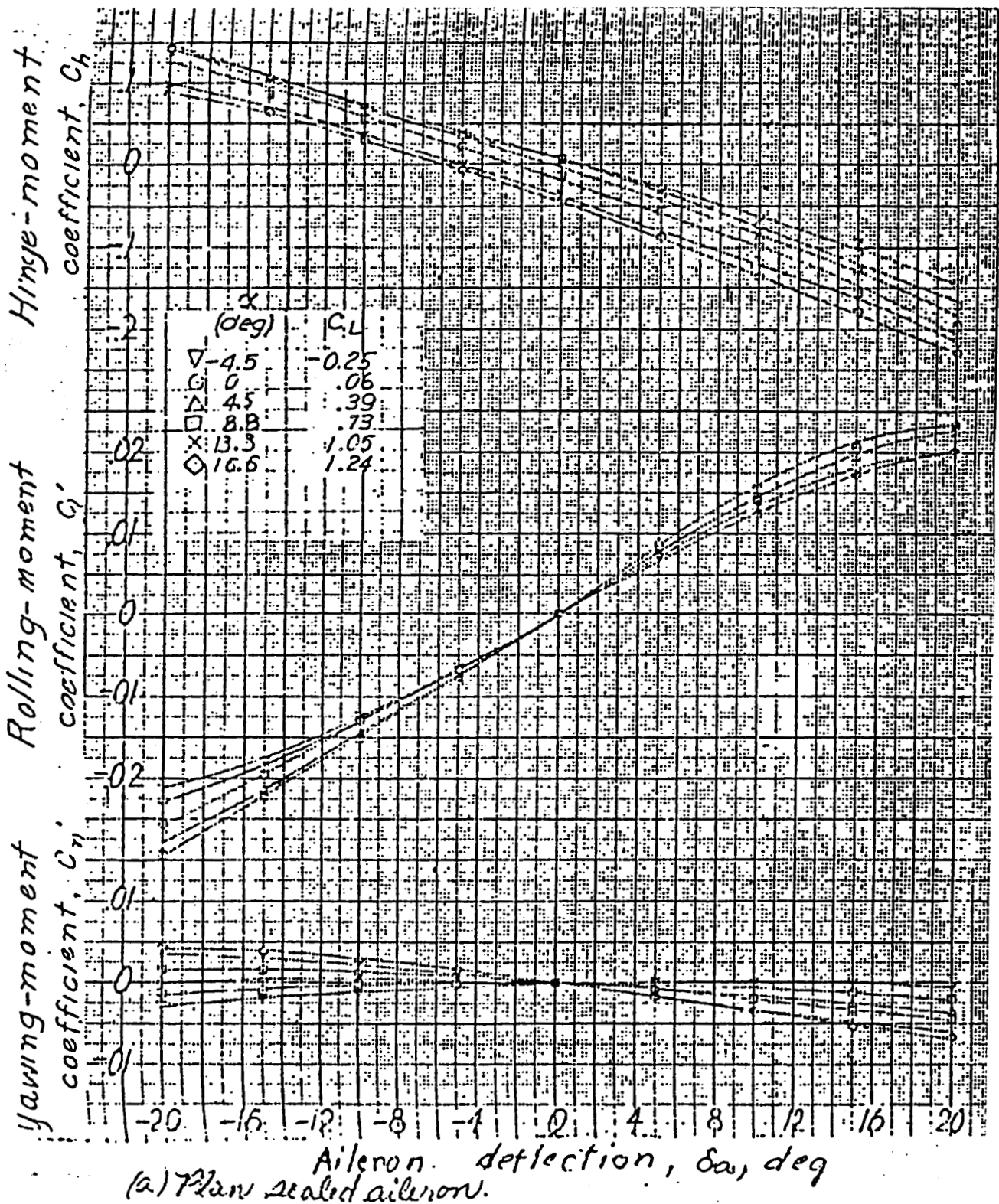
Figure A-4.   Aileron Characteristics of Model C-X With Flaps

APPENDIX B
FLIGHT CONDITION ANALYSIS

(if IS=1)   _LANDING STABLE_

Input File Name: _F,W,L,A,N,S,T,G,.,/,N,P,_   Output File Name; |_,_,_,_,_,_,_,_,.,_,_,_|

AFTF LONGITUDINAL LIFT/DRAG NONDIMENSIONAL DERIVATIVES   Date: _22_ - _FEB_ -_88_
                                                                  dd - mmm - yy

Flight Condition Identifier; <FCI: 60 Characters or Numerals

_F,L,Y,I,N,G,W,I,N,G,/,L,A,N,D,I,N,G,/,S,T,A,B,L,E,C,O,N,F,I,G,/,S,L,/,H,E,A,V,Y,_

# of Controls include Throttle but not Gust; ≤ 6

With Gusts = 1; W/O Gusts = 0

Polynomial Coeff. = 1; Without = 0

With CPLG NUM = 1; Without = 0

Save Eqn. = 1; W/O Save Eqn. = 0

Long.	NRHS	NG	NPC	Nondim	C_L, C_D	ICC	IS
0				1	0		
0	2	O	O	1	0	1	1

$S(ft^2)$ c(ft) ξ_o(deg) l_i(ft) W(lb) I_y(slgft^2) l_{x_a}(ft) l_{x_h}(ft) l_{x_d}(ft)

_4000_ , _26.2_ , _O_ , _O_ , _194143_ , _1190245_ , _20_ , _O_ , _255_

(h(ft) if ρ=0)

$\rho\left(\dfrac{slg}{ft^3}\right)$ a(fps) V_{T_o}(fps)   MACH α_o(deg) γ_o(deg)

_O_ , _O_ , _198_ , _O_ , _O_ , _O_

C_L C_{L_α} $C_{L_{\dot\alpha}}$ C_{L_M} C_D C_{D_α} C_{D_M}

_1.04_ , _4.39_ , _O_ , _O_ , _.258_ , _.655_ , _O_

C_{m_α} $C_{m_{\dot\alpha}}$ C_{m_q} C_{m_M} $\partial T/\partial M$ ✓ $\partial T/\partial\delta Th$

_-.22_ , _O_ , _-1.56_ , _O_ , _-8528_ , _1.0_

C_{D_δ} C_{L_δ} C_{m_δ} (define δ_i below)

_O_ , _.74_ , _-.26_ : _Elevon in Pitch_

_____ , _____ , _____ : _____

_____ , _____ , _____ : _____

_____ , _____ , _____ : _____

Control Symbols (except thrust) $\delta_{1,2,...6}$. Use 3 characters; left justified:

_D,E,P,_ , |_,_,_| , |_,_,_| , |_,_,_| , |_,_,_| , |_,_,_|

02-26-88   10:35:18

FLYINGWING/LANDING/STABLECONFIG/SL/HEAVY

GEOMETRY:

VT	ALPHA	GAMMA	LX A	LX H	LX D
198.0	0.0	0.0	20.0	0.0	-25.50
A	RHO	MACH	XIO	ZJ	
1116.5	.002377	.17735	0.0	0.0	–
S	C	WEIGHT	IY	ALTITUDE	
4000.0	26.20	194140.	.11903E+7	0.0	–

(LX D circled) prop location

NON-DIMENSIONAL DERIVATIVES:

CL	CLA	CLAD	CLM
1.040	4.390	0.0	0.0
CMA	CMAD	CMQ	CMM
-.220	0.0	-1.560	0.0
CD	CDA	CDM	TM	TDTH
.2580	.6550	0.0	-8528.0	1.000	–
CDDEP	CLDEP	CMDEP		
0.0	.740	-.260		

DIMENSIONAL DERIVATIVES:

XU	XU *	XW	TU
-.08049	-.08176	.06006	-.0012659
ZU	ZU *	ZWD	ZW
-.3245	-.3245	0.0	-.7250
MU	MU *	MWD	MW
0.0	0.0	0.0	-.004558
MAD	MA	MQ	
0.0	-.9025	-.4234	
XDEP	ZDEP	MDEP	
0.0	-22.86	-1.0666	
XDTH	ZDTH	MDTH	
.00016572	0.0	0.0	

Key

Roots Locus gain

$K [\zeta, \omega \quad$ Real Imag $]$

$(s+a)$

$\langle$Bode Gain$\rangle$

TRFN DATA FILE NAME :   A:FWLANSTA.SAV   .
OLD file, write over it (Y/N)?   Y
U ,W ,THE,DD ,AZ ,AZ',HD ,
Enter no. of eqns to output from 4 thru 7   7

FLYINGWING/LANDING/STABLECONFIG/SL/HEAVY

$\zeta \quad \omega \quad$ Real Imag

DENOMINATOR: [.1268;.1972 .0250;.1956][.533;1.107 .590;.936]
               <.0476> Bode Gain

FLYINGWING/LANDING/STABLECONFIG/SL/HEAVY

DEP NUMERATORS:

Root Locus Gain (S+a) (S+a) Bode Gain

N(U-DEP)   -1.373(.962)(-16.32) <21.5>

N(W-DEP)   -22.9(9.67)[.1703;.225   .0382;.221] <-11.14>

N(THE-DEP) -1.067(.1202)(.589) <-.0755>

N(DD-DEP)   50.1(.0291)(-1.348)(1.935) <-3.80>

N(AZ-DEP)   -22.9(0.0)(.0288)(-2.18)(2.65) <3.80>

N(AZ'-DEP) -1.523(0.0)(.0286)(8.23)(-10.61) <3.80>

N(HD-DEP)   22.9(.0288)(-2.18)(2.65) <-3.80>

FLYINGWING/LANDING/STABLECONFIG/SL/HEAVY

DTH NUMERATORS:

N(U-DTH)   .0001657(0.0)[.522;1.10   .574;.938] <.00020>

N(W-DTH)   -.538E-4(0.0)(.423) <-.228E-4>

N(THE-DTH) .245E-6 <.245E-6>

N(DD-DTH)   .538E-4[.1617;.950   .1536;.938] <.485E-4>

N(AZ-DTH)   -.538E-4(0.0)[.223;.950   .212;.926] <-.485E-4>

N(AZ'-DTH) -.538E-4(0.0)[.271;.950   .257;.915] <-.485E-4>

N(HD-DTH)   .538E-4[.223;.950   .212;.926] <.485E-4>

FLYINGWING/LANDING/STABLECONFIG/SL/HEAVY

DEP/DTH COUPLING NUMERATORS:

N(U-DEP/W-DTH)   .00379(0.0)(9.66) <.0366>

N(U-DEP/THE-DTH)   .0001768(.627) <.0001109>

N(U-DEP/DD-DTH)   -.00830(-1.382)(1.916) <.0220>

N(U-DEP/AZ-DTH)   .00379(0.0)(-2.21)(2.63) <-.0220>

N(U-DEP/AZ'-DTH)   .000252(0.0)(8.19)(-10.62) <-.0220>

N(U-DEP/HD-DTH)   -.00379(-2.21)(2.63) <.0220>

N(W-DEP/THE-DTH)   -.574E-4 <-.574E-4>

```
N(W-DEP/DD-DTH)      .001462(-7.76) <-.01136>

N(W-DEP/AZ-DTH)      .01136(0.0) <.01136>

N(W-DEP/AZ'-DTH)     .001147(0.0)(9.90) <.01136>

N(W-DEP/HD-DTH)     -.01136 <-.01136>

N(THE-DEP/DD-DTH)   -.574E-4 <-.574E-4>

N(THE-DEP/AZ-DTH)    .574E-4(0.0) <.574E-4>

N(THE-DEP/AZ'-DTH)   .574E-4(0.0) <.574E-4>

N(THE-DEP/HD-DTH)   -.574E-4 <-.574E-4>

N(DD-DEP/AZ-DTH)    -.001462(0.0)(0.0) <-.001462>

N(DD-DEP/AZ'-DTH)   -.00261(0.0)(0.0) <-.00261>

N(DD-DEP/HD-DTH)     .001462(0.0) <.001462>

N(AZ-DEP/AZ'-DTH)    .001147(0.0)(0.0)(0.0) <.001147>

N(AZ-DEP/HD-DTH)    0.0 <0.0>

N(AZ'-DEP/HD-DTH)    .001147(0.0)(0.0) <.001147>
```

                    02-26-88   10:36:25
AFTF completed
```
```

LANDING

A. Stable
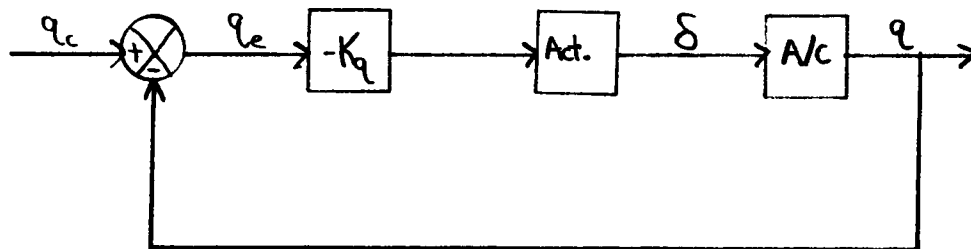
Program CC T.F.'s

$$G_{ACT} = \frac{-K_c 12^2}{[.707, 12]} = G100$$

$$G_{A/c} = \frac{q/\delta_E}{\Delta} = \frac{-1.067(\phi)(.1202)(.589)}{[.1268, .1972][.533, 1.107]} = G101$$

OLTF = G102 = $G_{ACT} * G_{A/c}$

From the Root Locus, Figure B-1,(6), $K_c = 1.0$

G_{CL} = G102/(1+G102) = G103

G114 = Acceleration @ CG

G115 = Acceleration @ Pilot

G116 = H @ CG

G118 = $\dot{H}$ @ CG

G119 = H @ Pilot (From $\dot{H}$)

G125 = $\delta_{Response}$

(a)

(b)
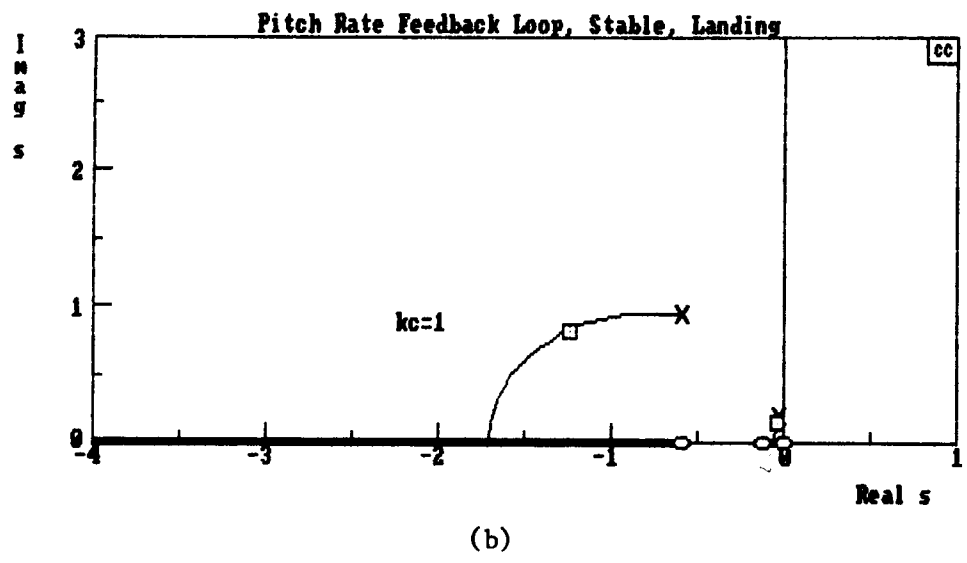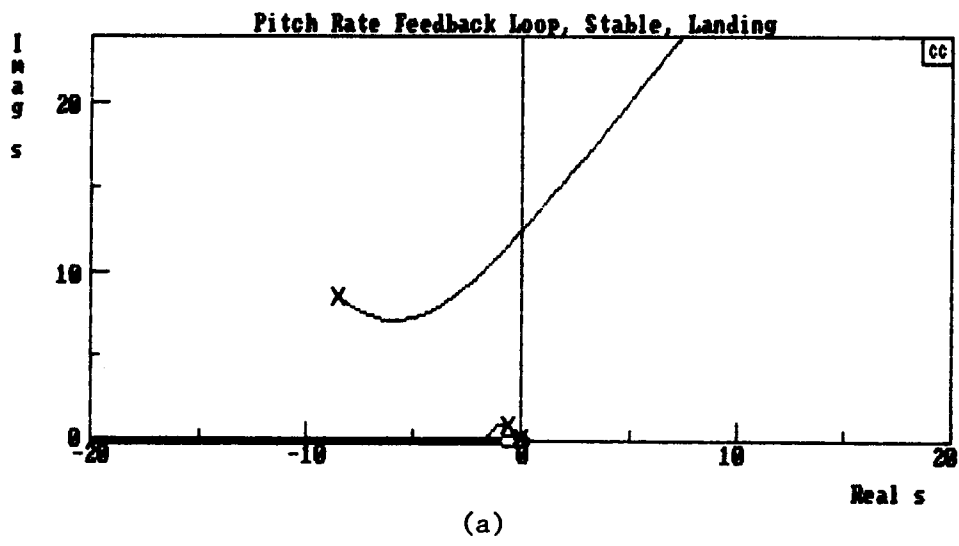
Figure B-1. Stable Configuration Pitch Rate
Feedback Loop Root Locus

LANDING

A. Stable , Add θ feedback to the system
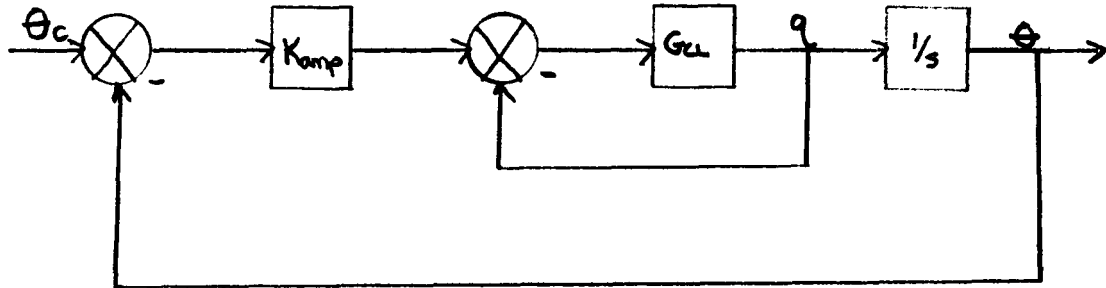
Program CC Transfer Functions

G_{120} = Kamp $*$ Gcl $*$ $1/s$

From Figure B-2 (a), Kamp = 0.6

$$G_{121} = Gclo = \frac{92.2(.12)(.589)}{[.62,.21][.7,1.56][.7,11.2]}$$

Plot H at various locations to check for non-minimum

phase effects.

H @ CG = G136 , Figure B-4

H @ Pilot = G137 , Figure B-3

H @ Prop Tip = G138 , Figure B-5

C-2
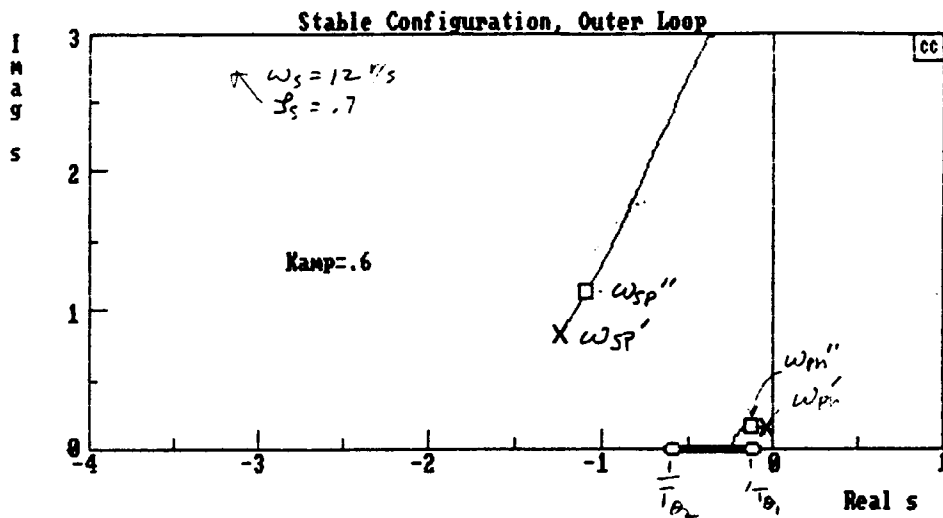
(a) Root Locus
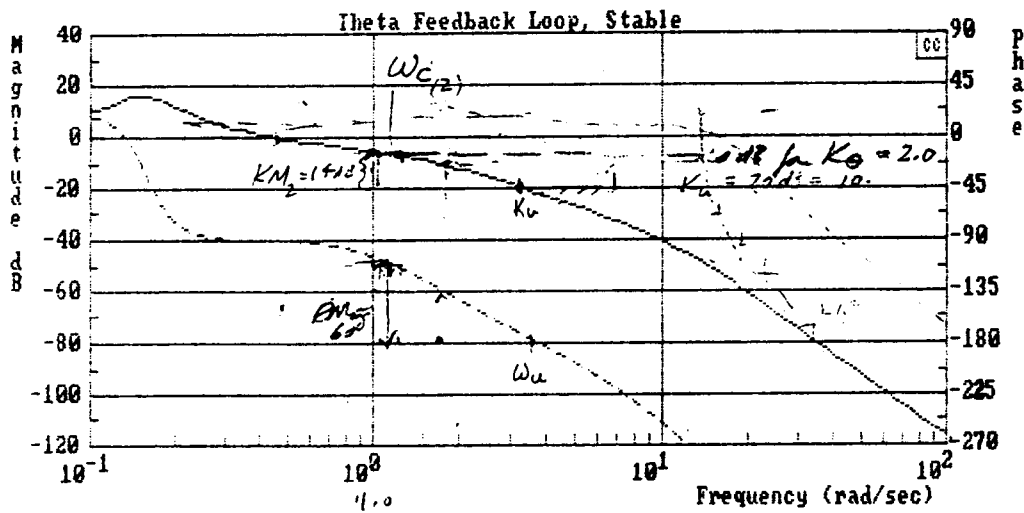
(b) Bode Plot

Figure B-2. Stable Configuration Pitch Angle
Feedback Loop Root Locus and Bode Plot
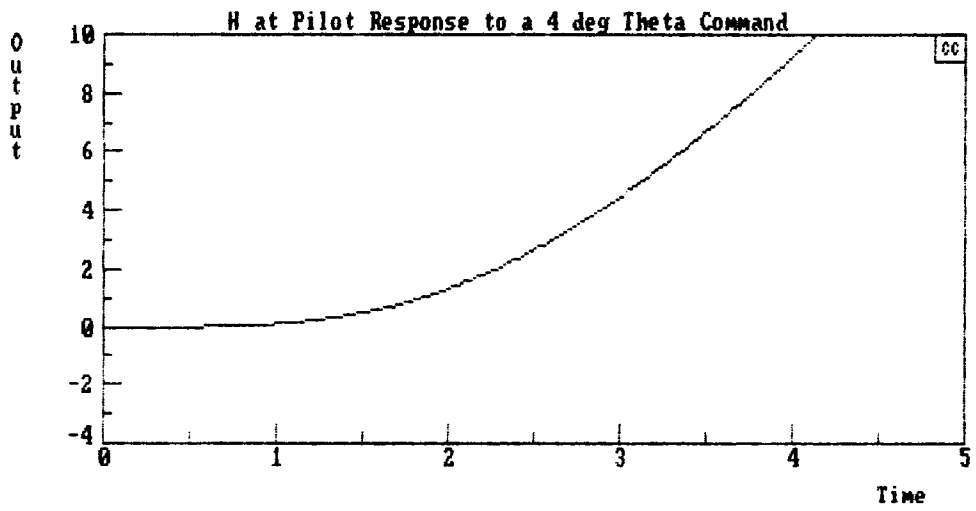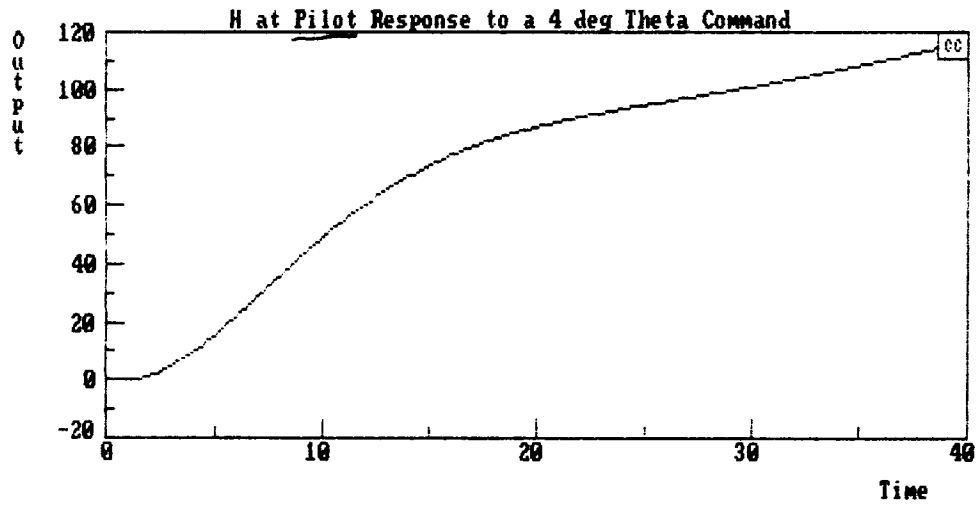
Figure B-3. Change In Altitude At The Pilot Location
For The Stable Configuration
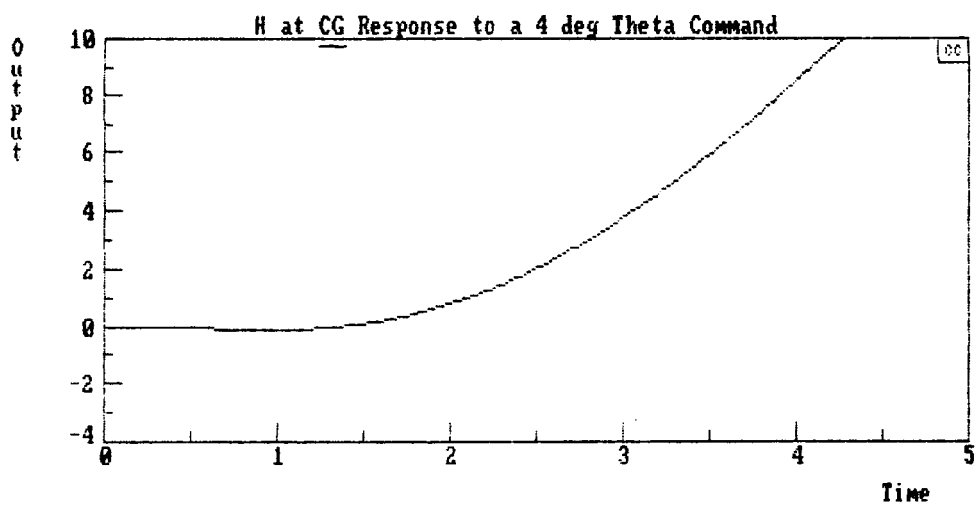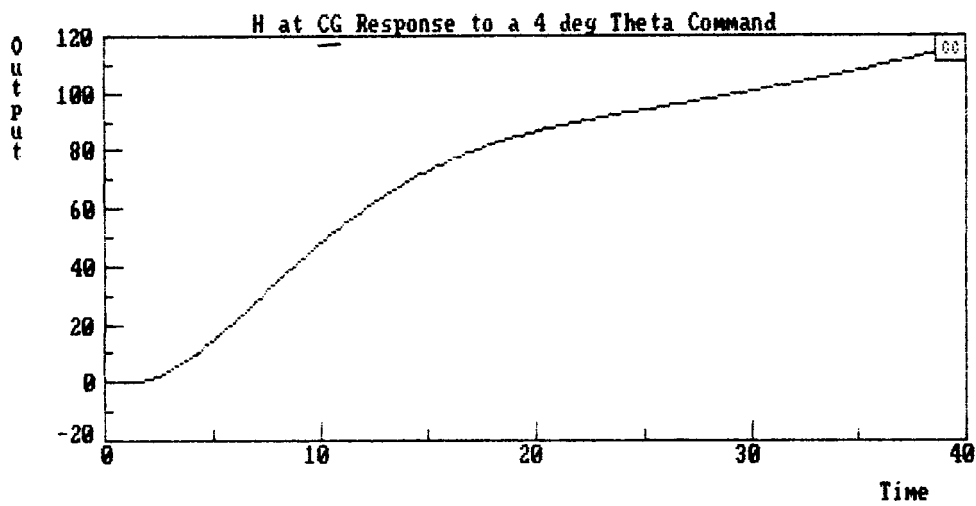
Figure B-4.   Change In Altitude At The CG
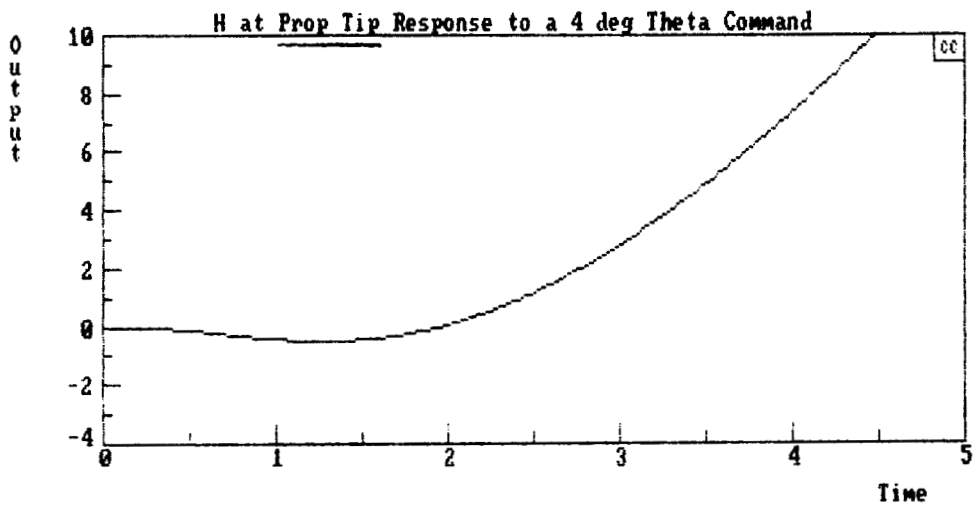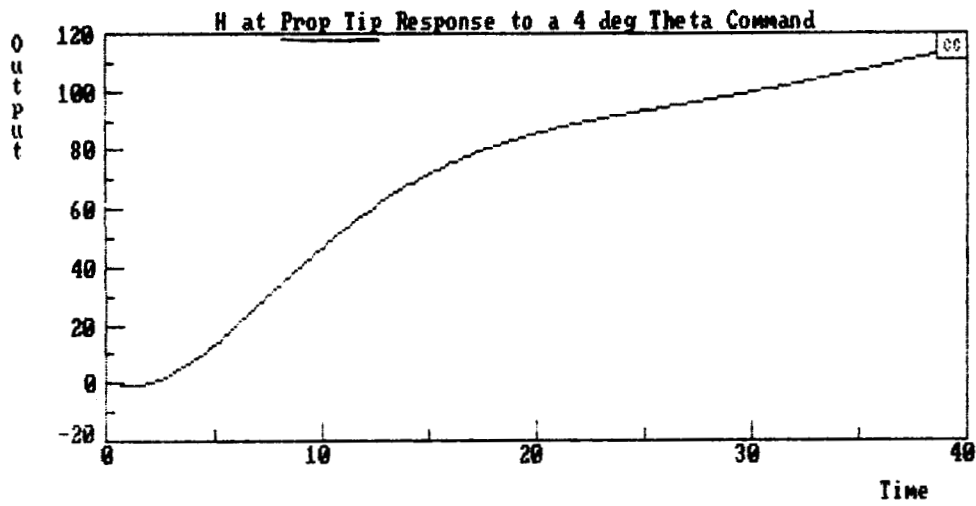   For The Stable Configuration

Figure B-5. Change In Altitude At The Prop Tip
For The The Stable Configuration

LANDING

A. Stable, Higher Gain, Less Conservative Case

$K_a = 2$

$$G_{140} = G_{CL} = \frac{307.296(.1202)(.589)}{[.99,.25][.45,1.92][.7,11.2]}$$

$G_{141} = \delta/\theta_c$, Figure B-6

$G_{142} = h @ CG$, Figure B-9

$G_{143} = h @ pilot$, Figure B-8
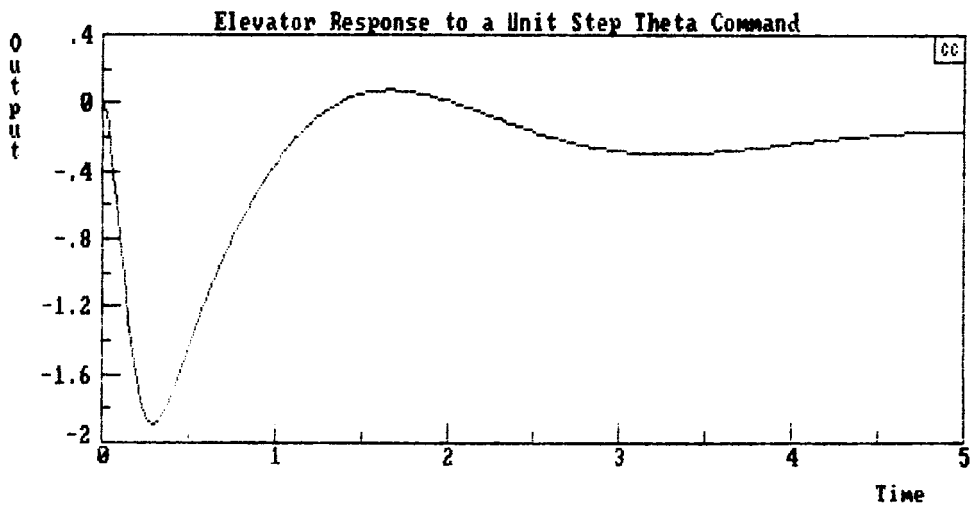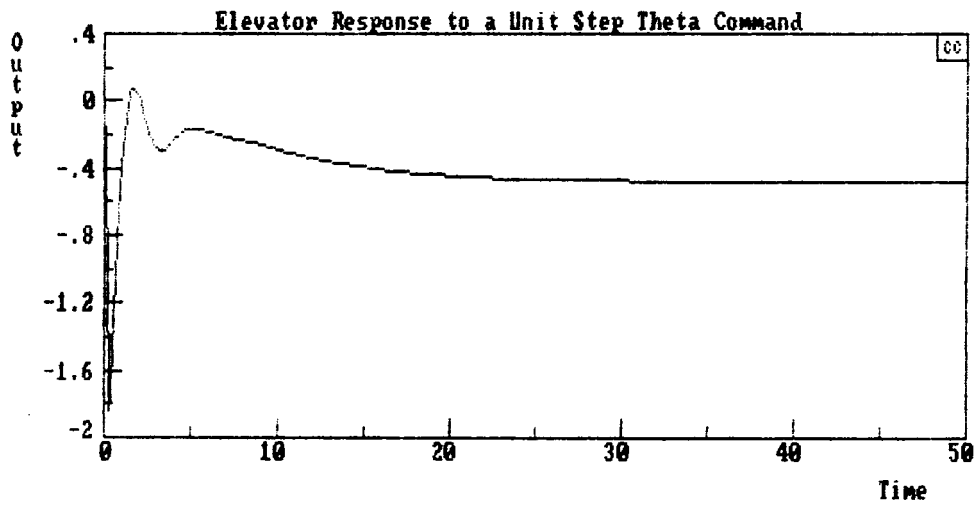
$G_{144} = h @ prop tip$, Figure B-10

Figure B-6. Stable Configuration Elevator Response
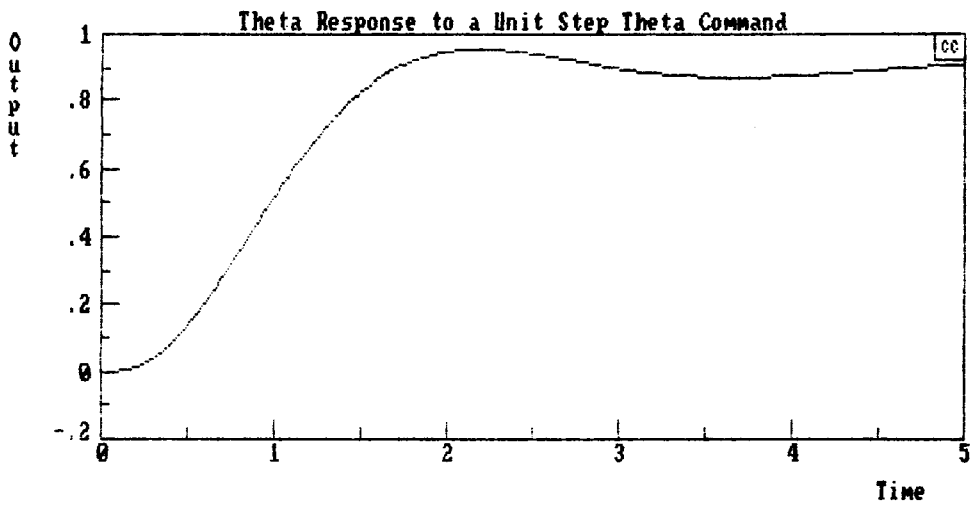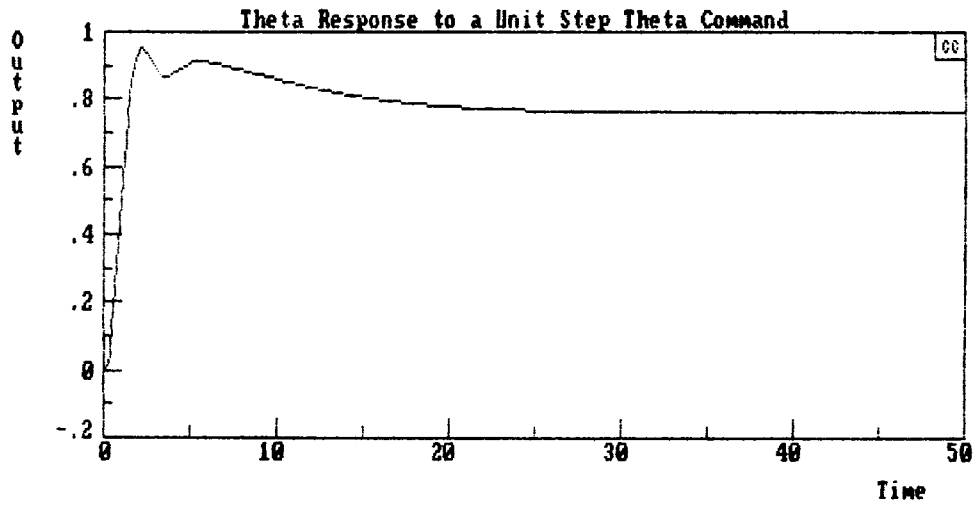(Higher Gain Case)

Figure B-7. Stable Configuration Pitch Angle Response
(Higher Gain Case)

Figure B-8.   Change In Altitude At The Pilot Location
For The Stable Configuration (Higher Gain Case)

Figure B-9. Change In Altitude At The CG For The
Stable Configuration (Higher Gain Case)

Figure B-10. Change In Altitude At The Prop Tip For The
Stable Configuration (Higher Gain Case)

LANDING

A. Stable, High Gain Case

$K_\alpha = 3$

$$G_{150} = G_{CL} = \frac{460.944 (.1202)(.589)}{(.167)(.389)[.34, 2.2][.7, 113]}$$

$G_{151} = \delta/\theta_c$, Figure B-11

$G_{152} = h @ CG$, Figure B-13

$G_{153} = h @ pilot$, Figure B-12

$G_{154} = h @ prop tip$, Figure B-14

Stable Configuration: High Gain Case

Elevator Response to a Unit Step Theta Command

Elevator Response to a Unit Step Theta Command
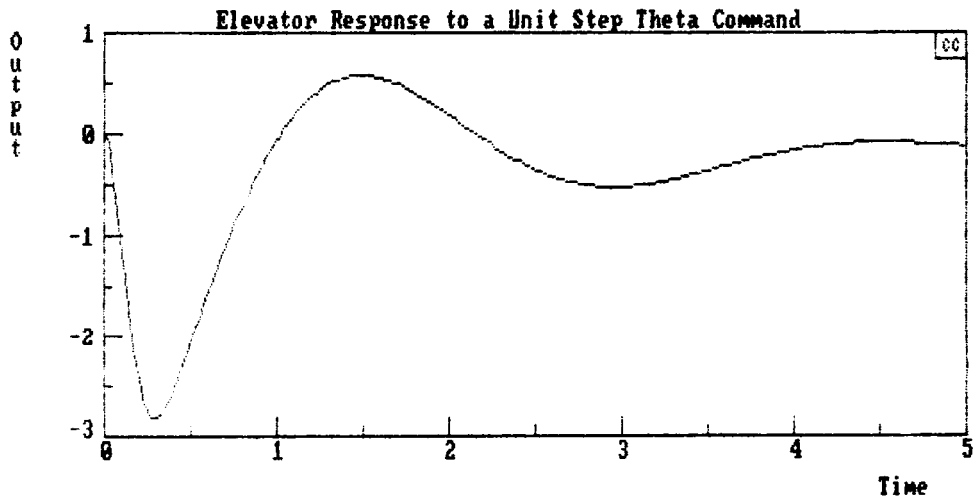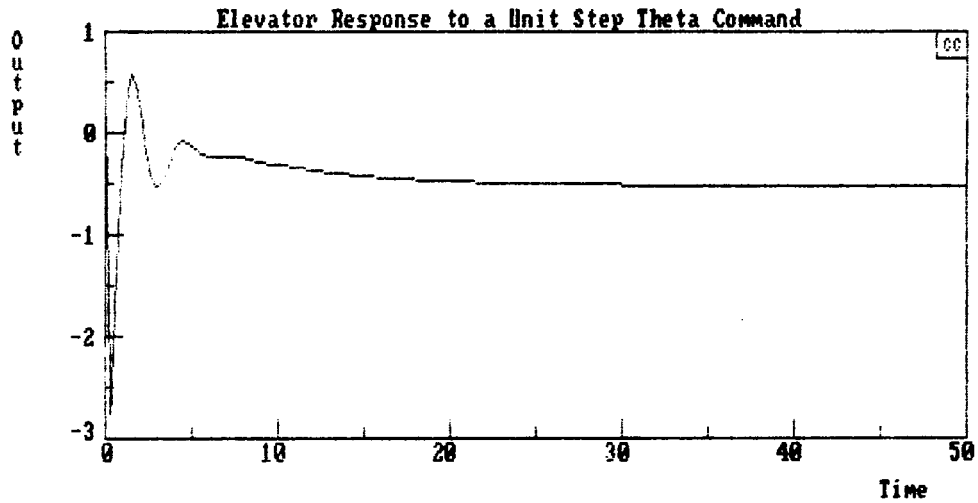
Figure B-11. Stable Configuration Elevator Response
(Highest Gain Case)

Stable Configuration: High Gain Case

H at Pilot Response to a Unit Step Theta Command

Output

70
60
50
40
30
20
10
0
-10

0   10   20   30   40   50

Time

H at Pilot Response to a Unit Step Theta Command

Output

10
8
6
4
2
0
-2
-4

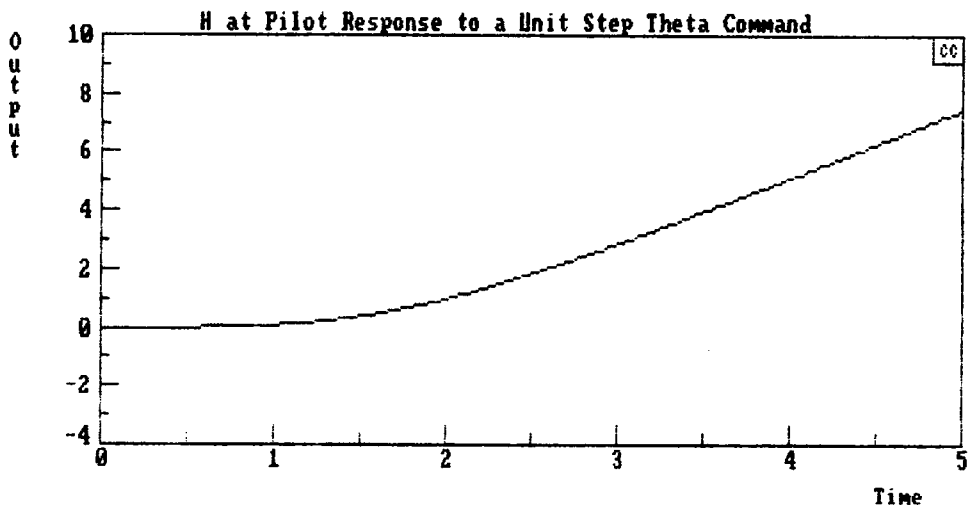0   1   2   3   4   5

Time

Figure B-12. Change In Altitude At The Pilot Location
For The Stable Configuration (Highest Gain Case)
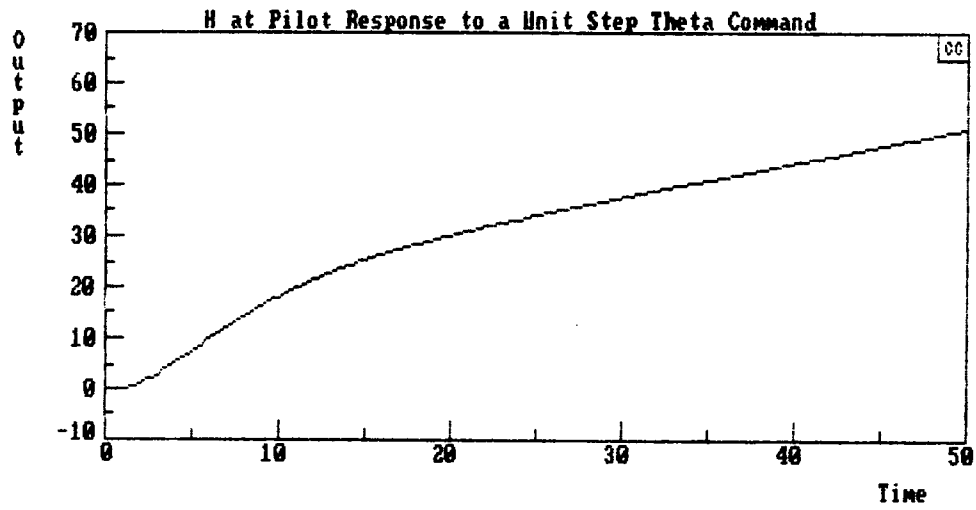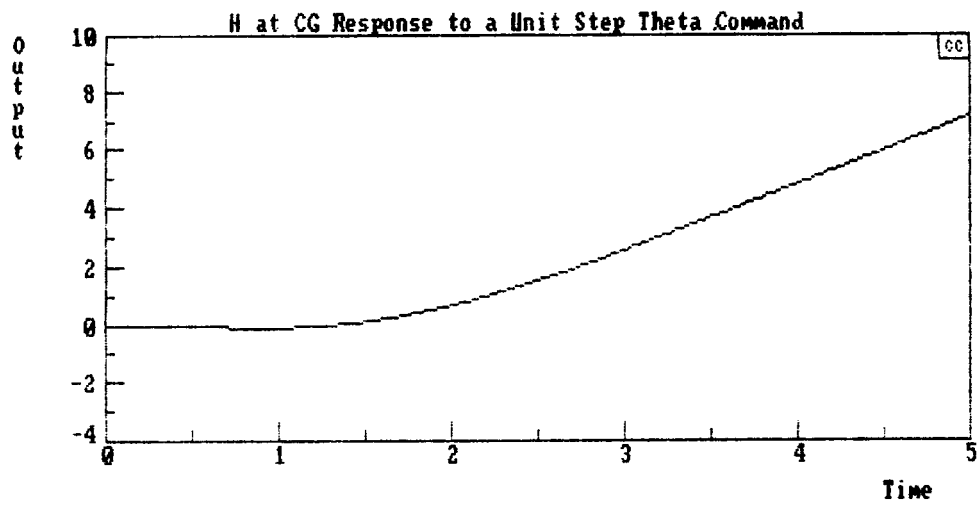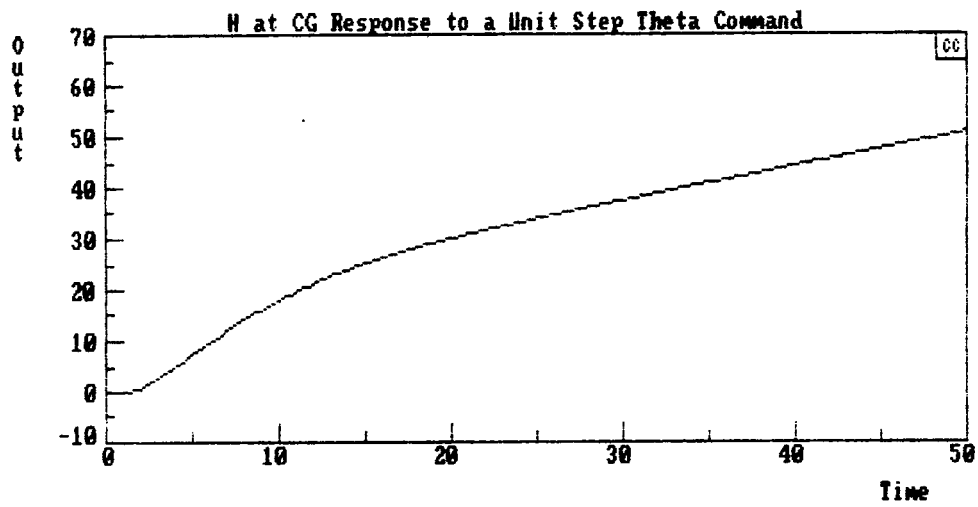
B-22

Stable Configuration: High Gain Case
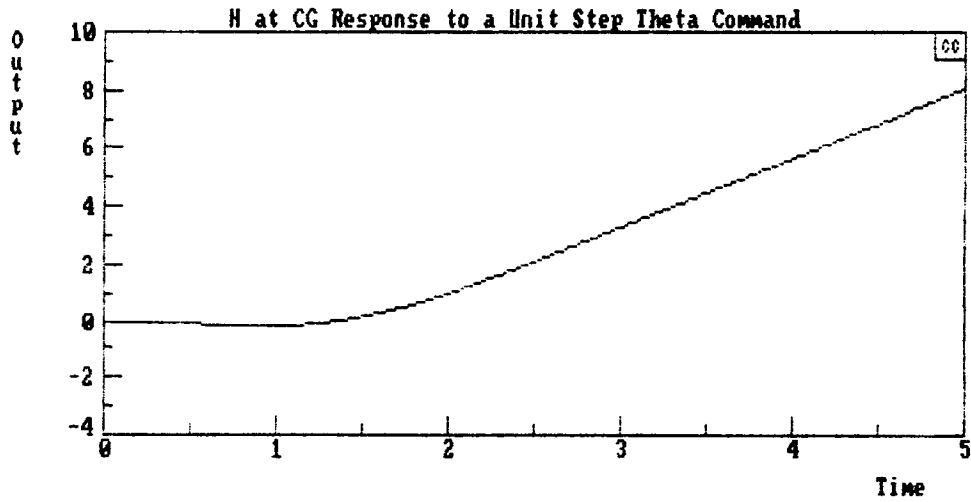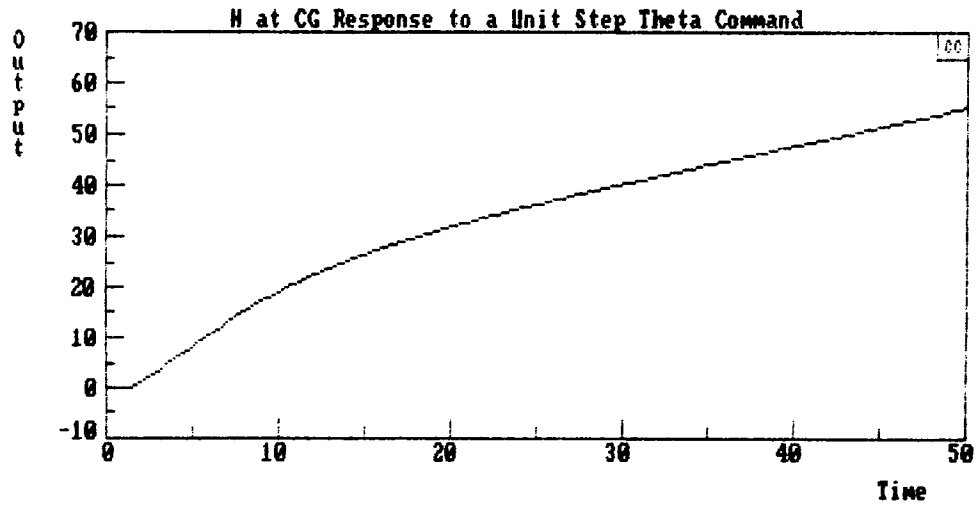
Figure B-13. Change In Altitude At The CG For The
Stable Configuration (Highest Gain Case)

Figure B-14. Change In Altitude At The Prop Tip For The
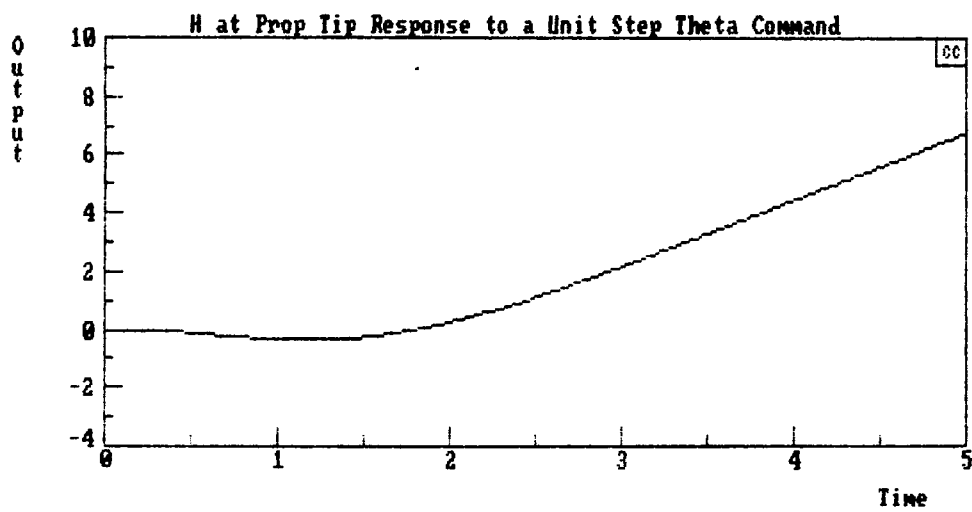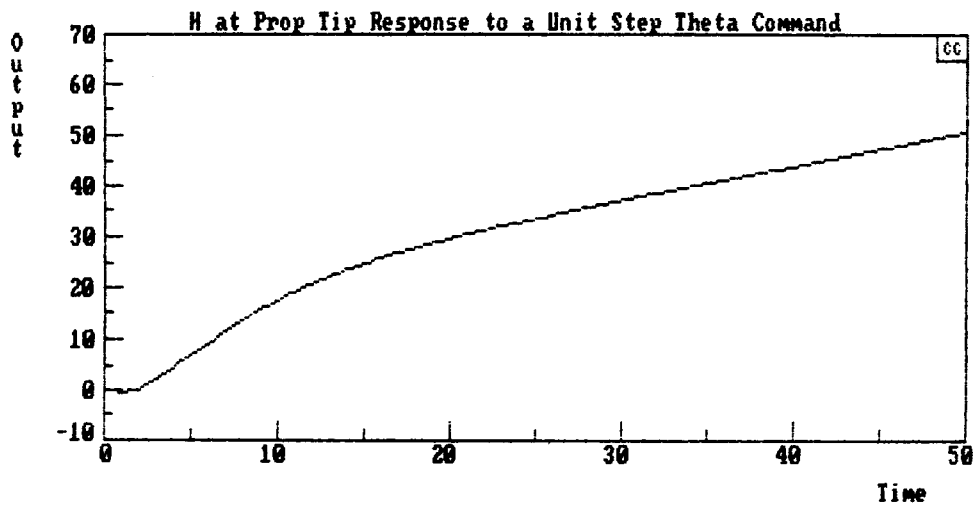Stable Configuration (Highest Gain Case)

(if IS-1)

Input File Name: F,W,L,A,N,U,S,B,.,1,N,P,   Output File Name: |_,_,_,_,_,_,_,_,_,.,_,_,_,|

AFTF LONGITUDINAL LIFT/DRAG NONDIMENSIONAL DERIVATIVES   Date: 24 - FEB - 81

dd - mmm - yy

Flight Condition Identifier; <FCI: 60 Characters or Numerals

F,L,Y,I,N,G,V,I,N,G,/,L,A,N,D,I,N,G,/,U,N,S,T,A,B,L,E,/,O,N,F,I,G,/,S,L,/,H,E,A,V,Y,_,_,_

# of Controls include Throttle but not Gust; ≤ 6

With Gusts = 1; W/O Gusts = 0

Polynomial Coeff. = 1; Without = 0

With CPLG NUM = 1; Without = 0

Save Eqn. = 1; W/O Save Eqn. = 0

Long.	NRHS	NG	NPC	Nondim	C_L, C_D	ICC	IS
0				1	0		
0 ,	2 ,	0 ,	0 ,	1 ,	0 ,	1 ,	1
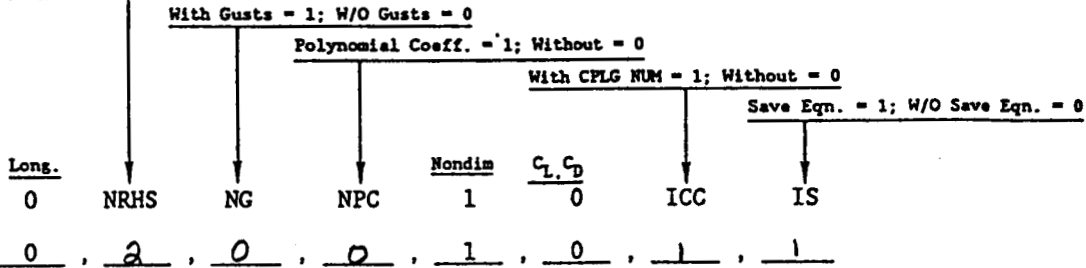
$S(ft^2)$ $c(ft)$ $\xi_o(deg)$ $l_j(ft)$ $W(lb)$ $I_y(slgft^2)$ $l_{x_a}(ft)$ $l_{x_h}(ft)$ $l_{x_d}(ft)$

2800 , 21.9 , 0 , 0 , 194143 , 834266 , 16.7 , 0 , 21.3

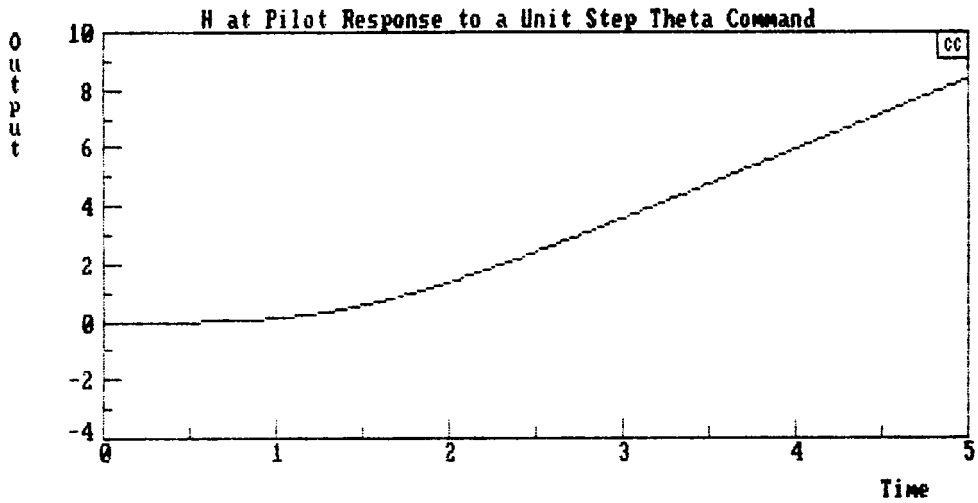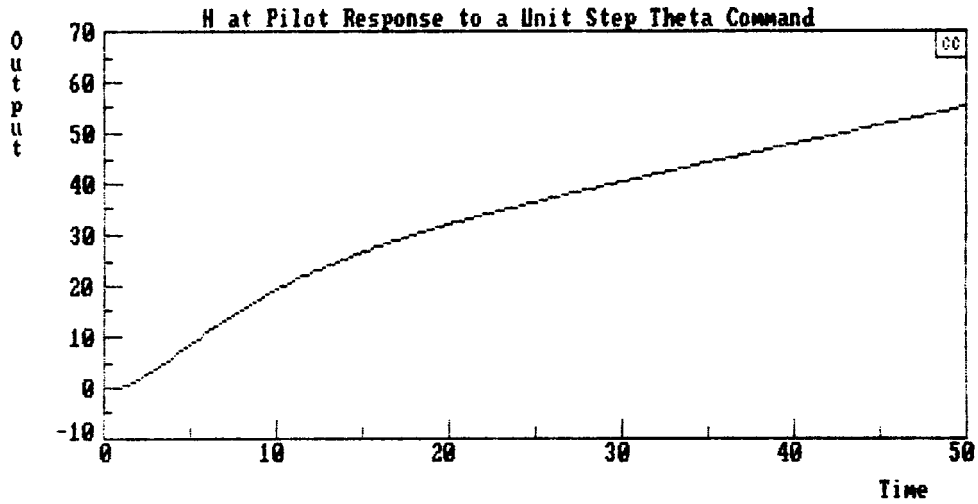$\rho\left(\dfrac{slg}{ft^3}\right)$ (h(ft) if $\rho=0$) $a(fps)$ $V_{T_o}(fps)$✓   MACH $\alpha_o(deg)$ $\gamma_o(deg)$

0 , 0 , 198 , 0 , 0 , 0

C_L ✓ C_{L_α} $C_{L_{\dot\alpha}}$ C_{L_M} C_D ✓ C_{D_α} ✓ C_{D_M}

1.48 , 4.39 , 0 , 0 , .407 , .932 , 0

C_{m_α} $C_{m_{\dot\alpha}}$ C_{m_q} C_{m_M} $\partial T/\partial M$ $\partial T/\partial \delta Th$

.35 , 0 , -1.38 , 0 , -9417 , 1

C_{D_δ} C_{L_δ} C_{m_δ} (define δ_i below)

0 , .74 , -.26   : ELEVON IN PITCH

___ , ___ , ___   : _____

___ , ___ , ___   : _____

___ , ___ , ___   : _____

Control Symbols (except thrust) $\delta_{1,2,...6}$. Use 3 characters; left justified:

D,E,P, , |_,_,_,_| , |_,_,_,_| , |_,_,_,_| , |_,_,_,_| , |_,_,_,_|

AFTF FILE NAME : A:FWLANUSA.INP

02-26-88   10:23:26

FLYINGWING/LANDING/UNSTABLECONFIG/SL/HEAVY

GEOMETRY:

VT	ALPHA	GAMMA	LX A	LX H	LX D
198.0	0.0	0.0	16.70	0.0	(-21.30) prop location
A	RHO	MACH	XIO	ZJ	
1116.5	.002377	.17735	0.0	0.0	—
S	C	WEIGHT	IY	ALTITUDE	
2800.0	21.90	194140.	834300.	0.0	—

NON-DIMENSIONAL DERIVATIVES:

CL	CLA	CLAD	CLM
1.480	4.390	0.0	0.0
CMA	CMAD	CMQ	CMM
.350	0.0	-1.380	0.0
CD	CDA	CDM	TM	TDTH
.4070	.9320	0.0	-9417.0	1.000	—
CDDEP	CLDEP	CMDEP
0.0	.740	-.260

DIMENSIONAL DERIVATIVES:

XU	XU *	XW	TU
-.08888	-.09028	.05984	-.0013978
ZU	ZU *	ZWD	ZW
-.3232	-.3232	0.0	-.5238
MU	MU *	MWD	MW
0.0	0.0	0.0	.006054
MAD	MA	MQ	
0.0	1.1986	-.2614	
XDEP	ZDEP	MDEP	
0.0	-15.999	-.8904	
XDTH	ZDTH	MDTH	
.00016572	0.0	0.0	

TRFN DATA FILE NAME : A:FWLANUSA.SAV
OLD file, write over it (Y/N)? Y
U ,W ,THE,DD ,AZ ,AZ',HD ,
Enter no. of eqns to output from 4 thru 7   7

FLYINGWING/LANDING/UNSTABLECONFIG/SL/HEAVY

DENOMINATOR: (-.745)(1.501)[.251;.237   .0597;.230] <-.0630>

FLYINGWING/LANDING/UNSTABLECONFIG/SL/HEAVY

DEP NUMERATORS:

N(U-DEP)   -.957(.965)(-19.63) <18.14>

N(W-DEP)   -16.0(11.29)[.1891;.227   .0428;.222] <-9.27>

N(THE-DEP)   -.890(.1287)(.594) <-.0681>

N(DD-DEP)   35.0(.0382)(-1.538)(2.05) <-4.21>

N(AZ-DEP)   -16.0(0.0)(.0378)(-2.49)(2.80) <4.21>

N(AZ'-DEP)   -1.129(0.0)(.0376)(7.94)(-12.51) <4.21>

N(HD-DEP)   16.0(.0378)(-2.49)(2.80) <-4.21>

FLYINGWING/LANDING/UNSTABLECONFIG/SL/HEAVY

DTH NUMERATORS:

N(U-DTH)   .0001657(0.0)(-.710)(1.495) <-.0001760>

N(W-DTH)   -.536E-4(0.0)(.261) <-.1400E-4>

N(THE-DTH)   -.324E-6 <-.324E-6>

N(DD-DTH)   .536E-4(-.917)(1.307) <-.642E-4>

N(AZ-DTH)   -.536E-4(0.0)(-.972)(1.233) <.642E-4>

N(AZ'-DTH)   -.536E-4(0.0)(-1.018)(1.178) <.642E-4>

N(HD-DTH)   .536E-4(-.972)(1.233) <-.642E-4>

FLYINGWING/LANDING/UNSTABLECONFIG/SL/HEAVY

DEP/DTH COUPLING NUMERATORS:

N(U-DEP/W-DTH)   .00265(0.0)(11.28) <.0299>

N(U-DEP/THE-DTH)   .0001476(.633) <.933E-4>

N(U-DEP/DD-DTH)   -.00579(-1.570)(2.03) <.01848>

N(U-DEP/AZ-DTH)   .00265(0.0)(-2.51)(2.77) <-.01848>

N(U-DEP/AZ'-DTH)   .0001871(0.0)(7.89)(-12.52) <-.01848>

N(U-DEP/HD-DTH)   -.00265(-2.51)(2.77) <.01848>

N(W-DEP/THE-DTH)   -.477E-4 <-.477E-4>

```
N(W-DEP/DD-DTH)      .001016(-9.30) <-.00944>

N(W-DEP/AZ-DTH)      .00944(0.0) <.00944>

N(W-DEP/AZ'-DTH)     .000796(0.0)(11.86) <.00944>

N(W-DEP/HD-DTH)     -.00944 <-.00944>

N(THE-DEP/DD-DTH)   -.477E-4 <-.477E-4>

N(THE-DEP/AZ-DTH)    .477E-4(0.0) <.477E-4>

N(THE-DEP/AZ'-DTH)   .477E-4(0.0) <.477E-4>

N(THE-DEP/HD-DTH)   -.477E-4 <-.477E-4>

N(DD-DEP/AZ-DTH)    -.001016(0.0)(0.0) <-.001016>

N(DD-DEP/AZ'-DTH)   -.001812(0.0)(0.0) <-.001812>

N(DD-DEP/HD-DTH)     .001016(0.0) <.001016>

N(AZ-DEP/AZ'-DTH)    .000796(0.0)(0.0)(0.0) <.000796>

N(AZ-DEP/HD-DTH)     0.0 <0.0>

N(AZ'-DEP/HD-DTH)    .000796(0.0)(0.0) <.000796>
```

                    02-26-88   10:25:09
AFTF completed

LANDING

B. Unstable
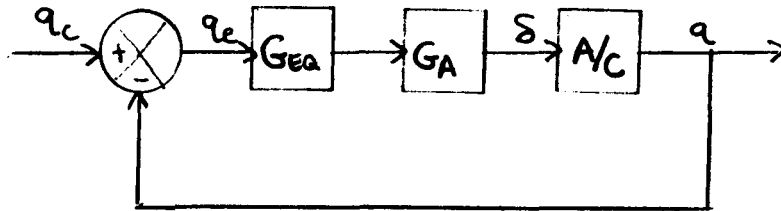
$$G_A = \frac{-12^2}{[.707, 12]} = G100$$

$$G_{EQ} = \frac{K_q (S + 1/T_q)}{S} = G110 \qquad K_q = 3.5, \; 1/T_q = 1.75$$

$$G_{A/C} = \frac{-.890(.1287)(.594)(0)}{(-.745)(1.501)[.251, .237]} = G111$$

$$G112 = OLTF = G100 * G110 * G111 \qquad , \; \text{Figure B-15}$$

$$G113 = CLTF = \frac{448.56(\phi)(.1287)(.594)(1.75)}{(.103)(.935)[.786, 2.52][.705, 9.12]}$$

$$G145 = \delta/\theta_c \qquad , \; \text{Figure B-16}$$

$$G146 = H @ CG \qquad , \; \text{Figure B-19}$$

$$G147 = H @ Pilot \qquad , \; \text{Figure B-18}$$

$$G148 = H @ Prop Tip \qquad , \; \text{Figure B-20}$$
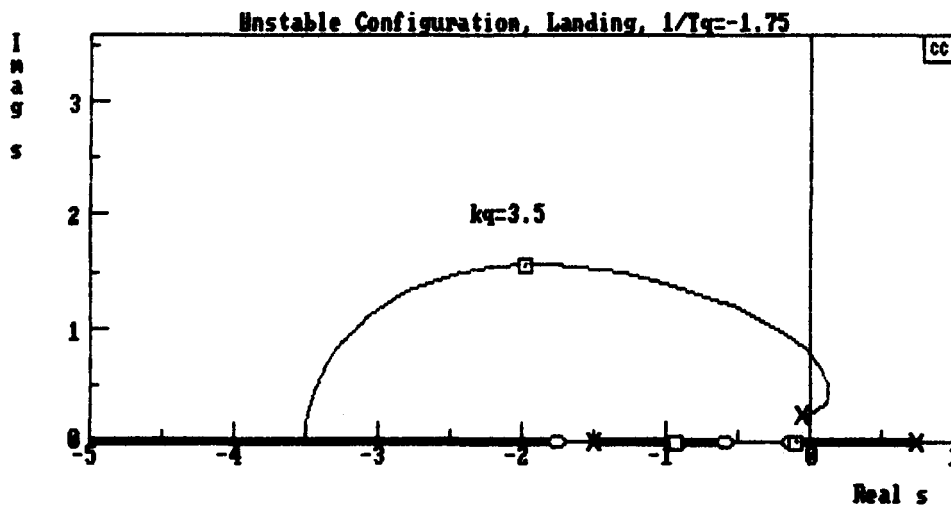
Figure B-15. Unstable Configuration Root Locus Plot
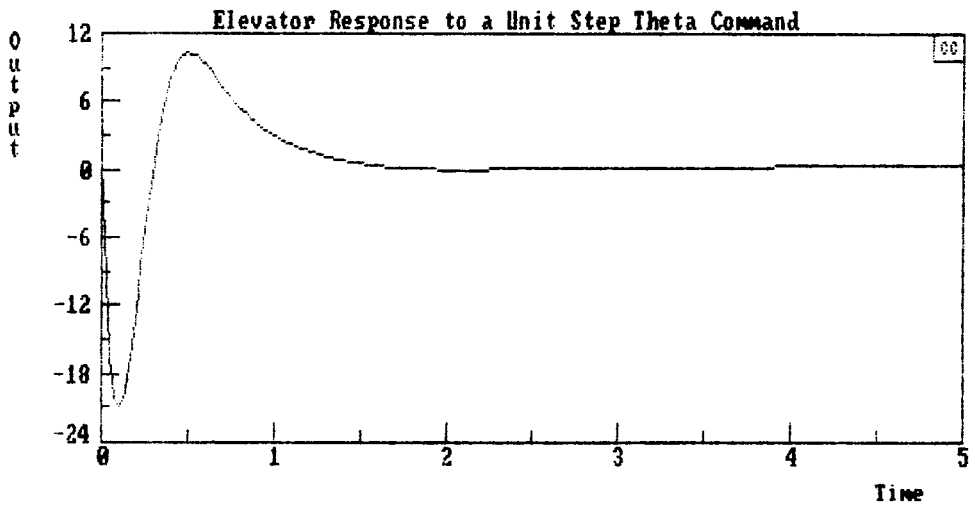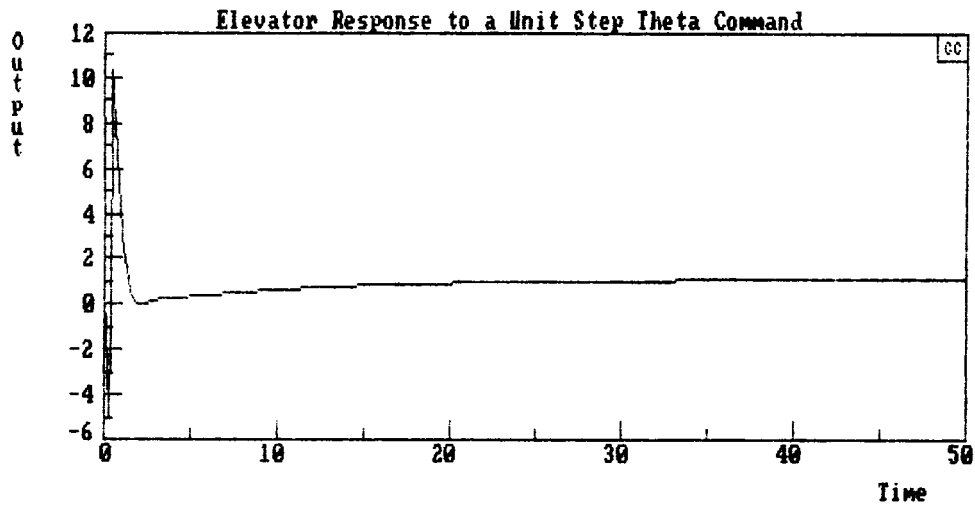
Figure B-16.   Unstable Configuration Elevator Response
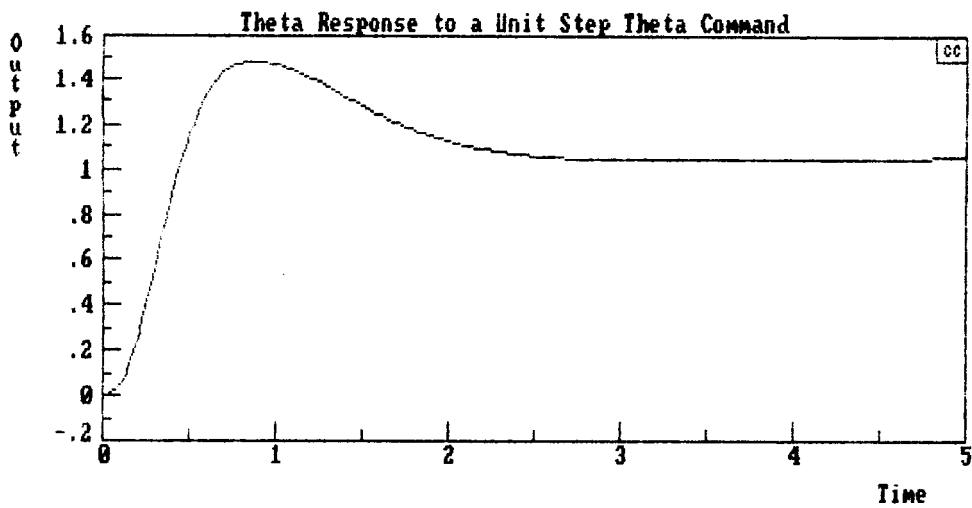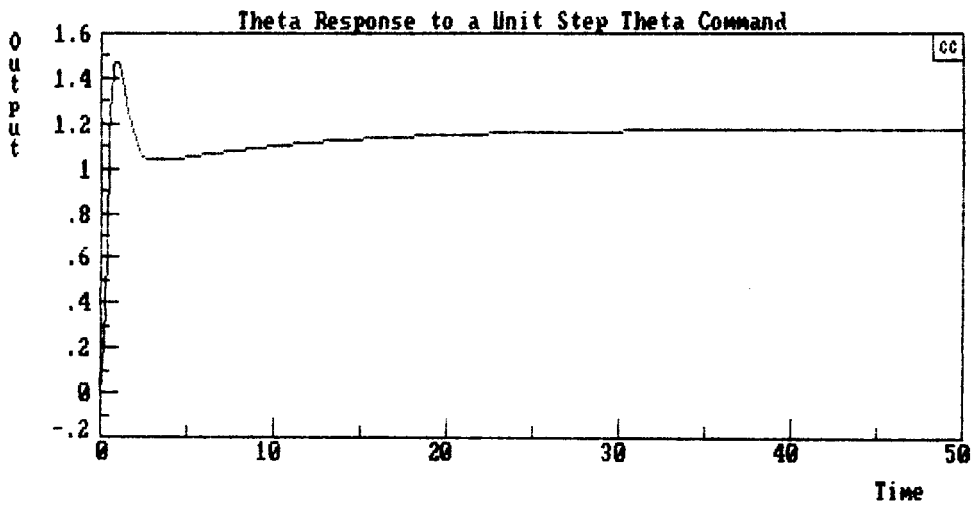
Figure B-17. Unstable Configuration Pitch Angle Response
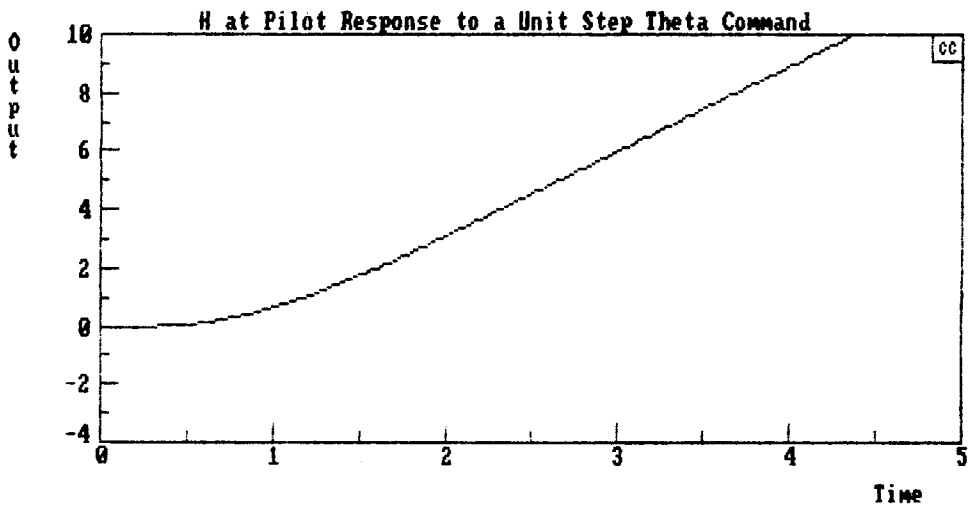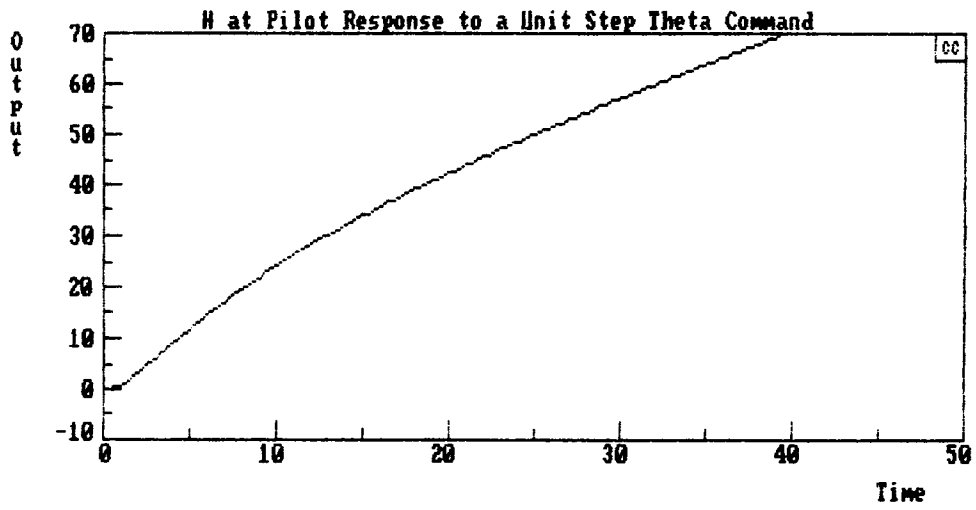
Figure B-18.   Change In Altitude At The Pilot
For The Unstable Configuration
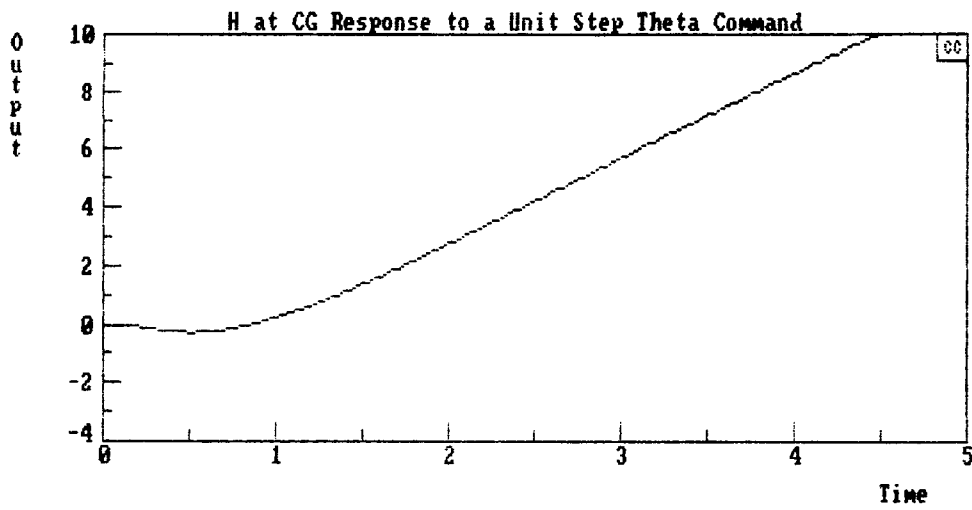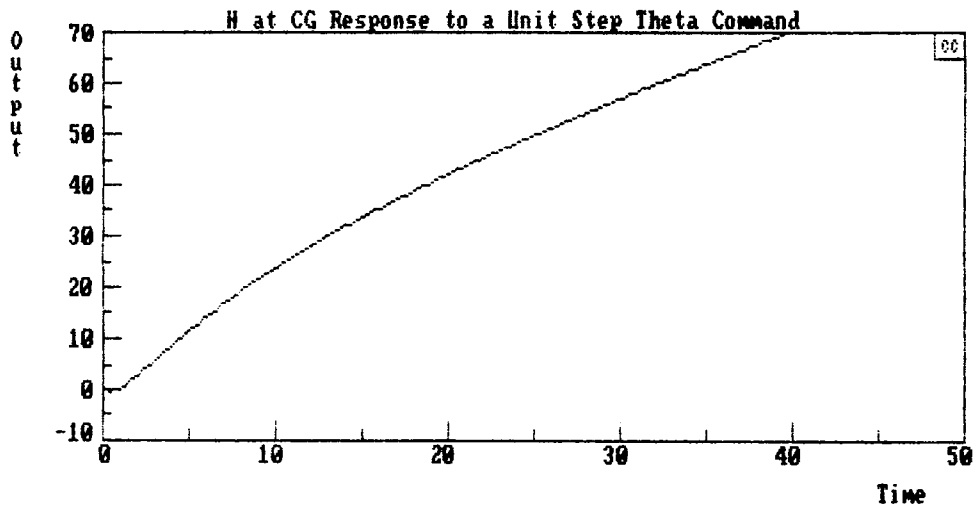
Figure B-19. Change In Altitude At The CG
For The Unstable Configuration
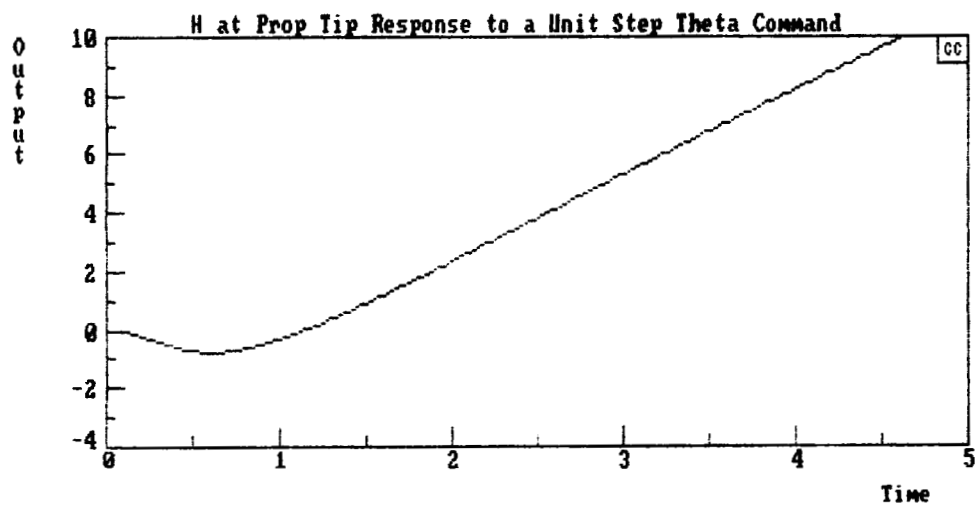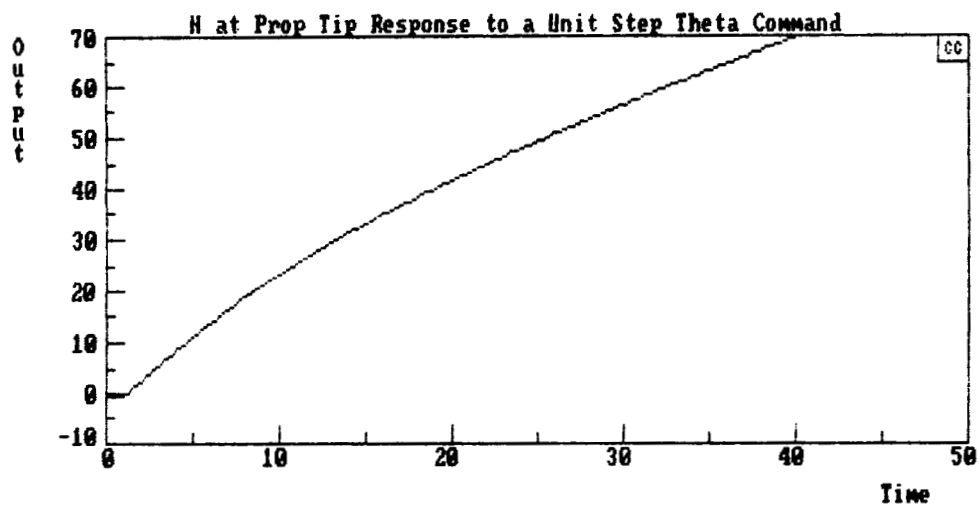
Figure B-20. Change In Altitude At The Prop Tip
For The Unstable Configuration

Elevator TF: Stable (high gain case)

$$G151(s) = \frac{-432[\ .1268,\ .1972][\ .533,\ 1.107]}{(\ .1679314)(\ .3891044)[\ .3394424,\ 2.175661][\ .7152076,\ 11.30022]}$$

Elevator TF: Unstable

$$G145(s) = \frac{-504[\ .251,\ .237](-.745)(\ 1.501)(\ 1.75)}{(\ .1033132)(\ .9348707)[\ .7857228,\ 2.519533][\ .7044609,\ 9.117243]}$$

CRUISE

(if IS=1)

Input File Name; F,V,L,A,T,C,A,1,.,1,N,P, Output File Name; |__|__|__|__|__|__|__|__|.|__|__|__|

AFTF LATERAL NONDIMENSIONAL INPUT   Date: 14 - JAN - 88
                                                                            dd - mmm - yy

Flight Condition Identifier; <FCI: 60 Characters or Numerals

,F,L,Y,I,N,G,W,I,N,G,/,C,R,U,I,S,E,/,S,T,A,B,L,E,/,C,L,=,.,3,5,/,L,A,T,D,I,R,|__|__|__|__ __.

# of Controls but not Gust; ≤ 6

With Gusts = 1; W/O Gusts = 0

Polynomial Coeff. = 1; Without = 0

With CPLG NUM = 1; Without = 0

Save Eqn. = 1; W/O Save Eqn. = 0

Lat. 1	NRHS	NG	NPC	Nondim 1	Unprimed 0	ICC	IS
1	2	0	0	1	0	0	1
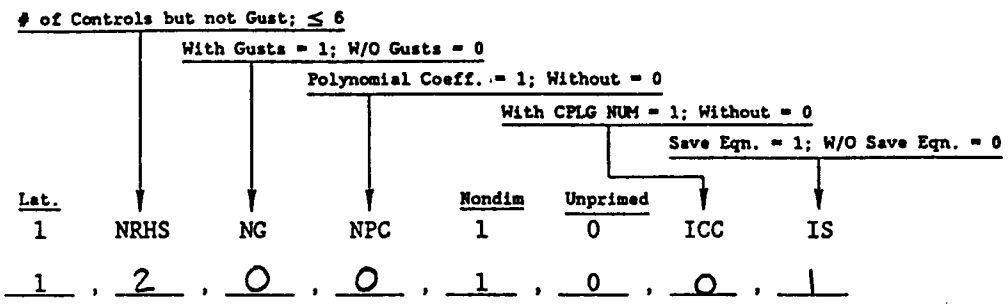
$I_x(\text{slg-ft}^2)$ $I_z(\text{slg-ft}^2)$ $I_{xz}(\text{slg-ft}^2)$ W(lb) $S(\text{ft}^2)$ b(ft)

5579273 , 6156439 , 0 , 194143 , 4000 , 172

(h(ft) if ρ=0)

$\rho\left(\dfrac{\text{slg}}{\text{ft}^3}\right)$ a(fps) V_{T_0}(fps) MACH

0 , 40000 , 629 , 0

α_o(deg) γ_o(deg) l_x(ft) l_z(ft) α_G(deg)

0 , 0 , 0 , 0 , 0

C_{y_β} C_{l_β} C_{n_β} C_{l_p} C_{n_p} C_{l_r} C_{n_r}

-.138 , -.0328 , 0.0155 , -.343 , -.0262 , 0.0722 , -0.0075

C_{y_δ} C_{l_δ} C_{n_δ} (define δ_{ij} below; 3 characters)

0 , 0.048 , -.003 : Elevon as Aileron

0 , 0 , .007 : Split Rudder

____ , ____ , ____ : _____

____ , ____ , ____ : _____

Control Symbols (except thrust) $\delta_{1,2,\ldots,6}$. Use 3 characters; left justified:

,D,E,A, , ,D,S,R, , |__|__|__| , |__|__|__| , |__|__|__| , |__|__|__|

ORIGINAL PAGE IS
OF POOR QUALITY

CRUISE, UNSTABLE

(if IS=1)

Input File Name; F.W.L.A.T.C.B.1...N.P.   Output File Name; �

AFTF LATERAL NONDIMENSIONAL INPUT   Date: 14 -JAN -87
                                                dd - mmm - yy

Flight Condition Identifier; <FCI: 60 Characters or Numerals

F.L.Y.I.N.G.W.I.N.G./.C.R.U.I.S.E./.U.N.S.T.A.B.L.E./.C.L.=.3.7./.L.A.T.D.R.⌎⌎⌎...

# of Controls but not Gust; ≤ 6
        With Gusts = 1; W/O Gusts = 0
                Polynomial Coeff. = 1; Without = 0
                        With CPLG NUM = 1; Without = 0
                                Save Eqn. = 1; W/O Save Eqn. = 0

Lat.	NRHS	NG	NPC	Nondim	Unprimed	ICC	IS
1	2	0	0	1	0	0	1
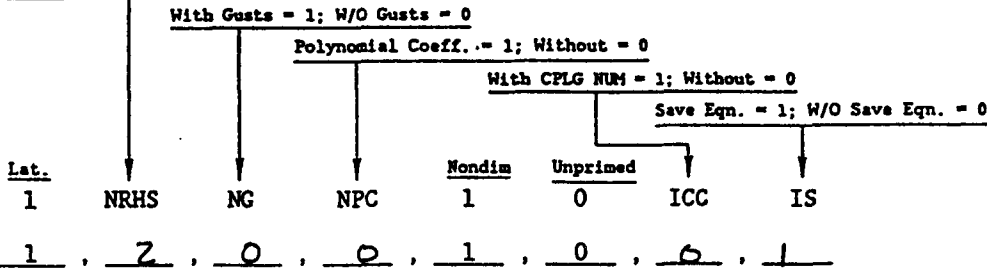
I_x(slg-ft^2) I_z(slg-ft^2) I_{xz}(slg-ft^2) W(lb) S(ft^2) b(ft)

3910620 , 4315168 , 0 , 194143 , 2800 , 144

$\rho\left(\frac{slg}{ft^3}\right)$ {h(ft) if ρ=0} a(fps) V_{T_o}(fps) MACH

0 , 40000 , 629 , 0

α_o(deg) γ_o(deg) l_x(ft) l_z(ft) α_G(deg)

0 , 0 , 0 , 0 , 0

C_{y_β} C_{l_β} C_{n_β} C_{l_p} C_{n_p} C_{l_r} C_{n_r}

-.152 , -.0459 , 0.0171 , -.343 , -.0275 , .0763 , -.007

C_{y_δ} C_{l_δ} C_{n_δ} (define δ_{ij} below; 3 characters)

0 , 0.048 , -.0058 : Elevon as Aileron
0 , 0 , .007 : Split Rudder
___ , ___ , ___ : _____
___ , ___ , ___ : _____

Control Symbols (except thrust) $\delta_{1,2,...6}$. Use 3 characters; left justified:

D.E.A. , D.S.R. , ⌎⌎⌎ , ⌎⌎⌎ , ⌎⌎⌎ , ⌎⌎⌎

B-39

02-08-88   10:13:49

FLYINGWING/CRUISE/UNSTABLE/CL=.37/LATDIR

GEOMETRY:

VT	ALPHA	GAMMA	LX	LZ
629.0	0.0	0.0	0.0	0.0
IX	IZ	IXZ	AG	ALTITUDE
.3911E+7	.4315E+7	0.0	0.0	████
S	B	RHO	W	A
2800.0	144.0	.0005890	194140.	968.1

NON-DIMENSIONAL DERIVATIVES:

CYB	CLB	CNB	
-.1520	-.04590	.01710	
CLP	CNP	CLR	CNR
-.3430	-.02780	.07630	-.00700
CYDEA	CLDEA	CNDEA	
0.0	.0480	-.00580	
CYDSR	CLDSR	CNDSR	
0.0	0.0	.00700	

UNPRIMED DIMENSIONAL DERIVATIVES:

YV	LB	NB	
-.013064	-.5514	.18615	
LP	NP	LR	NR
-.4716	-.03464	.10491	-.008723
YDEA	LDEA	NDEA	
0.0	.5766	-.06314	
YDSR	LDSR	NDSR	
0.0	0.0	.07620	

PRIMED DIMENSIONAL DERIVATIVES:

YB	LB '	NB '	
-8.218	-.5514	.18615	
LP '	NP '	LR '	NR '
-.4716	-.03464	.10491	-.008723
YDEA*	LDEA'	NDEA'	
0.0	.5766	-.06314	
YDSR*	LDSR'	NDSR'	
0.0	0.0	.07620	

TREN DATA FILE NAME : A:FWLATCB1.SAV
OLD file, write over it (Y/N)? Y
B ,P ,R ,PHI,AY ,LAD,
Enter no. of eqns to output from 4 thru 6   6

FLYINGWING/CRUISE/UNSTABLE/CL=.37/LATDIR

DENOMINATOR: (-.00553)(.566)[-.0683;.491 -.0335;.490]
                 <-.000754>

FLYINGWING/CRUISE/UNSTABLE/CL=.37/LATDIR

DEA NUMERATORS:

          N(B-DEA)   .0631(-.001029)(1.257) <-.816E-4>

          N(P-DEA)   .577(0.0)[.01452;.355   .00515;.355] <.0725>

          N(R-DEA)   -.0631(-.233)(.392)(.643) <.00371>

        N(PHI-DEA)   .577[.01452;.355   .00515;.355] <.0725>

         N(AY-DEA)   -.519(-.001029)(1.257) <.000671>

        N(LAD-DEA)   .0287[-.0354;.360   -.01275;.359] <.00371>

FLYINGWING/CRUISE/UNSTABLE/CL=.37/LATDIR

DSR NUMERATORS:

          N(B-DSR)   -.0762(-.01113)(.483) <.000409>

          N(P-DSR)   .00799(0.0)(5.27) <.0421>

          N(R-DSR)   .0762(.563)[-.1745;.224   -.0391;.221] <.00215>

        N(PHI-DSR)   .00799(5.27) <.0421>

         N(AY-DSR)   .626(-.01113)(.483) <-.00336>

        N(LAD-DSR)   .000996[.30;1.470   .441;1.402] <.00215>

                        02-08-88   10:14:38
          AFTF completed

02-08-88   10:12:04

FLYINGWING/CRUISE/STABLE/CL=.35/LATDIR

GEOMETRY:

VT	ALPHA	GAMMA	LX	LZ
629.0	0.0	0.0	0.0	0.0
IX	IZ	IXZ	AG	ALTITUDE
.5579E+7	.6156E+7	0.0	0.0	███████
S	B	RHO	W	A
4000.0	172.0	.0005890	194140.	968.1

NON-DIMENSIONAL DERIVATIVES:

CYB	CLB	CNB	
-.1380	-.03280	.01550	
CLP	CNP	CLR	CNR
-.3430	-.02620	.07220	-.00750
CYDEA	CLDEA	CNDEA	
0.0	.0480	-.00300	
CYDSR	CLDSR	CNDSR	
0.0	0.0	.00700	

UNPRIMED DIMENSIONAL DERIVATIVES:

YV	LB	NB	
-.016944	-.4712	.2018	
LP	NP	LR	NR
-.6738	-.04664	.14182	-.013351
YDEA	LDEA	NDEA	
0.0	.6896	-.03906	
YDSR	LDSR	NDSR	
0.0	0.0	.09114	

PRIMED DIMENSIONAL DERIVATIVES:

YB	LB '	NB '	
-10.658	-.4712	.2018	
LP '	NP '	LR '	NR '
-.6738	-.04664	.14182	-.013351
YDEA*	LDEA '	NDEA '	
0.0	.6896	-.03906	
YDSR*	LDSR '	NDSR '	
0.0	0.0	.09114	

TRFN DATA FILE NAME : A:FWLATCA1.SAV
OLD file, write over it (Y/N)? Y
B ,P ,R ,PHI,AY ,LAD,
Enter no. of eqns to output from 4 thru 6   6

FLYINGWING/CRUISE/STABLE/CL=.35/LATDIR

DENOMINATOR: (-.00622)(.734)[-.0232;.501 -.01164;.50]
                 <-.001143>

FLYINGWING/CRUISE/STABLE/CL=.35/LATDIR

DEA NUMERATORS:

        N(B-DEA)   .0391(.0020)(2.40) <.0001878>

        N(P-DEA)   .690(0.0)[.0266;.419   .01113;.418] <.1208>

        N(R-DEA)   -.0391(-.289)(.386)(1.417) <.00618>

        N(PHI-DEA)   .690[.0266;.419   .01113;.418] <.1208>

        N(AY-DEA)   -.416(.0020)(2.40) <-.0020>

        N(LAD-DEA)   .0346[-.0274;.422   -.01159;.422] <.00618>

FLYINGWING/CRUISE/STABLE/CL=.35/LATDIR

DSR NUMERATORS:

        N(B-DSR)   -.0911(-.01061)(.684) <.000662>

        N(P-DSR)   .01293(0.0)(3.34) <.0432>

        N(R-DSR)   .0911(.721)[-.0835;.1829   -.01527;.1822]
                          <.00220>

        N(PHI-DSR)   .01293(3.34) <.0432>

        N(AY-DSR)   .971(-.01061)(.684) <-.00705>

        N(LAD-DSR)   .001544[.462;1.193   .551;1.058] <.00220>

                      02-08-88   10:12:56
    AFTF completed

02-08-88   10:15:20

FLYINGWING/S-CRUISE/STABLE/CL=.37/LATDIR

GEOMETRY:

VT	ALPHA	GAMMA	LX	LZ
456.0	0.0	0.0	0.0	0.0
IX	IZ	IXZ	AG	ALTITUDE
.5579E+7	.6156E+7	0.0	0.0	2000
S	B	RHO	W	A
4000.0	172.0	.0012673	194140.	1036.9

NON-DIMENSIONAL DERIVATIVES:

CYB	CLB	CNB		
-.1520	-.04590	.01710		
CLP	CNP	CLR	CNR	
-.3430	-.02780	.07630	-.00700	
CYDEA	CLDEA	CNDEA		
0.0	.0480	-.00300		
CYDSR	CLDSR	CNDSR		
0.0	0.0	.00700		

UNPRIMED DIMENSIONAL DERIVATIVES:

YV	LB	NB		
-.02911	-.7457	.2518		
LP	NP	LR	NR	
-1.0510	-.07720	.2338	-.019438	
YDEA	LDEA	NDEA		
0.0	.7799	-.04417		
YDSR	LDSR	NDSR		
0.0	0.0	.10307		

PRIMED DIMENSIONAL DERIVATIVES:

YB	LB '	NB '		
-13.276	-.7457	.2518		
LP '	NP '	LR '	NR '	
-1.0510	-.07720	.2338	-.019438	
YDEA*	LDEA '	NDEA '		
0.0	.7799	-.04417		
YDSR*	LDSR '	NDSR '		
0.0	0.0	.10307		

TRFN DATA FILE NAME : A:FWLATCA2.SAV
OLD file, write over it (Y/N)? Y
B .P ,R ,PHI,AY ,LAD,
Enter no. of eqns to output from 4 thru 6   6

FLYINGWING/S-CRUISE/STABLE/CL=.37/LATDIR

DENOMINATOR: (-.00827)(1.116)[-.00679;.583   -.00396;.583]
                 <-.00313>

FLYINGWING/S-CRUISE/STABLE/CL=.37/LATDIR

    DEA NUMERATORS:

            N(B-DEA)   .0442(.00211)(3.66) <.000341>

            N(P-DEA)   .780(0.0)[.0386;.458   .01765;.458] <.1636>

            N(R-DEA)   -.0442(-.296)(.373)(2.37) <.01154>

          N(PHI-DEA)   .780[.0386;.458   .01765;.458] <.1636>

           N(AY-DEA)   -.586(.00211)(3.66) <-.00453>

          N(LAD-DEA)   .0538[-.0555;.463   -.0257;.462] <.01154>

FLYINGWING/S-CRUISE/STABLE/CL=.37/LATDIR

    DSR NUMERATORS:

            N(B-DSR)   -.1031(-.01548)(1.066) <.001702>

            N(P-DSR)   .0241(0.0)(3.22) <.0776>

            N(R-DSR)   .1031(1.096)[-.0363;.219   -.00796;.219] <.00543>

          N(PHI-DSR)   .0241(3.22) <.0776>

           N(AY-DSR)   1.368(-.01548)(1.066) <-.0226>
                            ,
          N(LAD-DSR)   .0030[.602;1.345   .809;1.074] <.00543>

                        02-08-88   10:16:02
    AFTF completed

                                                                B-45

02-08-88   10:16:33

FLYINGWING/S-CRUISE/UNSTABLE/CL=.37/LATDIR

GEOMETRY:
VT	ALPHA	GAMMA	LX	LZ
539.0	0.0	0.0	0.0	0.0
IX	IZ	IXZ	AG	ALTITUDE
.3911E+7	.4315E+7	0.0	0.0	~~2000~~
S	B	RHO	W	A
2800.0	144.0	.0012673	194140.	1036.9

NON-DIMENSIONAL DERIVATIVES:
CYB	CLB	CNB	
-.1520	-.04590	.01710	
CLP	CNP	CLR	CNR
-.3430	-.02780	.07630	-.00700
CYDEA	CLDEA	CNDEA	
0.0	.0480	-.00580	
CYDSR	CLDSR	CNDSR	
0.0	0.0	.00700	

UNPRIMED DIMENSIONAL DERIVATIVES:
YV	LB	NB	
-.02409	-.8712	.2941	
LP	NP	LR	NR
-.8696	-.06387	.19345	-.016084
YDEA	LDEA	NDEA	
0.0	.9110	-.09976	
YDSR	LDSR	NDSR	
0.0	0.0	.12040	

PRIMED DIMENSIONAL DERIVATIVES:
YB	LB '	NB '	
-12.984	-.8712	.2941	
LP '	NP '	LR '	NR '
-.8696	-.06387	.19345	-.016084
YDEA*	LDEA'	NDEA'	
0.0	.9110	-.09976	
YDSR*	LDSR'	NDSR'	
0.0	0.0	.12040	

TRFN DATA FILE NAME : A:FWLATCB2.SAV
OLD file, write over it (Y/N)? Y
B ,P ,R ,PHI,AY ,LAD,
Enter no. of eqns to output from 4 thru 6   6

FLYINGWING/S-CRUISE/UNSTABLE/CL=.37/LATDIR

DENOMINATOR: (-.00699)(.954)[-.0303;.620 -.01879;.619]
            <-.00256>

FLYINGWING/S-CRUISE/UNSTABLE/CL=.37/LATDIR

DEA NUMERATORS:

N(B-DEA)   .0998(-.001391)(2.00) <-.000278>

N(P-DEA)   .911(0.0)[.0213;.446   .00949;.446] <.1809>

N(R-DEA)   -.0998(-.241)(.322)(1.396) <.01082>

N(PHI-DEA)   .911[.0213;.446   .00949;.446] <.1809>

N(AY-DEA)   -1.295(-.001391)(2.00) <.00360>

N(LAD-DEA)   .0520[-.0794;.456   -.0362;.455] <.01082>

FLYINGWING/S-CRUISE/UNSTABLE/CL=.37/LATDIR

DSR NUMERATORS:

N(B-DSR)   -.1204(-.01309)(.883) <.001391>

N(P-DSR)   .0233(0.0)(4.53) <.1055>

N(R-DSR)   .1204(.931)[-.0794;.236   -.01876;.236] <.00627>

N(PHI-DSR)   .0233(4.53) <.1055>

N(AY-DSR)   1.563(-.01309)(.883) <-.01807>

N(LAD-DSR)   .00290[.459;1.470   .675;1.306] <.00627>

                    02-08-88   10:17:20
    AFTF completed

02-08-88   10:17:45

FLYINGWING/E-CRUISE/STABLE/CL=.37/LATDIR

GEOMETRY:

VT	ALPHA	GAMMA	LX	LZ
259.0	0.0	0.0	0.0	0.0
IX	IZ	IXZ	AG	ALTITUDE
.18651E+7	.2058E+7	0.0	0.0	██████
S	B	RHO	W	A
4000.0	172.0	.0012673	64900.	1036.9

NON-DIMENSIONAL DERIVATIVES:

CYB	CLB	CNB	
-.1520	-.04590	.01710	
CLP	CNP	CLR	CNR
-.3430	-.02780	.07630	-.00700
CYDEA	CLDEA	CNDEA	
0.0	.0480	-.00300	
CYDSR	CLDSR	CNDSR	
0.0	0.0	.00700	

UNPRIMED DIMENSIONAL DERIVATIVES:

YV	LB	NB	
-.04947	-.7197	.2430	
LP	NP	LR	NR
-1.7857	-.13117	.3972	-.03303
YDEA	LDEA	NDEA	
0.0	.7526	-.04263	
YDSR	LDSR	NDSR	
0.0	0.0	.09947	

PRIMED DIMENSIONAL DERIVATIVES:

YB	LB '	NB '	
-12.812	-.7197	.2430	
LP '	NP '	LR '	NR '
-1.7857	-.13117	.3972	-.03303
YDEA*	LDEA '	NDEA '	
0.0	.7526	-.04263	
YDSR*	LDSR '	NDSR '	
0.0	0.0	.09947	

TREN DATA FILE NAME : A:FWLATCA3.SAV
OLD file, write over it (Y/N)? Y
B ,P ,R ,PHI,AY ,LAD,
Enter no. of eqns to output from 4 thru 6   6

FLYINGWING/E-CRUISE/STABLE/CL=.37/LATDIR

DENOMINATOR: (-.01436)(1.914)[.0579;.589 .0341;.588]
                (-.00904)

FLYINGWING/E-CRUISE/STABLE/CL=.37/LATDIR

DEA NUMERATORS:

N(B-DEA)   .0426(.00367)(6.29) <.000985>

N(P-DEA)   .753(0.0)[.0666;.450   .030;.449] <.1526>

N(R-DEA)   -.0426(-.294)(.371)(4.07) <.01892>

N(PHI-DEA)   .753[.0666;.450   .030;.449] <.1526>

N(AY-DEA)   -.546(.00367)(6.29) <-.01262>

N(LAD-DEA)   .0915[-.0921;.455   -.0419;.453] <.01892>

FLYINGWING/E-CRUISE/STABLE/CL=.37/LATDIR

DSR NUMERATORS:

N(B-DSR)   -.0995(-.0272)(1.813) <.00491>

N(P-DSR)   .0395(0.0)(1.861) <.0735>

N(R-DSR)   .0995(1.814)[.0484;.222   .01075;.222] <.00890>

N(PHI-DSR)   .0395(1.861) <.0735>

N(AY-DSR)   1.274(-.0272)(1.813) <-.0629>

N(LAD-DSR)   .00492(1.033)(1.751) <.00890>

                    02-08-88   10:18:34
AFTF completed

02-08-88   10:19:12

FLYINGWING/E-CRUISE/UNSTABLE/CL=.37/LATDIR

GEOMETRY:

VT	ALPHA	GAMMA	LX	LZ
311.0	0.0	0.0	0.0	0.0
IX	IZ	IXZ	AG	ALTITUDE
.11683E+7	.12892E+7	0.0	0.0	████
S	B	RHO	W	A
2800.0	144.0	.0012673	58000.	1036.9

NON-DIMENSIONAL DERIVATIVES:

CYB	CLB	CNB	
-.1520	-.04590	.01710	
CLP	CNP	CLR	CNR
-.3430	-.02780	.07630	-.00700
CYDEA	CLDEA	CNDEA	
0.0	.0480	-.00580	
CYDSR	CLDSR	CNDSR	
0.0	0.0	.00700	

UNPRIMED DIMENSIONAL DERIVATIVES:

YV	LB	NB	
-.04652	-.9708	.3278	
LP	NP	LR	NR
-1.6796	-.12337	.3736	-.03106
YDEA	LDEA	NDEA	
0.0	1.0152	-.11117	
YDSR	LDSR	NDSR	
0.0	0.0	.13418	

PRIMED DIMENSIONAL DERIVATIVES:

YB	LB '	NB '	
-14.469	-.9708	.3278	
LP '	NP '	LR '	NR '
-1.6796	-.12337	.3736	-.03106
YDEA*	LDEA'	NDEA'	
0.0	1.0152	-.11117	
YDSR*	LDSR'	NDSR'	
0.0	0.0	.13418	

```
TRFN DATA  FILE NAME :  A:FWLATCB3.SAV
OLD file, write over it ( Y/N )?  Y
B  ,P  ,R  ,PHI,AY ,LAD,
Enter no. of eqns to output from 4 thru  6      6
```

FLYINGWING/E-CRUISE/UNSTABLE/CL=.37/LATDIR

DENOMINATOR: (-.01222)(1.726)[.0320;.673   .0215;.673]
               <-.00956>

FLYINGWING/E-CRUISE/UNSTABLE/CL=.37/LATDIR

DEA NUMERATORS:

N(B-DEA)   .1112(-.00248)(3.75) <-.001035>

N(P-DEA)   1.015(0.0)[.0390;.470   .01834;.470] <.224>

N(R-DEA)   -.1112(-.240)(.314)(2.78) <.0233>

N(PHI-DEA)   1.015[.0390;.470   .01834;.470] <.224>

N(AY-DEA)   -1.609(-.00248)(3.75) <.01498>

N(LAD-DEA)   .0999[-.1612;.483   -.0778;.476] <.0233>

FLYINGWING/E-CRUISE/UNSTABLE/CL=.37/LATDIR

DSR NUMERATORS:

N(B-DSR)   -.1342(-.0227)(1.702) <.00519>

N(P-DSR)   .0501(0.0)(2.64) <.1326>

N(R-DSR)   .1342(1.715)[.0235;.242   .00569;.242] <.01349>

N(PHI-DSR)   .0501(2.64) <.1326>

N(AY-DSR)   1.941(-.0227)(1.702) <-.0751>

N(LAD-DSR)   .00624[.854;1.470   1.256;.764] <.01349>

                    02-08-88   10:20:10
AFTF completed

1. Report No. NASA CR- 181806	2. Government Accession No.	3. Recipient's Catalog No.
4. Title and Subtitle Tailless Aircraft Performance Improvements with Relaxed Static Stability		5. Report Date March 1989
		6. Performing Organization Code
7. Author(s) Irving L. Ashkenas and David H. Klyde		8. Performing Organization Report No. STI-TR-1252-1
9. Performing Organization Name and Address Systems Technology, Inc. 13766 South Hawthorne Boulevard Hawthorne, CA 90250		10. Work Unit No. 505-66-01-02
		11. Contract or Grant No. NAS1-18524
12. Sponsoring Agency Name and Address National Aeronautics and Space Administration Langley Research Center Hampton, VA 23665-5225		13. Type of Report and Period Covered CONTRACTOR REPORT
		14. Sponsoring Agency Code

15. Supplementary Notes

Langley Technical Monitor: William D. Grantham

16. Abstract

The purpose of the work reported here is to determine the tailless aircraft performance improvements gained from relaxed static stability, to quantify this potential in terms of range-payload improvements, and to identify other possible operational and handling benefits or problems. Two configurations were chosen for the study: a "modern" high aspect ratio, short-chord wing proposed as a high-altitude long endurance (HALE) RPV; a wider, lower aspect ratio, high volume wing suitable for internal stowage of all fuel and payload required for a manned long-range reconnaissance mission. Flying at best cruise altitude, both unstable configurations were found to have a 14 percent improvement in range and a 7 to 9 percent improvement in maximum endurance compared to the stable configurations. The unstable manned configuration also shows a 15 percent improvement in the 50 ft takeoff obstacle distance and an improved height response to elevator control. However, it is generally more deficient in control power due to its larger adverse aileron yaw and its higher takeoff and landing C_L, both due to the downward trimmed (vs upward trimmed for stable configurations) trailing edge surfaces.

17. Key Words (Suggested by Author(s)) taillless, relaxed stability, improved performance, flying wing, control power	18. Distribution Statement UNCLASSIFIED - UNLIMITED Subject Category 08		
19. Security Classif. (of this report) Unclassified	20. Security Classif. (of this page) Unclassified	21. No. of Pages 140	22. Price A07